# Development of oligomer-specific antibodies against tau protein and testing of therapeutic potential in a cell model of tau pathology

**Dissertation**

**zur**

**Erlangung des Doktorgrades (Dr. rer. nat.)**

**der**

**Mathematisch-Naturwissenschaftlichen Fakultät**

**der**

**Rheinischen Friedrich-Wilhelms-Universität Bonn**

**vorgelegt von**


## Ram Reddy Chandupatla

**Parkal, INDIA**


**Bonn**

**2018**

**Angefertigt mit Genehmigung der Mathematisch-Naturwissenschaftlichen Fakultät der Rheinischen Friedrich-Wilhelms-Universität Bonn**

**1. Gutachter: Prof. Dr. Eckhard Mandelkow**

**2. Gutachter: Prof. Dr. Michael Hoch**

**Tag der Promotion: 24. April 2019**

**Erscheinungsjahr: 2020**

## Contents

## Abbreviations

°C – degree Celsius

µg – microgram

µl – microliter

µm – micrometer

µM – micromolar

aa- aminoacid

AFM – Atomic Force Microscopy

APC – Allophycocyanin

BCA – Bicinchoninic acid

BLI – Bio-layer Interferometry

BSA – Bovine serum albumin

Butyl FF – Butyl Fast Flow column

CNS – Central Nervous System

DLS – Dynamic Light Scattering

DMSO – Dimethyl Sulfoxide.

DTT – Dithiothreitol

FCS – Fetal Calf Serum

FL – Full length Tau protein

FTDP – Fronto Temporal Dementia linked with Parkinsonism

Low-n oligomers – dimers to hexamers

LucN – Click beetle green luciferease N-terminal sequence

LucC – Click beetle green luciferease C-terminal sequence

HCl – Hydrochloric Acid

High-n oligomers - ≥15mers

hTau40$^{WT}$ –Wild type full length human tau, longest CNS isoform (441 residues)

$k_a$ – Association rate constant

$k_d$ – Dissociation rate constant

$K_D$ – Dissociation constant ($k_d$ / $k_a$)

mA – milliAmpere

mAb – Monoclonal antibody

MAP – Microtubule Associated Protein

mg – milligram

ml – milliliter

mm – millimeter

mM – millimolar

mTau40 – Full length mouse tau, longest CNS isoform

MWCO – Molecular Weight Cut Off

$NaN_3$ – Sodium Azide

NFT – Neurofibrillary Tangles

ng – nanogram

nm – nanometer

nM – nanomolar

NMR – Nuclear Magnetic Resonance

OD – Optical Density

PAGE – Polyacrylamide Gel Electrophoresis

PBS – Phosphate Buffer Saline

PHF – Paired Helical Filaments

PNS – Peripheral Nervous System

PVDF – Polyvinylidenedifluoride

RD – Repeat domain of tau protein

Rpm – Rotations per minute

RT – Room temperature

s – second

SDS – Sodium Dodecyl Sulfate

SEC – Size Exclusion Chromatography

$Tau^{RD\Delta K}$ – Tau Repeat Domain protein with deletion of lysine 280

$Tau^{FL\Delta K}$ – Full length human tau with deletion of lysine at 280 position

TEA – Triethanolamine

ThS – Thioflavin S

V – Volt

WT – Wildtype

## Summary

Tau, a microtubule associated protein, forms abnormal aggregates in many neurodegenerative diseases such as Alzheimer disease (AD). There is an urgent need for disease-modifying therapies of AD and related tauopathies. Inhibiting the aggregation of tau and the accumulation of neurofibrillary tangles (NFTs) could be helpful in combating tau pathology. Recent studies show that tau induced toxicity is mainly due to the presence of oligomers of tau rather than the monomers and fibrillar aggregates (Kaniyappan et al., 2017, Flach et al., 2012, Lasagna-Reeves et al., 2010).

To combat the toxicity of tau oligomers we developed antibodies against the purified low-n tau oligomers (dimers to hexamers) of $Tau^{RD\Delta K}$, the strongly aggregating repeat domain of tau. Monoclonal antibodies were tested by various biochemical and biophysical methods for their specificity to bind to the toxic oligomers. Some antibodies show specificity to aggregates of tau while others detect all forms of tau. Antibodies 2B10 and 6H1, described as representative examples, bind to tau oligomers with high specificity as judged by dotblot, dynamic light scattering (DLS) and immunofluorescence analysis. As these antibodies are dependent on tau conformations, they appear non-specific in denaturing methods like western blotting. 2B10 and 6H1 antibodies are able to inhibit the tau aggregation up to ~90% *in vitro* ($Tau^{RD\Delta K}$, $hTau^{P301L}$), as judged by the Thioflavin S fluorescence assay which is sensitive to β-structure. In the presence of antibodies tau protein forms only up to low-n oligomers as judged by light scattering and atomic force microscopy (AFM). The choice of the pH of the column elution buffer of the antibodies plays a key role in determining the activity of the antibodies, as antibodies eluted at low pH have a higher activity compared to the same antibodies eluted at high pH.

The ability of antibodies to inhibit the aggregation of tau was tested in an N2a cell model of tau pathology which expresses the pro-aggregant tau repeat domain $Tau^{RD\Delta K}$. Antibodies were added to the extracellular medium, without or with protein transfection reagent (Xfect) which stimulates cellular uptake. In this assay, 2B10 antibody failed to inhibit tau aggregation (ThS signal) and failed to prevent aggregation induced apoptosis (Annexin V signal). By contrast, in the split-luciferase complementation assay the antibody 2B10, applied extracellularly, was able to prevent the dimerization/oligomerization of tau.

Surprisingly this antibody has only a relatively low affinity to tau but is still very active in inhibiting tau aggregation in vitro. Antibodies added extracellularly were taken up by the cells and sorted into lysosomes. Their inhibitory effect can be explained by the fact that the internalized antibody recruits the toxic tau protein or oligomers to the lysosomes for degradation (Figure 0.1). In summary, a subset of antibodies raised against the purified low-n oligomers of $Tau^{RD\Delta K}$ are able to inhibit tau aggregation both *in vitro* and in a cell model of tau pathology.

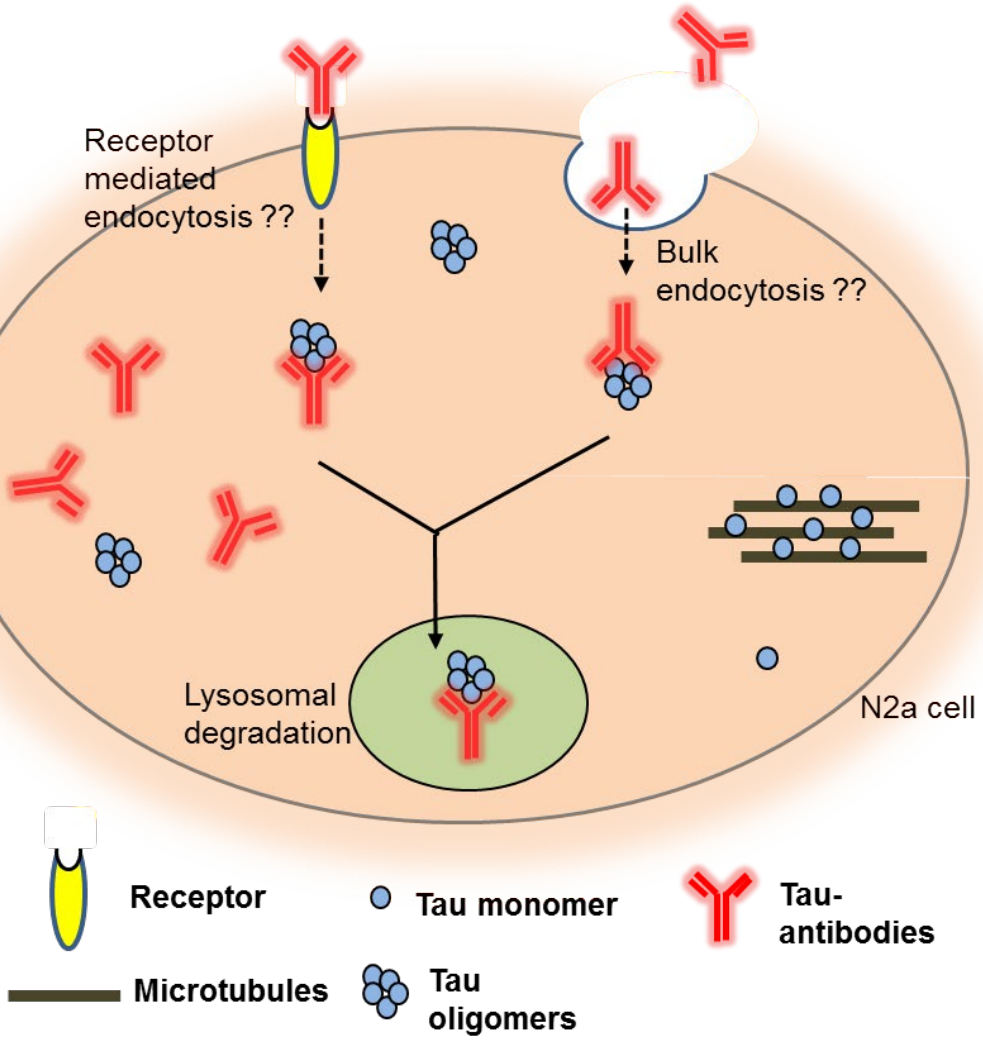


**Figure 0.1: Mode of activity of anti-tau low-n oligomer antibodies**
Cartoon representation of the modes of activity of the anti-tau low-n oligomer antibodies. Extracellularly added antibodies enter the N2a cells expressing $Tau^{RD\Delta K}$ and are released into the cytosol by some unknown mechanism (either receptor mediated or bulk endocytosis, dotted arrows) where they interact with tau oligomers and promote their entry into lysosomes presumably for degradation.

## List of tables



## List of figures

# 1 Introduction

## 1.1 Neurodegenerative diseases

Neurodegenerative diseases are a group of diseases in which loss of structure and function of neurons results in cell death. Aging is an important risk factor for many neurodegenerative diseases (Brookmeyer et al., 1998). The majority of the neurodegenerative diseases are proteinopathies which are characterized by the accumulation of misfolded and insoluble filamentous protein aggregates (Przedborski et al., 2003). These proteinopathies are called amyloid diseases, as the filamentous aggregates display amyloid properties (cross- β-pleated sheet structures). Brain amyloidoses display phenotypic diversity. Even though amyloidogenic proteins are typically expressed systemically, they accumulate in specific regions of the brain and their aggregates are composed of different protein constituents (Skovronsky et al., 2006). An example is Alzheimer disease (AD), the most prevalent form of neurodegenerative diseases which is characterized by the deposition of extracellular plaques composed of amyloid-β and intracellular tangles containing aggregates of tau protein.

## 1.2 Tauopathies

Tau, a microtubule-associated protein (MAP), was discovered in 1975 (Weingarten et al., 1975). Tau occurs mainly in the brain, particularly in the axons of mature neurons, but traces can be detected in glia as well (Miller et al., 2004). Tau plays a major role in binding, stabilization and assembly of microtubules (Mandelkow and Mandelkow, 2012). Tau is a highly soluble (hydrophilic) and natively unfolded protein with little or no tendency to aggregate (Jeganathan et al., 2008). In disease conditions, tau accumulates to form insoluble, fibrillary deposits in a wide range of neurodegenerative diseases called tauopathies (Wang and Mandelkow, 2016). AD is the best-known form of tauopathy, but aggregation or accumulation of abnormal tau occurs also in other tauopathies, such as Frontotemporal dementia with Parkinsonism linked to Chromosome 17 (FTDP-17), Corticobasal degeneration (CBD), Progressive Supranuclear Palsy (PSP), Argyrophilic Grain Disease (AGD), Huntington Disease (HD), Pick Disease (PiD) and Traumatic Brain Encephalopathy (TBE). The ability of tau to cause neurodegenerative diseases has been confirmed by the identification of tau mutants in patients with FTDP-17 which indicates that

mutations in the tau gene are sufficient to trigger neurodegeneration (Spillantini et al., 2000). The trigger for tau aggregation and the mechanisms involved in tau-induced neurodegeneration are still poorly understood. Over the years, several research groups have created transgenic mouse lines with different tau mutations (P301L, P301S, ΔK280, G272V, A152T) to study the pathophysiology and role of tau in neurodegenerative diseases (Mocanu et al., 2008, Ramsden et al., 2005, Yoshiyama et al., 2007, Sydow et al., 2016, Alonso. et al., 2004, Eckermann et al., 2007, Van der Jeugd et al., 2012).

## 1.3 Tau

Human tau is encoded by the microtubule-associated protein tau gene (MAPT), which is located on chromosome 17q21 and comprises 16 exons (Neve et al., 1986). Transcribed RNA undergoes alternative splicing which produces different mRNA species which translates to different tau isoforms. The human brain contains six tau isoforms which differ in their presence or absence of N-terminal (0N, 1N, 2N) and C-terminal (R2) inserts which are encoded by the alternative splicing of the exons E2, E3 and E10 (Figure 1.1). Tau isoforms with exon 10 are called 4R tau as they have 4 repeats and tau isoforms lacking exon 10 are called 3R tau as they have only 3 repeats (lacking R2) (Avila et al., 2004). Exons 2 and 3 encode two N-terminal inserts of tau. Exons 2 and 3 are also alternatively spliced, exon 2 can appear alone, but not exon 3 (Andreadis et al., 1995). There is an additional tau isoform in the peripheral nervous system which is encoded by an extra exon, exon 4a. It is also referred to as "big tau" because of additional 242 residues (Goedert et al., 1992).

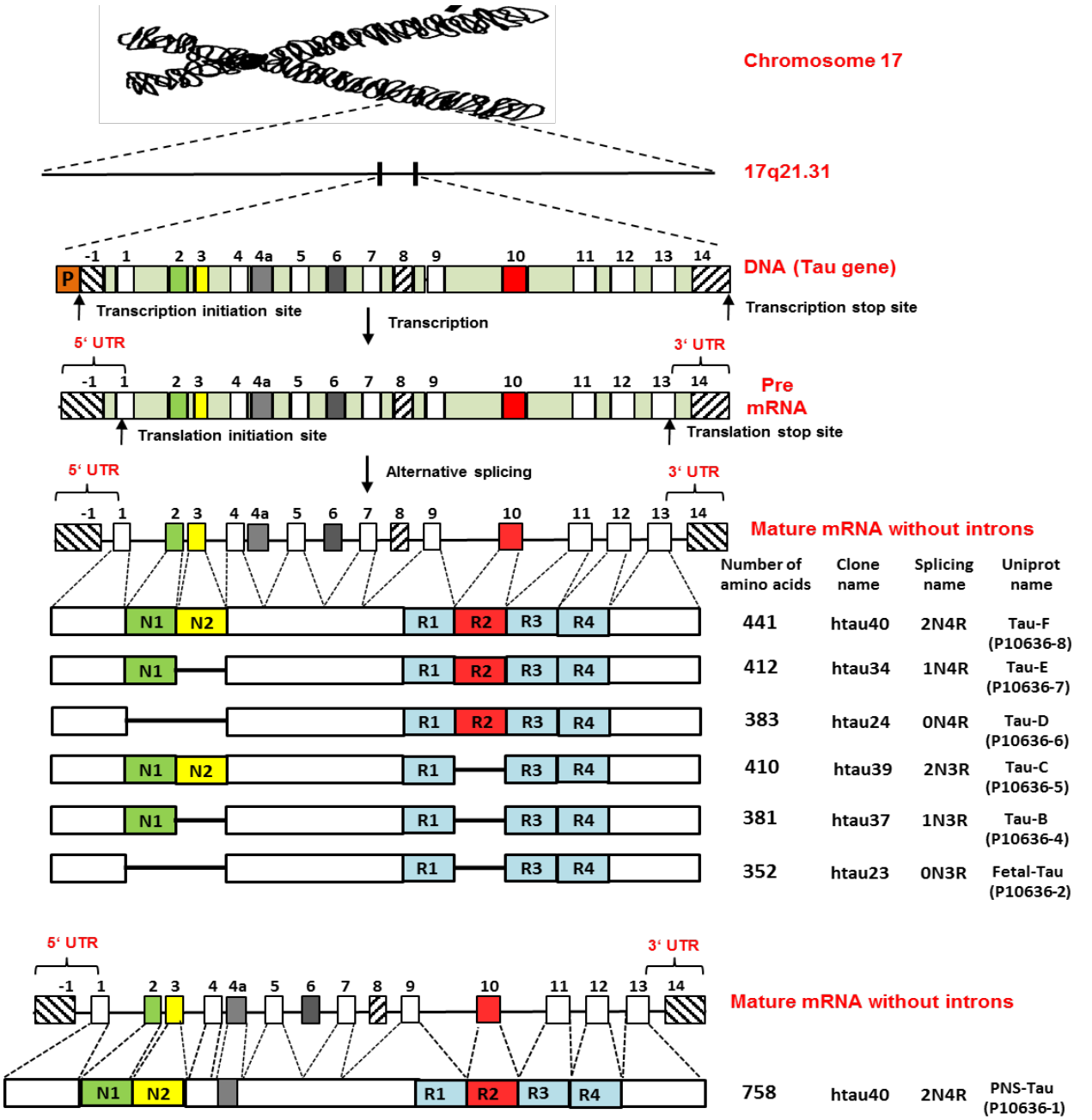


**Figure 1.1: Tau gene and protein organization**

Diagram showing the MAPT gene encoding human tau located on chromosome 17 at position 17q21.31. The tau gene contains 16 exons. The start and stop codons are present in the exon 1 and 13 respectively. The human CNS contains six major tau isoforms which differ in their presence or absence of near N-terminal inserts (1N, 2N) and near-C-terminal (R2) inserts which are encoded by the alternative splicing of the exons E2, E3 and E10 (green, yellow and red). 8 out of 16 exons (E1, E4, E5, E7, E9, E11, E12 and E13) are constitutive. Removal of exons 2, 3, 4a, 6, 8, 10 by alternative splicing results in different protein isoforms (Andreadis, 2005, Andreadis, 2006). Exons 4a, 6 and 8 are not transcribed in CNS. Exons -1 (part of 5' UTR) and 14 (part of 3'UTR) are transcribed but not translated (Lee et al., 2001). In PNS (peripheral nervous system) exon 4a alone or in combination with exon 6 encode a larger tau isoform called big tau. There is no evidence for tau isoforms containing exon 8. Expression of tau isoforms is developmentally regulated. Adult human brain contains six main isoforms and the fetal brain expresses only the shortest isoform. The ratio of 3R and 4R tau are almost equal in adult brain. Figure adapted from (Wang and Mandelkow, 2016).

### 1.3.1 Tau domains

The six main tau isoforms in human brain range from 352-441 residues with the molecular weight (Mr) ranging from 36.7-45.7 kDa but the tau isoforms run on 12% SDS gel show an apparent Mr ranging from 45-65 kDa, as the protein is natively unfolded. Tau protein can be subdivided into various domains, depending on protein interactions and composition (Gustke et al., 1994). Chymotryptic cleavage at Y197 generates a carboxy-terminal fragment which binds to microtubules and promotes their assembly (assembly domain), and an amino-terminal fragment which projects away from the microtubules (projection domain). The N-terminal region is highly charged (acidic region 1-120, basic region 120-150), followed by a proline rich region (residues 150-240, also basic). This is followed by the basic repeat domain (244-368) consisting of 3 or 4 pseudo-repeats of 31 or 32 residues. Residues 369-400 (R' or $5^{th}$ repeat) are followed by the acidic C-terminal tail (residues 401-441) (Gustke et al., 1994). The repeat domain is important for pathological aggregation (notably the hexapeptide motifs at the beginning of R2 and R3 which have a high propensity for β-structure (von Bergen et al., 2000)). The repeat domain plus adjacent flanking domains are required for strong microtubule binding (Mandelkow and Mandelkow, 2012).

### 1.3.2 Tau structure

The primary structure reveals tau as an unusually hydrophilic, highly soluble and natively unfolded protein (Lee et al., 1988). The disordered nature of tau is maintained in the N-terminal and C-terminal domains of tau without contributing to microtubule binding (Jeganathan et al., 2008). Tau belongs to the class of intrinsically disordered proteins with little detectable secondary structure by circular dichroism (CD) and Fourier transform infrared spectroscopy (FT-IR) (Schweers et al., 1994, Mukrasch et al., 2009, von Bergen et al., 2005). Because of this property, tau is resistant to high temperatures and acidic conditions which is used as basis for its preparation *in vitro*. Because of its unfolded structure tau cannot be studied by X-ray crystallography (Fischer et al., 2007) but NMR studies confirm its disordered structure (Mukrasch et al., 2009). Because of its flexibility tau is able to bind to many proteins in the cell. In solution amino and carboxy terminals of tau fold over the repeat domain, forming a "paperclip" -like structure (Jeganathan et al., 2006).

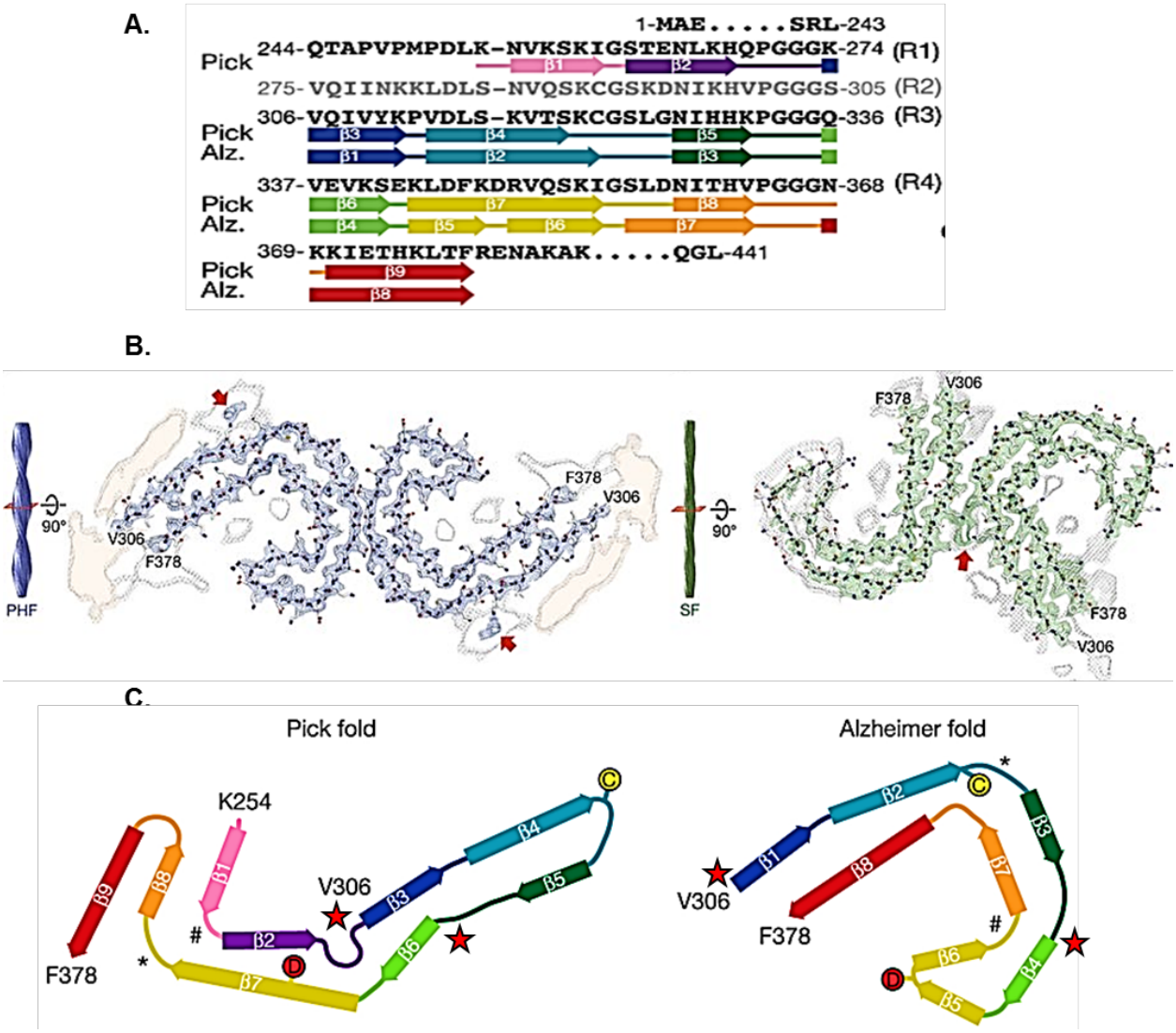


**Figure 1.2: Structure of tau filaments in AD and Pick disease**
**A)** Sequence alignment of the repeat domain (R1-R4) showing the differences in the β-strand regions between the Alzheimer fold (eight β-strands) and Pick fold (nine β-strands). **B)** Cryo-EM structures of tau filaments from AD. Cryo-EM density and atomic models of PHFs (blue) and straight filaments (green). Red arrows indicate additional densities in contact with K317 and K321. **C)** Secondary structure elements in the Pick and Alzheimer folds. The positions of Cys322 (yellow 'C') and Asp348 (red 'D') in the two folds are highlighted. The asterisk and hash symbols mark conserved turns of homologous regions in the Pick and Alzheimer folds. Red stars indicate epitopes of antibody DC8E8 capable of disrupting filament formation and used for developing the AADvac1 vaccine (Kontsekova et al., 2014). The epitopes lie close to the repetitive PGGG motifs at the end of each repeat. Figure adapted from (Falcon et al., 2018, Fitzpatrick et al., 2017).

Recently, partial structures of tau aggregated into paired helical filaments have been solved by cryo-electron microscopy and image reconstruction. They confirm earlier results from spectroscopic and x-ray experiments about the prominence of β-structure in the repeat domain (Figure 1.2). The structures reveal distinct folds in the repeats and differences between disease types (e.g. Alzheimer vs. Pick disease) (Fitzpatrick et al., 2017, Falcon et al., 2018).

### 1.3.3 Cellular functions of tau

A major role of tau or other MAPs is to support the assembly of microtubules. These are involved in diverse cellular functions like cell division, segregation of chromosomes, outgrowth of cell processes, and intracellular transport of vesicles by motor proteins. Tau maintains the dynamic instability of microtubules that allows reorganization of the cytoskeleton (Mandelkow and Mandelkow, 2012). In adult neurons tau is localized mainly in axons where it binds to the outer surface of microtubules. The repeat region of tau (R1-R4) form the core of the microtubule binding region, but strong binding requires additionally the flanking regions N and C-terminal of the repeats. Tau with more repeats (4R) have stronger affinity to microtubules than the tau with less repeats (3R) (Goode et al., 2000, Gustke et al., 1994). The affinity of tau to microtubules can be influenced by post-translational modifications like phosphorylation, acetylation, glycosylation etc. (Martin et al., 2011, Wang and Mandelkow, 2016). Especially the phosphorylation of S262 in R1, phosphorylated by the kinase MARK, decreases the affinity of tau to microtubules strongly (Biernat et al., 1993, Schwalbe et al., 2013).

Tau is also involved in various other functions apart from binding to microtubules. Tau competes with the motor protein dynein and kinesin in binding to the microtubules and decreases the motile fraction of motor proteins and their run length, thereby decreasing the anterograde and retrograde transport (Stamer et al., 2002). Tau interacts with other cytoskeletal fibers, e.g. actin filaments, intermediate filaments and spectrin which may allow microtubules to interconnect with other cellular structures (Cabrales Fontela et al., 2017, Mandelkow and Mandelkow, 2012).

### 1.3.4 Tau aggregation

Although Tau is natively unfolded and highly soluble (>200 µM in cells (Tepper et al., 2014)), it can be induced to aggregate into well-structured fibers in neurodegenerative diseases like AD. The inducers for tau aggregation in vivo are still not well established, but likely candidates are extended polyanions (e.g. RNA, acidic proteins, and heparin) because these are capable of stimulating tau aggregation in vitro (Goedert et al., 1996, Kampers et al., 1996). Consistent with this, the cationic repeat domain of tau forms the core of tau fibers. This domain is also important for the binding of tau to the anionic surface of

microtubules, illustrating that the physiological and pathological roles of tau are encoded in the same domain. PHF formation is facilitated by two hexapeptide motifs with enhanced propensity for β-structure, located in repeat R2 (PHF6*- $^{275}$VQIINK$^{280}$) and in R3 (PHF6- $^{306}$VQIVYK$^{311}$). They play a key role in forming the β-sheet structures necessary for the aggregation process and pathological inclusions (von Bergen et al., 2000, von Bergen et al., 2001, von Bergen et al., 2005). The formation of PHF's can be influenced by many factors like mutations, post-translational modifications and biochemical modifications of tau protein. For instance, sulphated glycosaminoglycan like heparin sulfate compensates the basic charge of tau and thus enables PHF formation. Lipid micelles like arachidonic acid and polyanions like RNA increase tau self-assembly by overcoming the nucleation barrier (Wilson and Binder, 1997, Kampers et al., 1996). Phosphorylation of tau is the major post-translational modification of tau. Because of the protein's disordered structure and multiple potential sites (> 80), many protein kinases can phosphorylate tau (Noble et al., 2013, Stoothoff and Johnson, 2005, Mandelkow and Mandelkow, 2012, Hanger et al., 2009). However, the contribution of phosphorylation to PHF aggregation is still a matter of debate since even highly phosphorylated tau can remain soluble in cells (Tepper et al., 2014). Oxidation of cysteines C291 and C322 (in R2 and R3) to form intra-chain disulfide bridges retards aggregation, whereas inter-molecular bridges (C322-C322) can enhance the aggregation propensity of tau (Schweers et al., 1995).

Mutations in the tau gene are correlated with FTLD disorders, presumably by enhancing the β-propensity of tau and thereby promoting tau aggregation. Since the repeat domain of tau forms the core of the PHFs (Mukrasch et al., 2009), mutations in the repeat domain can induce a strong conformational change in repeat 2 and promote aggregation. FTDP-17 mutants in the repeat domain, like the ΔK280 or P301L, strongly promote the aggregation of tau into PHFs (Barghorn et al., 2000). Indeed, the ΔK280 mutation in the repeat domain construct K18 can promote slow aggregation even without any inducers *in vitro*, illustrating the strong influence of mutations in inducing and accelerating tau aggregation (Barghorn et al., 2000, von Bergen et al., 2001, Kaniyappan et al., 2017). The β-structure in tau has been verified by various biophysical techniques (Mukrasch et al., 2005, Barghorn et al., 2004). Introducing anti-aggregant mutations which prevent β-structure in the hexa-peptide motifs lead to blockage of tau aggregation. This confirms that the formation of β-structure is necessary for tau aggregation (von Bergen et al., 2000).

### 1.3.5 Tau-dependent toxicity

Tau gene mutations reported in FTDP has confirmed the role of tau in neurodegeneration (Spillantini et al., 1998). Various studies suggest the correlative association of tau aggregation with neuronal dysfunction and neurodegeneration (Ramsden et al., 2005, Yoshiyama et al., 2007, Mocanu et al., 2008). Elevated tau levels alone can initiate neuronal dysfunction which is clearly evident in transgenic worm, fly, and mouse models of tau pathology (Andorfer et al., 2005, Sydow et al., 2011, Pir et al., 2016). Regulatable tau transgenic animals and cell models expressing the pro-aggregant repeat domain of human tau ($Tau^{RD\Delta K}$) show pronounced aggregation and cause severe neuronal dysfunction inducing memory deficits (Mocanu et al., 2008, Pickhardt et al., 2017). However, when the expression of pro-aggregant human tau in transgenic mouse models is switched off the tau pathology is reduced and memory is recovered (Sydow et al., 2011). In contrast, introducing two proline mutations (I277P/I308P, breakers of β-structure) in the hexapeptide motifs of R2 and R3 prevents tau aggregation, so that this anti-aggregant mouse model does not show abnormalities (Mocanu et al., 2008). These data suggests that tau aggregation (β-sheet conformation) causes toxicity. In the case of the regulatable transgenic mouse model expressing full length human tau with the pro-aggregant mutation ΔK280 ($hT40^{\Delta K280}$) at a low level (1X endogenous mouse tau) synaptic loss and memory deficits are detectable, but aggregation is slow and reaches only the "pre-aggregate" stage (Eckermann et al., 2007, Van der Jeugd et al., 2012). These data suggest that pre-NFTs or smaller species of tau (oligomers) are likely the toxic species.

Tau oligomers have been reported to cause cell death, synaptic dysfunction and memory deficits when injected into the brains of wild type mice (Lasagna-Reeves et al., 2011). Some tau oligomer preparations have been reported to decrease cell viability and increase phospholipid vesicle leakage in SH-SY5Y cells (Flach et al., 2012). On the contrary, other authors reported that tau oligomers can induce synaptotoxicity without affecting the cell viability (Kaniyappan et al., 2017).These discrepancies may be related to different methods of oligomer preparation and observation of effects. Methods included the preparation of tau oligomers *in vitro* such as cross-seeding with Aβ42 oligomers (Lasagna-Reeves et al., 2010), or oligomerization in the presence of arachidonic acid or heparin (Patterson et al., 2011, Flach et al., 2012). The uncertainty of oligomer preparations from the above reported

preparations is that tau oligomers might not mimic the natural oligomers as they are induced to aggregate in vitro with some inducers like heparin, arachidonic acid micelles and Aβ42 oligomers. In our studies we prepared oligomers using the pro-aggregant tau repeat domain without any inducers (Kaniyappan et al., 2017) in order to mimic the oligomers in disease conditions. Because of the toxic properties of tau oligomers, they can be potential targets for therapeutic studies. Small drug molecules or antibodies can be designed to counteract the toxicity caused by tau oligomers.

## 1.4 Approaches to disease modifying therapies

AD is the most common form of dementia, affecting worldwide around 36 million people currently and expected 96 million people by 2050 (Reitz and Mayeux, 2014). AD is characterized by the presence of extracellular plaques composed of Aβ and intracellular tangles of tau. Disease modifying therapy is an intervention in the clinical progression of the disease by interfering with the pathophysiological mechanisms of the disease leading to cell death (Cummings and Fox, 2017). In AD, the disease progression could be retarded by blocking the pathogenic process like aggregation of Aβ or tau, inflammation, oxidative damage, cholesterol metabolism, and others. Several therapies have been tried with the aim of targeting Aβ pathology (Liu et al., 2018, Honig et al., 2018), but so far they have failed to show significant benefits in clinical trials (Nelson et al., 2012). Therefore therapies targeting tau pathology have gained importance, especially as cognitive decline in AD correlates better with tau pathology than with amyloid burden (Huber et al., 2018, Reas, 2017). Disease modifying therapies targeting tau pathology could include the interference with tau aggregation by aggregation inhibitor drugs, reduction of tau levels by drugs or antisense oligonucleotides, gene therapy targeting tau gene, active/passive immunization to neutralize toxic tau species, and others. A brief summary of different therapies that have been explored for tau pathology in animal models are presented below.

### 1.4.1 Therapies targeting kinases

Tau becomes "hyperphosphorylated" at several sites in AD, and it is assumed that hyperphosphorylated tau has a weaker affinity to microtubules and greater propensity to aggregate and form NFTs (Avila, 2006). This provides the rationale for down-regulating kinases which phosphorylate tau or upregulate phosphatases. Tested kinases include

GSK3β, CDK5, p38, MARK, PKA etc. (Mandelkow and Mandelkow, 2012, Tell and Hilgeroth, 2013). GSK3β is increased (Pei et al., 1997) and co-localized with NFTs in AD brain (Leroy et al., 2007). Lithium inhibits GSK3β and reduces tau pathology in transgenic mice (Engel et al., 2006). However, treatment of patients with mild AD did not show any improvement in cognitive performance (Hampel et al., 2009). Another GSK3β inhibitor (SB-216763) was shown to decrease phospo-tau in mice, but had toxic effects (Boutajangout and Wisniewski, 2014). Another example is the microtubule-affinity regulating kinase (MARK) which phosphorylates tau at S262 (KXGS motif) and decreases the affinity of tau to microtubules (Biernat et al., 1993, Drewes et al., 1997). Our group showed four low-molecular weight anti-MARK2 compounds (30019, 30195, 30197, 30199) sharing a common 9-OXO-9H-acridin-10-yl functional group which inhibited the MARK2-mediated hyperphosphorylation of tau (Timm et al., 2011). Overall, the interest in kinase inhibitors to combat AD has waned since positive effects observed in transgenic animals have not been reproduced in patients, and since interference with the network of kinases may lead to unpredictable results.

### 1.4.2 Therapies targeting inhibition of tau aggregation

As tau aggregates in a pathological manner in AD, combating tau pathology would be expected to be beneficial. A number of potential drugs to inhibit the aggregation of tau *in vitro* and in cell or animal models have been described (Pickhardt et al., 2005, Bulic et al., 2013). The phenothiazine compound methylene blue, which penetrates the blood brain barrier (BBB), has been shown to inhibit tau aggregation *in vitro* and in animals (Wischik et al., 1996, Hochgrafe et al., 2015). However, despite extensive efforts, this and related compounds (LMTX) have failed in human trials (Gauthier et al., 2016). Rhodanine based inhibitor bb14 inhibits tau aggregation *in vitro* and in organotypic hippocampal slice cultures (OHSCs) expressing pro-aggregant tau (Pickhardt et al., 2015, Messing et al., 2013). The phenylthiazolylhydrazide based inhibitor BSc3094 is effective in reducing aggregation in N2a cells expressing pro-aggregant tau and also in worms (Pickhardt et al., 2007b, Fatouros et al., 2012). A naturally occurring compound curcumin reduces tau aggregation by binding to β-sheet conformation (Rane et al., 2017). In animal models curcumin decreases both tau and Aβ pathology and ameliorates behavioral and synaptic deficits (Ma et al., 2013, Shytle et al., 2012). The antioxidant and anti-inflammatory properties of

curcumin, as well as its safety in humans, make it an attractive candidate for clinical development. It is currently under clinical trial phase II (Congdon and Sigurdsson, 2018).

### 1.4.3 Therapies targeting clearance of tau aggregates

Another approach directed at tau pathology is to enhance the degradation of polymerized tau. As a fact, heat shock protein 90 (HSP 90) is involved in re-folding of the denatured proteins for their degradation. In case of tau, HSP 90 fails to regulate tau protein and prevents tau from degradation (Blair et al., 2014). EC102, an Hsp90 inhibitor promoted selective decrease of phospho-tau species in a transgenic mouse model of AD (Dickey et al., 2007). Similarly, the antibiotic Geldanamycin (GA) inhibits HSP90 and reduces phospho-tau levels, although with a high degree of toxicity (Blair et al., 2014). Another HSP90 inhibitor, 17-(allylamino)-17-demethoxygeldanamycin (17-AAG) decreases NFTs in a mouse model of tauopathy. This compound has already been in clinical studies for cancer treatment (Ho et al., 2013). The co-chaperone Aha1 enhances the HSP90 ATPase activity and dramatically increases tau aggregation. Accordingly, the Aha1 inhibitor KU-177 reduces the accumulation of insoluble tau (Shelton et al., 2017).

## 1.5 Tau immunotherapy

Treatments aimed at reducing amyloid-β or tau pathology (aggregation inhibition) appeared to be promising in animal models (Hosokawa et al., 2012, Lai and McLaurin, 2012) but they failed in clinical trials (Medina, 2018, Panza et al., 2014). Immunotherapy targeting Aβ were also unsuccessful in clinical trials. Therefore tau based immunotherapies are expected to be positive and are currently in clinical trials. Since this is early days for tau immunotherapies, more antibodies with different targets and properties are needed (Hung and Fu, 2017, Nisbet and Gotz, 2018). Recent research focused on investigating new treatment strategies promoting the immunological clearance of tau pathology, which employs active and passive immunization against pathological tau.

### 1.5.1 Active immunization

Active tau immunotherapy involves eliciting an immune response against tau protein as immunogen to generate specific antibodies capable of binding and then reducing or

clearing pathological tau to ameliorate overall neuronal function. The choice of the epitope on tau is crucial for the success of tau immunotherapy (Pedersen and Sigurdsson, 2015). AADvac1 is an active immunogen containing the tau sequence 294-305 including a PGGG motif that occurs repetitively just upstream of the hexapeptide motifs that promote beta structure during aggregation. This tau sequence had been identified because it was targeted by a monoclonal antibody (DC8E8) capable of disrupting tau aggregation (Kontsekova et al., 2014). Hence the synthetic tau peptide was coupled to keyhole limpet hemocyanine (KLH) and aluminum hydroxide (adjuvant) to be used as a vaccine (Axon Neuroscience, Bratislava, Slovakia). Vaccine treated transgenic animals showed reduced tau oligomerization, phosphorylation and improved sensorimotor functions. This treatment did not show any adverse effects and it displayed a favorable safety and tolerability profile in all toxicology studies (Kontsekova et al., 2014). AADvac1 was the first anti-tau vaccine to enter human trial phase 1. Phase 2 clinical studies started for AADvac1, which includes cognitive and clinical assessments with exploratory outcomes of CSF biomarkers (Medina, 2018, Novak et al., 2017).

During the events leading to neurofibrillary pathology, tau undergoes numerous post-translational modifications such as phosphorylation, truncation, glycosylation and ubiquitination (Martin et al., 2011). Phospho-tau as an epitope has received the most attention for both active and passive immunotherapy. ACI-35 is a liposomal active vaccine with the adjuvant monophosphoryl lipid A (MPLA) developed by AC Immune (Lausanne, Switzerland). It is a palmitoylated phospho-tau synthetic peptide which has 16-amino acids corresponding to human tau sequence 393–408, with phosphorylated residues S396 and S404, which become hyperphosphorylated in AD and form the basis of the diagnostic antibody PHF-1 (Greenberg et al., 1992). In a T-cell independent immune response the immunogen elicits very specific tau antibodies in tau P301L mice, resulting in reduced phospho-tau aggregates, less tangled neurons in the brain, improvement in cognitive behavior and prolonged survival of ageing in tau P301L mice. These beneficial effects were not associated with any adverse inflammatory response or neurological side-effects, which suggest a good safety profile for human studies. ACI-35 (Trial ID- ISRCTN13033912) is currently under clinical trial phase 1b (Medina, 2018, Theunis et al., 2013).

Several other active immunization studies were performed. The tau peptide with residues 417-427 containing pSer422 was tested in THY-Tau22 transgenic mice. The immunized mice showed a reduction in tau pathology which correlated with improved performance on spatial memory (Troquier et al., 2012). In another study, active immunization of transgenic mice expressing tau-P301L with a tau peptide containing residues 379-408 (including pS396 and pS404) showed a reduction in tau pathology and improved sensorimotor tasks compared to controls. The generated anti-tau antibodies were able to cross the blood brain barrier and reduce tau pathology by binding to phosphorylated tau without showing any adverse effects (Asuni et al., 2007). One caveat is that autoimmune reactions are a threat associated with active immunotherapy. Hence there is a need for more elaborate preclinical assessment of safety before clinical trials can be performed (Theunis et al., 2013).

### 1.5.2 Passive immunization

In passive immunotherapy, antibodies raised against tau (as antigen) are used to attenuate tau pathology. Several anti-tau antibodies are currently under preclinical and clinical studies for treatment of AD and other tauopathies. The Holtzman lab generated two series of antibodies against human and mouse tau (Yanamandra et al., 2013). Antibodies HJ9.3 and HJ9.4 detect residues 306-320 and 7-13 respectively in both human and mouse tau whereas antibody HJ8.5 (ABBV-8E12) detects residues 25-30 and binds specifically to human tau. Antibody HJ8.5 was able to inhibit the transfer of pathology in a trans-cellular propagation assay. Chronic intracerebroventricular (ICV) injection of antibodies in P301S mice showed a prominent decrease in hyperphosphorylated tau and reversal of behaviour deficits in the contextual fear conditioning test (Yanamandra et al., 2013). Phase 1 studies showed an acceptable safety and tolerability profile of single doses of ABBV-8E12 (West et al., 2017). A phase 2 trial on PSP subjects is still ongoing (Budur et al., 2017).

Antibodies developed against phosphorylated tau have also been explored in pre-clinical experiments. The efficacy of tau based immunotherapy has been tested by injecting the phospho-tau specific PHF1 antibody (pS396 and pS404) intraperitoneally in the JNPL3 mouse model which prevented the tau pathology and functional impairments (Boutajangout et al., 2011). Similar studies were done with antibodies against PHF1 and MC1 epitopes in two other mouse models (JNPL3 and P301S). Passive immunization of these two

antibodies showed the prevention of tau pathology as well as a reduction of neurofilament positive axonal spheroids in the spinal cord with an improvement in locomotor activity. Despite the fact that both antibodies (PHF1 and MC1) have different epitopes they yielded similar phenotypic improvement (Chai et al., 2011).

Passive tau immunotherapy not only enables recovery of animals from tau pathology but also retards Aβ pathology in some AD models of tau + Aβ pathology. Anti-tau antibodies 4E6 (raised against residues 6-18 of tau) and 77E9 (against residues 184-195) raised against the N-terminal domain of tau injected in 3XTg AD mice showed reduced levels of total tau and hyperphosphorylated tau with improved cognitive performance. Antibody treated animals also showed a decreased amyloid precursor protein (APP) and amyloid plaques (Dai et al., 2015, Dai et al., 2017).

One study clearly highlighted the choice of antigen used to generate therapeutic antibodies. A comparative study of the efficacy of pan tau antibody with two phospho-tau (pS404) specific antibodies with similar affinity but different isotypes (IgG1/k and igG2a/k) showed differences in their efficacy (Ittner et al., 2015). A reduction in tau-positive neurofibrillary inclusions and pS422-positive tau was observed in the mice treated with the IgG2a/k pS404 antibody. A trend towards reduction of pS422-positive tau was observed with the IgG1/k pS404 antibody, whereas no reduction was observed in the pan-tau antibody-treated mice. This study suggests that the activity of antibodies is dependent on the isotype and specificity of the antibody (Ittner et al., 2015). Thus there is a need for careful consideration of antibody design, affinity, specificity and efficacy for immunotherapy.

Some antibodies were raised against certain oligomeric species of tau (T22, TOMA-tau oligomeric monoclonal antibody, both oligomer specific conformation dependent antibodies), or TOC1-tau oligomeric complex 1 (recognizing tau oligomers at residues 209-224) (Lasagna-Reeves et al., 2012, Castillo-Carranza et al., 2014b, Ward et al., 2013) which show strong affinity to tau oligomers without binding to monomers or polymers of tau. Treatment of tau tg-mice with TOMA antibody resulted in lower cognitive and behavioral deficits compared with un-treated animals. There is a need for further characterization of these antibodies regarding their specificities as the specificity of T22/TOMA antibody is still a matter of debate.

All the approaches of tau-directed therapy mentioned above are currently in late-stage pre-clinical development and likely to enter clinical trials in the near future. Other promising tau immunotherapies are actively being studied, but it is not yet clear if those will be used in clinical trials (Pedersen and Sigurdsson, 2015).

Although immunotherapy for AD is gaining popularity, there are certain pros and cons associated with the applications of active and passive immuninzations. Active immunotherapy is long lasting and cost-effective but the success of the therapy depends on the host immune system (which may be compromised in older animals). In passive immunization, the injected immunoglobulins provide immediate immunity which are pharmacologically controlled. However the efficacy of passive antibody therapies is limited by the half-life time of the immunoglobulins, resulting in the need for regular reinjections and enormous costs. One great advantage of passive immunotherapy is that it can be discontinued at any point of time unlike active immunization. These factors should also be taken into consideration for a successful immunotherapy (Jensen-Jarolim and Singer, 2011).

## 1.6 Aims of the study

Tau aggregation is known to correlate well with the disease progression in AD (Braak and Braak, 1991b, Braak and Del Tredici, 2016). Inhibiting tau aggregation might overcome the tau induced pathology in AD. Cell and animal models expressing pro-aggregant forms of tau display AD-like tau pathology, whereas anti-aggregant forms do not (Khlistunova et al., 2006, Sydow et al., 2011). Moreover, the toxicity of tau appears to reside in the early oligomeric forms of tau (Kaniyappan et al., 2017). Therefore the aim of the current study is to develop novel antibodies against toxic species and conformations (low-n oligomers) of $Tau^{RD\Delta K}$ which can be of therapeutic application for diagnosis or treatment (passive immunotherapy) of transgenic animal models, with the aim of future applications to human patients.

**The current study addresses the following questions:**

1. Generation of antibodies against toxic species of tau (antigen) and screening them for inhibition of tau aggregation.
2. Determination of the specificity and affinity of the antibodies against low-n oligomers of tau.
3. Characterization of antibodies (in terms of their specificity and stability) that can block tau aggregation to a high degree (>90%) *in vitro* and *ex vivo*.
4. Characterization of the ability of antibodies to neutralize the tau induced toxic effects in an N2a cell model of tauopathy.
5. Analysis of the mechanism of antibody-mediated inhibition of tau-aggregation in N2a cell model of tauopathy.

# 2 Materials and Methods

## 2.1 Materials (instruments & equipment)

### 2.1.1 Centrifuges

| Name | Company |
|---|---|
| Eppendorf centrifuge 5415C | Eppendorf, Hamburg |
| Eppendorf centrifuge 5810R | Eppendorf, Hamburg |
| Eppendorf centrifuge 5810 | Eppendorf, Hamburg |
| Optima$^{TM}$ LE-80K Ultracentrifuge | Beckman Coulter, München |
| Avanti$^{R}$Centrifuge J-26 XP | Beckman Coulter, München |
| Optima$^{TM}$ Max Ultracentrifuge | Beckman Coulter, München |

### 2.1.2 HPLC

| Name | Company |
|---|---|
| Äkta explorer100 | GE Healthcare Life Sciences, Freiburg |

### 2.1.3 Columns

| Name | Company |
|---|---|
| Superdex G200 HR 16/60 | Amersham Biosciences, Freiburg |
| SP Sepharose 16/10 | Amersham Biosciences, Freiburg |
| HiPrep Butyl FF 16/10 | GE Healthcare Life Sciences, Freiburg |
| NAP5 column | Pharmacia Biotech, USA |
| PD 10 column | Pharmacia Biotech, USA |

### 2.1.4 Spectrophotometers

| Name | Company |
|---|---|
| Ultrospec 3100 *pro* | Amersham Biosciences, Freiburg |
| Tecan Spectrophotometer | Lab System, Frankfurt |
| Dynamic Light Scattering Nano S | MALVERN, Germany |

### 2.1.5 Microscopes

| Name | Company |
|---|---|
| Atomic Force Microscope (Nanowizard 3) | JPK instruments, Germany |
| LSM 700 Confocal Microscope | Zeiss, Germany |

### 2.1.6 Cell culture equipment

| Name | Company |
|---|---|
| HERA Safe Laminar air flow | Heraeus Instruments, Germany |
| HERA Cell 240 $CO_2$Incubator | Heraeus Instruments, Germany |
| Neubauer chamber | MARIENFELD, Germany |

### 2.1.7 Others

| Name | Company |
|---|---|
| French Press | G-Heinemann Ultraschall und Labortechnik, Germany |
| Ice flaking machine (SPR 80) | Nord Cap, Germany |
| Water filtration apparatus | Millipore, Germany |
| Deep freezer (-80°C) | SANYO, USA |
| Image Quant LAS 4000 mini | GE Healthcare Life Sciences, Freiburg |
| Blotting Apparatus | BIO-RAD trans-blot SD transfer cell |
| Gel apparatus for SDS-PAGE | SE 250, Hoefer, USA |
| Electrophoresis power supply | Pharmacia Biotech, USA |
| Micropipettes (2, 10, 20, 100, 200 and 1000µl) | GILSON, Austria |
| Weighing balance BP 310S | Sartorius, Germany |
| Incubators | Memmert, Germany |
| Incubator with shaker | INFORS HT Multitron, Switzerland |
| Heating-agitator | Eppendorf, Germany |

| | |
|---|---|
| Incubator with rotator | Shake and Stack, HYBAID, Germany |
| Laminar flow for bacterial inoculation | LaminAir HB 2448, Heraeus Instruments, Germany |
| pH-Meter | Schott Instruments, Germany |
| Water bath | GFL AND JULABO UC, Germany |
| Vortexer | JANKE & KUNKEL. IKA-WERK, Germany |
| Pasteur pipette | Assistant, UK |
| well plates (6,12,24,48, and 96) | Corning, Germany |
| SNL 10 cantilever | Bruker, München |
| Glass wares | VWR international, UK |
| PVDF membrane (0.45µm pore size), | Millipore, Germany |
| Quartz microcuvettes | Hellma, Muhlheim, Germany |
| Magnetic steel disks (diameter 12mm) | Ted Pella, Inc., Redding, CA, USA |
| Teflon sheets (0.2 mm thickness) | Maag Technic AG, Birsfelden, Switzerland |
| Mica sheets | Muscovite, Kolkata, India |
| Cantilever (Si3N4) | Di-Veeco, Santa Barbara, California, USA |

## 2.2 Methods

### 2.2.1 Molecular biology

#### 2.2.1.1 Plasmid DNA isolation

Plasmid DNA was transformed into DH5α competent cells using the heat shock method. Positive colonies were inoculated for the starter culture and further transferred to 100 ml LB medium containing respective antibiotic and cultured overnight at 37°C with agitation at 180 rpm. Plasmid DNA was isolated using the Endofree maxi-kit QIAGEN according to the manufacturer protocol. The quality of DNA was estimated by

running an agarose gel electrophoresis and the quantity of DNA was estimated using NanoDrop spectrophotometer (Peqlab ND-1000).

### 2.2.1.2 Polymerase chain reaction (PCR)

Click beetle luciferase complementation fragments were generated using the pCBG99 plasmid (Promega). Primer designing was carried out using SnapGene 4.0 software. PCR amplification of N-terminal (aa 2-413) and C-terminal (aa 395-542) of pCBG99 was performed to split the whole gene in to two parts using the following primers.

**N-terminus forward primer:**

5' CCCGGGATCCACCGGTGGTGAAGCGTGAGAAAAATGTCATCTATGGC 3'

**N-terminus reverse primer:**

5' TCTAGAGTCGCGGCCGCCTAGCCGTCGTCGTCGATGGC 3'

**C-terminus forward primer**

5' CCCGGGATCCACCGGTGAGCAAGGGTTATGTCAATAACGTTGAAG 3'

**C-terminus reverse primer**

5' TCTAGAGTCGCGGCCGCCTAACCGCCGGCCTT 3'

**PCR reaction mixture:**

| | |
|---|---|
| ds DNA template | 20 ng (10 ng/µl) |
| Forward primer | 400 nM |
| Reverse primer | 400 nM |
| PCR-grade $H_20$ | 15 µl |
| PWO master mix | 25 µl |
| Total volume | 50 µl |

**PCR program**

| Heat lid to 105°C | | | |
|---|---|---|---|
| **Step** | **Condition** | **Temperature** | **Time** |
| 1. | Initial denaturation | 94°C | 2 min |
| 2. | Denaturation | 94°C | 1 min |
| 3. | Annealing | 60°C | 1 min |
| 4. | Elongation | 72°C | 1 min |
| Repeat step 3-4 for 30 cycles | | | |
| 5. | Final elongation | 72°C | 10 min |
| 6. | Hold | 4°C | Until required. |

#### 2.2.1.3 Restriction endonuclease digestion

5 µg of plasmid DNA or 2 µg of PCR amplified products was mixed with 2 units of restriction enzymes and 5 µl of 10X fast digest green buffer (Thermo Fisher) and the reaction mixture was incubated at 37°C for 15 min. Restriction digestion of DNA was analyzed by 1% agarose gel electrophoresis.

#### 2.2.1.4 DNA isolation from agarose gels

PCR amplified products or restriction digestion products run on an agarose gel were excised under UV light by using a clean scalpel. Excised products were purified from the agarose gel by using the NucleoSpin gel and PCR clean-up kit (Macherey-Nagel, Germany) according to the manufacturer's instructions.

#### 2.2.1.5 Agarose gel electrophoresis

0.8-1% agarose gel (depending on the size of the DNA) was prepared in 1x TAE buffer. 5 µl of DNA ladder (Smart ladder, Eurogentec) and DNA samples were loaded on the gel. Horizontal gel electrophoresis was performed by using Tris-acetate (TAE) buffer at 80 mA for 30-60 min. Detection of DNA was performed by staining the agarose gel in EtBr (Ethidium Bromide) solution (4 µg/ml in $H_2O$) for 20 min followed by detection using BioDocAnalyze (Biometra).

#### 2.2.1.6 Ligation

Ligation of the restriction digestion products was carried out by using the DNA quick ligase (NEB). The ligation mix contained 50 ng of vector DNA fragment, 3-fold molar excess of insert DNA fragment, 1 µl of T4 DNA Ligase, 5 µl 2X ligase buffer and 0.1 µl 100X BSA with final volume of 10 µl adjusted with elution buffer. Ligation mixture was incubated at RT for 5 min.

#### 2.2.1.7 Transformation

10 µl of ligation product was added to 1 vial of One Shot TOP10 chemically competent *E. coli* (*In vitro*gen, C4040) cells and incubated on ice for 30 min. Heat shock treatment was given by incubating the cells at 42°C for 50 sec and immediately transferring them to ice for 10 min. In the next step 200 µl of autoclaved LB medium were added to the cells and incubated at 37°C with shaking at 180 rpm for 1 h. Finally 150 µl of the cells were inoculated on LB-medium plates containing 50 µg/ml Kanamycin antibiotic (LBK) and incubated overnight at 37°C.

#### 2.2.1.8 Screening for positive colonies

Positive colonies (10-20 isolated colonies) were picked and colony PCR was done for the selected colonies. 4-5 positive colonies (after gel detection) were inoculated separately in 5 ml of LB medium containing Kanamycin (50 µg/ml) and incubated with shaking at 180 rpm at 37°C overnight. From the positive clones, plasmid DNA was purified using Qiagen Endofree mini plasmid DNA preparation kit (Qiagen, Germany) according to the manufacturer's instructions and the presence of gene of interest was confirmed by restriction digestion that yielded the desired size of the product on the agarose gel. Plasmids from positive clones were sequenced by Microsynth Seqlab, Germany.

#### 2.2.1.9 DNA quantification

The concentration of the DNA was determined by NanoDrop spectrophotometer (Peqlab ND-1000). Absorbance at 260 nm was used to calculate the concentration of nucleic acids. Elution buffer was used as buffer blank.

### 2.2.2 Biochemistry

#### 2.2.2.1 Protein preparation and purification

For pre-culture or starter culture, 100 ml of LB broth was prepared and autoclaved. Carbenicillin (50 µg/ml) was added before the inoculation of the glycerol stock of different tau constructs in pNG2 plasmid. This pre-culture was grown in a shaking incubator at 37°C with 180 rpm overnight. 2 liters of autoclaved "terrific broth"

containing Ampicillin (100 mg/l) was inoculated with 100 ml of pre-culture. Before inoculation, 2 ml of terrific broth were removed for optical density (OD) measurement as 0-time point control. The inoculated culture was grown at 37°C with 180 rpm rotation until the OD reached a minimum of 0.8 (approximately 4 h) as determined by spectrophotometer at 600 nm (Ultrospec 3100 pro, Amersham Biosciences, Freiburg). 0.4 mM of IPTG was added to the culture and incubated at 37°C with 180 rpm for 3 h. The culture was pelleted by centrifuging at 7000 rpm for 12 min in JLA-8.1000 rotor (AvantiRCentrifuge J-26 XP, Beckman Coulter, München). The pellet was collected in 90 ml of resuspension buffer and homogenized at 4°C by magnetic stirring (at this stage the cells can be frozen for future usage. Defrosting/thawing the cells should be done slowly in water at RT). The bacteria from the resuspended pellet were crushed twice using a French press to completely break down the cell wall, DNA, and other cell components. The bacteria lysates were collected in 50ml Falcon tubes. NaCl and DTT were added at a final concentration of 500mM and 5mM respectively. The samples were mixed well and boiled at 97°C for 20 min followed by centrifugation at 40,000 rpm (Ti 45 rotor), for 1 h at 4°C (OptimaTM LE-80K Ultracentrifuge, Beckman Coulter, München). The supernatant was collected and dialyzed with a 45 kDa MWCO membrane. The supernatant was dialyzed at 4°C twice in Mono S A buffer with an exchange of buffer after 2 h and second round of dialysis was done overnight. (Note: The volume of dialysis buffer should be at least 10 times higher than the sample volume). The dialyzed sample was centrifuged in a Ti 45 rotor at 40,000 rpm, for 1 h at 4°C. After centrifugation, the supernatant was transferred to the 150ml super loop and the protein purification was done by anion exchange chromatography using Äkta Explorer100 (GE Healthcare Life Sciences, Freiburg) system fitted with an SP Sepharose 16/10 column (Amersham Biosciences, Freiburg). The column was equilibrated prior to sample injection with 5 column volumes (CV) of Mono S A buffer. Once the sample was injected, the purified protein was eluted with Mono S A and Mono S B buffer in a gradient system (Mono S B 60% gradient for 5CV and 100% gradient for 1CV). The column was cleaned with Mono S B buffer for 4CV. The purified protein was collected in 2 ml fractions. The fractions were analyzed on a 10 or 17% SDS gel and stained with coomassie Blue. The protein containing fractions were pooled and concentrated using 3 kDa MWCO centrifugal filters (Amicon Ultra, Millipore, Ireland). Then the protein was further purified by gel filtration chromatography using a Superdex

G200 column for full length tau protein or Superdex G75 column for repeat domain tau protein with PBS pH 7.4, 1mM DTT as a mobile phase. The eluted protein was concentrated using 3 kDa MWCO amicon filters and then the protein concentration was measured using the BCA method.

#### 2.2.2.2 Protein quantification assay (BCA)

Quantification of proteins was carried out by BCA method (BCA protein assay reagent, Sigma). Using known concentrations (20-200 µg/ml) of BSA a standard curve was prepared and the concentration of unknown protein was determined by plotting against known BSA concentration. BSA and other protein samples were diluted in 50µl of $H_2O$ and mixed with 1 ml of reagent mixture consisting of 20 µl copper (II) sulfate [4% (w/v) (Sigma)] and 1 ml of bicinchoninic acid solution (Sigma). Samples were incubated at 60°C for 30 min and the absorption was measured at 562 nm using spectrophotometer (Ultrospec 3100 Pro Pharmachia Biotech). For the blank reference, $H_2O$ was used instead of the protein solution.

#### 2.2.2.3 Polymerization of tau protein into filaments

To prepare filaments, different tau constructs ($Tau^{RD\Delta K}$, $Tau^{FL\Delta K}$, $hT40^{WT}$) were diluted to 50 µM in BES buffer pH 7.0 with 1 mM DTT and heated at 95°C for 15 min, then the samples were cooled down to RT. 12.5 µM of heparin 16,000 was added to the samples and incubated at 37°C for 120 h. After 120 h the formation of filaments was assessed by ThS fluorescence and AFM.

#### 2.2.2.4 Dot blotting

Immobilon-P membrane (Millipore) was activated by soaking it in methanol for 1 min and then washed 3 times with doubly distilled water and 1 time with PBS buffer. PBS buffer soaked Whatman filter paper was arranged on dot blot apparatus and on top of it activated PVDF membrane was layered. The membrane was washed thrice with 100 µl of PBS and then 25 µl of 2 ng/µl protein in PBS buffer was loaded on the membrane and the buffer was imbibed using vacuum pump, during which the protein was retained on the PVDF membrane. The membrane was washed once more with 200 µl of PBS buffer. Then the membrane was blocked in 5% fat dry milk powder in

1X TBST (containing 0.01% Tween 20) for 1 h at room temperature on an orbital shaker. Later the membrane was incubated with primary antibody in 1X TBST at 4°C overnight on an orbital shaker or on a rotator and then the unbound or loosely bound antibody was washed away by washing the membrane with 1X TBST (3 times, 10 min each). The membrane was incubated in HRP labelled secondary antibody (1X TBST) at 37°C for 1 h on a rotator and the unbound antibody was washed away with 1X TBST buffer (3 times, 10min each). Membrane was developed using ECL reagent and the images were acquired using LAS ImageQuant (GE Healthcare).

#### 2.2.2.5 SDS-Polyacrylamide gel electrophoresis (SDS-PAGE)

SDS gels consisted of 4% acrylamide stacking gel and 10% or 17% acrylamide resolving gel. Protein samples were mixed with 5X SDS sample buffer and heated at 95°C for 10 min. The electrophoresis was carried out at constant 120V for 2 h at RT in SDS running buffer. The gels were stained with silver stain or transferred on to a PVDF membrane for immunoblotting.

#### 2.2.2.6 Western blotting

Recombinant protein and brain homogenates of transgenic animals or cell lysates were diluted in 5X SDS buffer with β-mercaptoethanol and heated at 95°C for 15 min before resolving. 50 ng of recombinant protein or 15 µg of brain lysates or 10 µg of whole cell lysate was resolved on 10% or 17% SDS- polyacrylamide gel. Then the SDS gels were incubated in 1X transfer buffer for 20 min on an orbital shaker at room temperature. Immobilon-P membrane (Millipore) was activated by soaking it in methanol for 1 min and then washed in transfer buffer. 3 pieces of wet Whatman filter papers are stacked on a transfer apparatus with the activated PVDF membrane, SDS gel and 3 wet Whatman filter papers are piled in sequence from bottom to top. The transfer of protein from SDS gel to PVDF membrane was initiated by applying 100 mA (1.5 mA per $cm^2$) for 2 h. The transfer was confirmed by prestained marker on the membrane. Then the membrane was blocked in 5% fat dry milk powder in 1X TBST for 1 h at room temperature on an orbital shaker. Later the membrane was incubated in primary antibody (1X TBST) at 4°C overnight on an orbital shaker and then the unbound or loosely bound antibody was washed away by washing the membrane with 1X TBST

(3 times, 10 min each). The membrane was incubated in HRP labelled secondary antibody (1X TBST) at 37°C for 1 h on a rotator and the unbound antibody was washed away with 1X TBST buffer (3 times, 10 min each). The membrane was developed using ECL reagent and the images were documented using LAS ImageQuant (GE Healthcare).

#### 2.2.2.7 Silver staining

After resolving the desired protein on SDS gel, the gel was incubated in a fixative solution for 15 min followed by cross-linking solution for 30 min or overnight. Then the gel was washed with doubly distilled water (3 times, 10 min each). The gel was incubated in silver nitrate staining solution for 20 min and then washed with doubly distilled water for 30 seconds. Then the gel was incubated in the developing solution until the protein was visible on the gel .Then the developing solution was immediately discarded and stopping reagent was added to prevent further development of the gel. All steps were carried out at room temperature and on an orbital shaker.

#### 2.2.2.8 Enzyme-linked immunosorbent assay (ELISA)

96-well plates were coated with 250 ng/well of recombinant tau protein dissolved in 0.05 M sodium bicarbonate, pH 9.6 as coating buffer and incubated at 4°C overnight. Plates were washed with 1X TBST (3 times, 10 min each), followed by blocking with 5% BSA in TBST for 2 h at room temperature. Primary antibodies (tissue culture supernatant) of interest (1:10) diluted in 5% BSA were incubated at 4°C, overnight. Plates were washed with 1X TBST (3 times, 10 min each), followed by incubating the plates with anti- rat or anti- mouse HRP conjugated secondary antibodies (1:1000) diluted in blocking solution, for 1 h at 37°C. . Finally, plates were washed with 1XTBST (3 times, 10 min each) and incubated with 100 µl of 3,3,5,5-tetramethylbenzidine (TMB liquid substrate; SIGMA) for 1 h in darkness. Then the reaction was stopped with 100 µl of 2 M HCl. Absorbance was read at 450 nm in TECAN spectrofluorimeter (Ascent, Lab systems, Frankfurt).

#### 2.2.2.9 Immunolabeling of an antibody

Monoclonal antibody was concentrated using 3000 MWT amicon filters (Millipore) in centrifuge (Eppendorf 5810R) at 2770 rpm, 4°C to achieve the final concentrations of 50-100 µM. 10X excess molar concentrations of TCEP (tris-(2-carboxyethyl) phosphine, Molecular Probes) to antibody was added and incubated on ice for 30 min, whereupon 11.85X excess molar concentrations of Alexa 647 dye (ThermoFischer, USA) was dissolved in DMSO, added and incubated on ice for 30min. NAP-5 column (GE-healthcare, USA) was equilibrated with 10 ml PBS and ~500 µl of the antibody mixture was transferred on the column bed and eluted with 1 ml PBS buffer. Protein yield (280 nm), dye concentration (650 nm) and labeling efficiency were determined using the NanoDrop spectrophotometer (Peqlab ND-1000). Degree of labeling (DOL) was calculated using the following equation.

$$DOL = \frac{\mathrm{A(dye)}\ X\ \epsilon\ (protein)}{A\ 280\ protein - (Adye\ X\ CF\ 280)\ X\ \epsilon\ \ dye}$$

Є IgG protein – 203000; Є $A_{647\ dye}$ – 265000; CF $_{280\ (A647)}$ - 0.03.

The quality of the protein was checked using 10% SDS-PAGE followed by coomassie staining.

### 2.2.3 Biophysical methods

#### 2.2.3.1 ThioflavinS (ThS) assay

ThS dye binds to cross β-sheet containing aggregates which are typical of amyloid aggregates. Inhibition of tau aggregation by monoclonal antibodies was monitored in presence of ThS dye. 10 µM of tau monomer in BES pH 7.0 with or without 2.5 µM heparin (MW 16,000), with or without different concentrations of antibody in presence of 40 µM of ThS was prepared for a maximum of 40µl and loaded in 384 well plates (black microtiter 384 plate round well, Thermolabsystems, Dreieich), and measurements were carried out using Magellan software in a TECAN spectrofluorimeter (Ascent, Lab systems, Frankfurt). Kinetics was carried out at 37°C for 24 h with measurement intervals of 15 min using excitation wavelength of 440 nm, an emission wavelength of 521 nm with spectral bandwidths of 2.5 nm for

excitation and emission. Samples were prepared in duplicates or triplicates and after the measurements, the background fluorescence from ThS alone was subtracted.

#### 2.2.3.2 Dynamic light scattering (DLS)

Using the principles of Brownian motion and Doppler shift the size and number of the particles in a suspension can be determined by dynamic light scattering (DLS) or quasi-elastic light scattering (QUELS). Using this technique the size differences between particles (monomers, oligomers or aggregates) can be determined provided the size differences are sufficiently large (minimum 5-fold). After 24 h, 20µl of the aggregated sample (with or without antibody) was placed in quartz batch cuvette (ZEN2112) and thermally equilibrated at 25°C for 2 min in Zetasizer Nano S (Malvern, Herrenberg) instrument fitted with 5-milliwatt helium-neon 633 nm laser at 173° measurement angle. Intensity of the scattered particle, their size and numbers were obtained as an average of 3 measurements with 20 runs each. The results are expressed as volume graph.

#### 2.2.3.3 Atomic force microscopy (AFM)

Atomic force microscopy is a powerful microscopy technology for studying samples at nanoscale. In AFM, imaging a surface topography by using attractive and repulsive interaction forces between a few atoms attached at a tip of a cantilever and a sample and these forces are received in photodiode and is proportional to the size of the particle. AFM sample preparation and imaging was performed as described earlier (Wegmann et al., 2012). In brief, mica discs pasted on a glass slide were freshly cleaved using a sticky tape. On these freshly cleaved mica, 1-2 µM of protein sample diluted in adsorption buffer (PBS, pH 7.4) was incubated for 10 min followed by washing with PBS, pH 7.4 (3-5 times) to remove loosely bound protein on the surface.

AFM Imaging: AFM imaging was done in oscillation mode for all Tau samples in liquid. The cantilever (MSNL10) was inserted in the cantilever holder attached with fluid cell. This assembled setup was attached to the AFM head. The laser was aligned on the end of the tip and the set up was thermally equilibrated for 10-20 min at room temperature. The oscillation of frequency and drive amplitude for oscillation mode

imaging was chosen using the inbuilt auto-tuning procedure. The surface was approached in an oscillation mode with an amplitude set point of 70% (0.7V) of the target amplitude (1V). Once the surface was reached, the minimal contact between the sample and cantilever was maintained by altering the amplitude set point manually. The images were acquired at a scan rate of 1Hz with the resolution of 512 by 512 pixels. During the scanning the gains and amplitude set points were altered manually often to keep a minimal force between the cantilever and the sample. The images were acquired using the JPK Nano Wizard ultra-speed AFM microscope facility at CAESAR. The acquired images were processed by the JPK data processing software.

#### 2.2.3.4 Bio-Layer Interferometry (BLI)

The BLI (bio-layer interferometry) technology used by BLItz provides real-time data on protein interactions. BLI is an analytical technique which measures the binding affinities of macromolecules. It is a label-free technology which measures the interference patterns caused by the binding of protein to its binding partner, which is immobilized on the biosensor surface. Kinetics assay was performed by capturing the monoclonal antibodies using anti-mouse IgG Fc capture (AMC) biosensors followed by buffer baseline for 30 s. mAb captured sensors were submerged in a sample with different tau constructs for 5 min followed by dissociation. The binding sensograms were obtained and the binding parameters (on and off rates $k_a$, $k_d$, dissociation constant $K_D$) were calculated by local fitting (1:1 Langmuir interaction model) by BLItz Pro 1.2 software.

### 2.2.4 Cell culture

#### 2.2.4.1 N2a cells maintenance

N2a wildtype and inducible cell lines were grown in minimal essential media (Sigma, Germany) supplemented with 10% FBS, 5 ml non-essential amino acids (PAA, Austria) and 1X penicillin and streptomycin antibiotic (complete media). The cells were grown at 37°C in a 5% $CO_2$ incubator. At 80-90% cell confluence they were sub-cultured by trypsin digestion as follows. Cells grown on T25 flask were washed twice with warm PBS and trypsinized with 1 ml of trypsin at 37°C in 5% $CO_2$ incubator for 2-3 min. 4 ml of complete media was added to inhibit the trypsin activity and the trypsinized cells

were centrifuged at 1250 rpm for 2-3 min at RT. Supernatant was removed and 5 ml of complete media was added to the pellet and sub-culture was established in 1:5-1:10 ratio. The inducible N2a cell lines expressing tau were generated in our lab previously (Khlistunova et al., 2006); these cells require antibiotics Geneticin (G418) (300 µg/ml) and Hygromycin (100 µg/ml).

#### 2.2.4.2 N2a cells freezing

N2a cell freezing media (50% FBS + 30% MEM + 20% DMSO) was prepared and sterile filtered using 0.22 µm filter. 90-100% confluent cells in T75 flask were washed twice with warm sterile PBS and 3 ml trypsin was added and incubated at 37°C in 5% $CO_2$ incubator for 2-3 min. 4 ml of complete media was added to inhibit the trypsin activity. Cells were centrifuged at 1250 rpm for 2-3 min at RT to pellet down the cells. 2-3 ml of freezing media was added to the pellet and the cells were counted using the Neubauer chamber. $1X10^6$ cells/cryo vial was prepared and transferred to isopropanol container for 24 h at -80°C and then transferred to liquid nitrogen for long-term storage.

#### 2.2.4.3 N2a cells recovery

One cryo vial with N2a cells retrieved from liquid nitrogen was thawed and the cells were washed twice with 4 ml of warm complete media by centrifugation (1250 rpm, RT, 3 min) to get rid of DMSO. To the final pellet 5 ml of complete media was added and the cells were plated in T25 flask. For inducible N2a cell lines antibiotics G418 (300 µg/ml) and Hygromycin (100 µg/ml) were added.

#### 2.2.4.4 Transfection (DNA) for luciferase complementation assay

Luciferase complementation fragments were generated using plasmid pCBG99 (click beetle green). The amino acid sequence of the luciferase complementation fragments 2-413 for N-terminus (Luc-N) and 395-542 for C-terminus (Luc-C) were amplified by PCR. The PCR fragments were cloned into the $pTau^{RD\Delta K}$-EGFPN1 (enhanced green fluorescent protein) vector by replacing the GFP with Luc-N or Luc-C (see appendix for the plasmid map). N2a cells were plated in a T25 flask to achieve uniform transfection efficiency. Plasmids pEGFPN1-Luc-N (3.24 µg) and pEGFPN1-Luc-C (2.7 µg) were mixed together in reduced-serum opti-MEM medium (1150 µl).

Lipofectamine2000 (25 µl) (*Invitro*gen) was also diluted in opti-MEM medium (1150 µl). Both the DNA and lipofectamine were mixed together and incubated at RT for 5 min. The cells were washed with warm PBS and the reaction mixture was added on the cells and incubated for 2 h at 37°C in 5% $CO_2$ incubator. After 2 h, 4 ml of complete medium was added and further incubated for another 2 h. Later the cells were trypsinized and all the cells were plated in 96 well plate equally in all wells.

#### 2.2.4.5 Antibody transfection into cells

Xfect protein transfection reagent kit (Clontech) was used to deliver the protein of interest into the cells. N2a cells were plated in 6 well plate with a density of $3x10^5$ cells per well. After 24 h, 15 µl of Xfect transfection reagent was mixed with 85 µl of deionized water. In another tube protein of our interest and Xfect transfection buffer was made to the final volume of 100 µl. Both the reaction mixtures were pooled and the solution was pipetted gently for 10-15 times. Afterwards the solution was incubated at RT for 30 min. 400 µl of serum free media was added to the mixture and the whole content of 600 µl was added to the cells for 2 h at 37°C in a $CO_2$ incubator. After 2 h, 1.4 ml of complete media was added on the cells and incubated for 15 h.

#### 2.2.4.6 Annexin V staining

Annexin V conjugate was used for detecting phosphatidylserine (PS) exposed on the outer plasma membrane, a hallmark of early apoptosis. Annexin V is 35-36 kDa $Ca^{2+}$ dependent phospholipid binding protein. APC (Allophycocyanin) labelled Annexin V can identify early stage apoptosis. Inducible N2a cells expressing $Tau^{RD\Delta K}$ were treated with desired antibodies and grown for 4 days. Cells were trypsinized and centrifuged, supernatant was removed and the cell pellet was suspended in 100 µl of 1X Annexin binding buffer and 5 µl of Annexin V dye was added and incubated in dark for 30 min at RT. Cells were washed in 1X binding buffer and collected in PBS buffer. Cell counting was performed in Gallios Beckman-Coulter Flow Cytometer. 20,000 cells per sample were counted to check Annexin V positive cells.

### 2.2.4.7 Thioflavin S staining of N2a cells

The ThS dye binds to protein aggregates containing cross β-sheet structures, a hallmark of amyloid aggregates. Inducible N2a cells expressing $Tau^{RD\Delta K}$ were treated with desired antibodies and 0.0001% of ThS dye and grown for 4 days at 37°C in a $CO_2$ incubator. Cells were trypsinized and centrifuged, supernatant was removed and the cell pellet was resuspended in PBS buffer. Using Gallios Beckman-Coulter Flow Cytometer 20,000 cells per sample were counted to check for ThS positive cells.

### 2.2.4.8 Flow cytometry-Fluorescence Activated Cell Sorting (FACS)

FACS is a laser based technology used to count cells by suspending cells in a stream of fluid and passing them by an electronic laser based detection system. Blue laser (488 nm) was used to excite ThS (excitation-440 nm; emission 521 nm) and red laser (683 nm) was used to excite Annexin V (excitation-633 nm; emission 665 nm). Trypsinized cells were centrifuged and collected into 1 ml PBS and then measured on the FITC channel/APC channel with a flow-rate of 30 µl/min. The instrument (Beckman) was allowed to count a maximum of 20,000 events. Counting was carried out at RT.

### 2.2.4.9 Staining lysosomes

N2a cells were grown to maximum confluence. Old medium was removed from the cells and diluted with 75 nM Lyso tracker red DND 99 (L7528, Molecular Probes) dye resolved in fresh complete warm medium and added to the cells and incubated for 2 h at 37°C in 5% $CO_2$ incubator. After 2 h the medium was removed and the cells were fixed using 4% sucrose and 3.7% formaldehyde in PBS for 30 min at 37°C and then cells were washed thrice with PBS buffer at RT. If required co-staining of other antibodies can be performed using immunocytochemistry protocol.

### 2.2.4.10 Immunocytochemistry

N2a cells were treated with desired antibodies at different concentrations for 24 h. Afterwards the cells were fixed in solution with 4% sucrose and 3.7% formaldehyde in PBS for 30 min at 37°C and then cells were washed thrice with PBS buffer. Later the cells were permeabilized and blocked using 5% BSA and 0.5% TritonX-100 in PBS for

6 min at room temperature and then washed thrice with PBS buffer. Primary antibody was diluted in blocking solution and incubated on cells at 4°C for overnight on a shaker. Unbound or loosely bound antibodies were washed thrice using PBS. Secondary antibody was diluted in blocking solution and incubated on cells for 1 h at 37°C. Cells were washed thrice with PBS. 10 µg/ml of DAPI in PBS buffer was incubated for 10 min at RT followed by washing with PBS. Finally, cells were mounted on a glass slide using poly mount solution and dried at 4°C.

#### 2.2.4.11 Confocal microscopy

Image acquisition of cells and tissue sections was carried out using Zeiss LSM 700 confocal microscope. Images were captured at 20X, 40X and 60X magnification. Image quantification was carried out using the software Zen blue edition (2012, Zeiss). For image acquisition gain values of positive control were considered as reference in order to minimize the overexposure of the samples.

#### 2.2.4.12 IVIS imaging

In vivo imaging system (IVIS, Spectrum; Caliper Life Sciences, Germany) allows high-sensitivity in vivo imaging of fluorescence and bioluminescence. The Click beetle fly luciferase gene was split in to two parts i.e. split luciferase N-terminal and split luciferase C-terminal and each split luciferase construct was cloned on to the C-terminal of the $Tau^{RD\Delta K}$ gene. The co-expression of these two plasmids leads to the translation of two tau-protein constructs fused to two complementary parts of the reporter protein Luciferase. If the tau protein molecules interact with each other the complementary fragments of the separated reporter Luciferase complement form active Luciferase which in the presence of the substrate D-Luciferin emits light detectable in the IVIS (Caliper Life Sciences, Germany) or another luminometer.

$$\text{Luciferin} + O_2 + \text{ATP} \xrightarrow{\text{Luciferase}} \text{Oxyluciferin} + CO_2 + \text{AMP} + \text{diphosphate} + \text{Light}$$

After 15 h of expression in N2a cells 5 µg/ml of D-luciferin was added and incubated for 10-20 min prior to the measurement. D-luciferin interacts with Luciferase in the cytoplasm in an ATP (Adenosine Triphosphate) dependent reaction and emits light

which can be recorded. Bioluminescence images are acquired using IVIS according to the manufacturer's protocol.

#### 2.2.4.13 Brain tissue homogenization

Animals were sacrificed by cervical dislocation and the whole brains were removed. Half of the brain (hemisphere) was frozen in liquid nitrogen for biochemistry. Other half of the brain was used for brain homogenate preparation, the brain sample was thawed on ice and 800 µl of 1x lysis buffer was added and the tissue was minced using a 1 ml syringe attached with 18G needle and later with 24G needle. The sample was incubated on ice for 30 min. Later the sample was resuspended with a pipette and was centrifuged at 14,000 rpm at room temperature. The supernatant was collected and the protein concentration was estimated using BCA method.

#### 2.2.4.14 Immunohistochemistry (IHC)

Animals were sacrificed by cervical dislocation and the whole brain was removed. Half of the brain (hemisphere) was fixed using 3.7% formaldehyde in PBS for 24 h at 4°C, followed by sucrose gradient (10%, 20% and 30%) fixation for 24 h in each gradient at 4°C. Brain was sliced (free floating sections) in to 50 µm equal sections from top to bottom using a vibratome (Leica VT 1200S, Germany) and the sections were collected and stored in PBS. Antigen epitope retrieval was carried out by adding 10 mM sodium citrate buffer (hot (80°C) to the sections and incubating the sections for 30 min at 80°C. Sections were washed with PBS (3 times, 10 min each). For permeabilization sections were incubated in 0.1% Triton-X 100 for 1 h at RT on an orbital shaker. Sections were washed with PBS (3 times, 10 min each).Sections were incubated in blocking solution (0.3% Triton-X 100, 2% horse serum in PBS) for 2 h at RT on a shaker. Primary antibody was diluted in blocking solution and incubated at 4°C overnight on a shaker. Sections were washed with 0.1% Triton-X100 in PBS (3 times, 10 min each) on a shaker. Secondary antibody was diluted in blocking solution and incubated on sections for 2 h at 37°C (shaker). Sections were washed with 0.1% Triton-X100 in PBS (3 times, 10 min each) on a shaker. 10 µg/ml of DAPI in PBS buffer was incubated for 10 min at room temperature followed by washing with PBS. Finally, sections were mounted using poly-mount solution and the coverslips were dried at 4°C.

### 2.2.5 Statistics

All experimental data were normalized with buffer controls. The statistics was done using Graph Pad (Prism) software. The significance of differences was analyzed by one- way ANOVA test with Tukey´s post hoc test. In all the experiments the confidence interval was set at 95%. Hence a p value $< 0.05$ was considered to be statistically significant.

# 3 Results

In Alzheimer disease models, the pathology induced by tau aggregation was previously analyzed in cell models (Khlistunova et al., 2006, Wang et al., 2007, Kaniyappan et al., 2017, Pickhardt et al., 2017) and in transgenic mouse models (Mocanu et al., 2008, Van der Jeugd et al., 2012, Decker et al., 2016). Tau aggregation inhibitors can block the aggregation by binding to tau (Pickhardt et al., 2007a, Yanamandra et al., 2013) or by blocking inducers of tau aggregation (Shelton et al., 2017). Recent reports suggest that passive immunization of mice with anti-tau antibodies can ameliorate tau pathology in tau transgenic animals (Yanamandra et al., 2013, Dai et al., 2015), but the underlying mechanisms and targets remain a matter of debate. The studies presented here demonstrate the targets and modes of activity of anti-tau monoclonal antibodies which are raised against toxic oligomers.

## 3.1 Purified Tau$^{RD\Delta K}$ oligomers as antigens for generating monoclonal antibodies

The antigens for generating monoclonal antibodies were the purified oligomers of the mutant tau repeat domain with the deletion of lysine 280 (Tau$^{RD\Delta K}$). Tau$^{RD\Delta K}$ readily forms aggregates and has the propensity to form β-sheet structure, hence its description as a pro-aggregant form of tau (Figure 3.1 A). Tau$^{RD\Delta K}$ oligomers were prepared and purified as described previously (Kaniyappan et al., 2017). Briefly, 50 µM recombinant Tau$^{RD\Delta K}$ (Mr~13.5 kDa) was diluted in TBS pH 9.0 and incubated at 37°C for 30 min for aggregation. The aggregated sample was cross-linked using 0.01% glutaraldehyde (GA) for 10 min at 37°C to stabilize the oligomers. The cross-linked sample was purified using a BFF 16/10 hydrophobic column. Figure 3.1 B represents the silver stained SDS gel with Tau$^{RD\Delta K}$ samples before and after purification. Tau$^{RD\Delta K}$ aggregated and cross-linked before purification (lane 1) shows different species of Tau$^{RD\Delta K}$ monomers and oligomers with some higher aggregates (see the gel pockets). The oligomers formed are mostly low-n oligomers ranging from dimer, trimer, and tetramer to some higher order oligomers. Cross-linked aggregates after purification (lane 3) have predominantly low-n oligomers with no monomers or higher aggregates (fibrils). The oligomers are separated from monomers due to their hydrophobicity. The

purified oligomers are predominantly low-n oligomers (dimers to hexamers) which were confirmed by AFM imaging.

The AFM-height image (Figure 3.1 C) reveals that the oligomers are globular in shape and are mostly in the range of 4-6 nm which corresponds to the height of dimers to hexamers of $Tau^{RD\Delta K}$. These purified and well characterized oligomers of $Tau^{RD\Delta K}$ were used as an antigen for generating the monoclonal antibodies.

## 3.2 Generation of monoclonal antibodies

The monoclonal antibodies were generated by our collaborator (Dr. Elizabeth Kremmer and Dr. Regina Feederle) at Helmholtz Center, Munich. We received tissue culture supernatants and purified antibodies of the clones that recognize the oligomers for further characterization.

## 3.3 Analysis of specificity of monoclonal antibodies

Monoclonal antibodies raised against purified oligomers of $Tau^{RD\Delta K}$ were screened for their specificity to potential targets. Aggregation of tau from non-toxic monomers to fibrils, implies various targets (protein species, conformations) for aggregation inhibitors and dis-aggregators (Howlett, 2001). In order to explore the specificity of antibodies to monomers or aggregation intermediates or fibrils, different constructs (repeat domain/full length) and different species (monomers, oligomers and fibrils) of tau were employed. Immunoassay methods like dot blots, western blots and ELISA were used to explore the affinity of antibodies in denaturing and non-denaturing conditions.

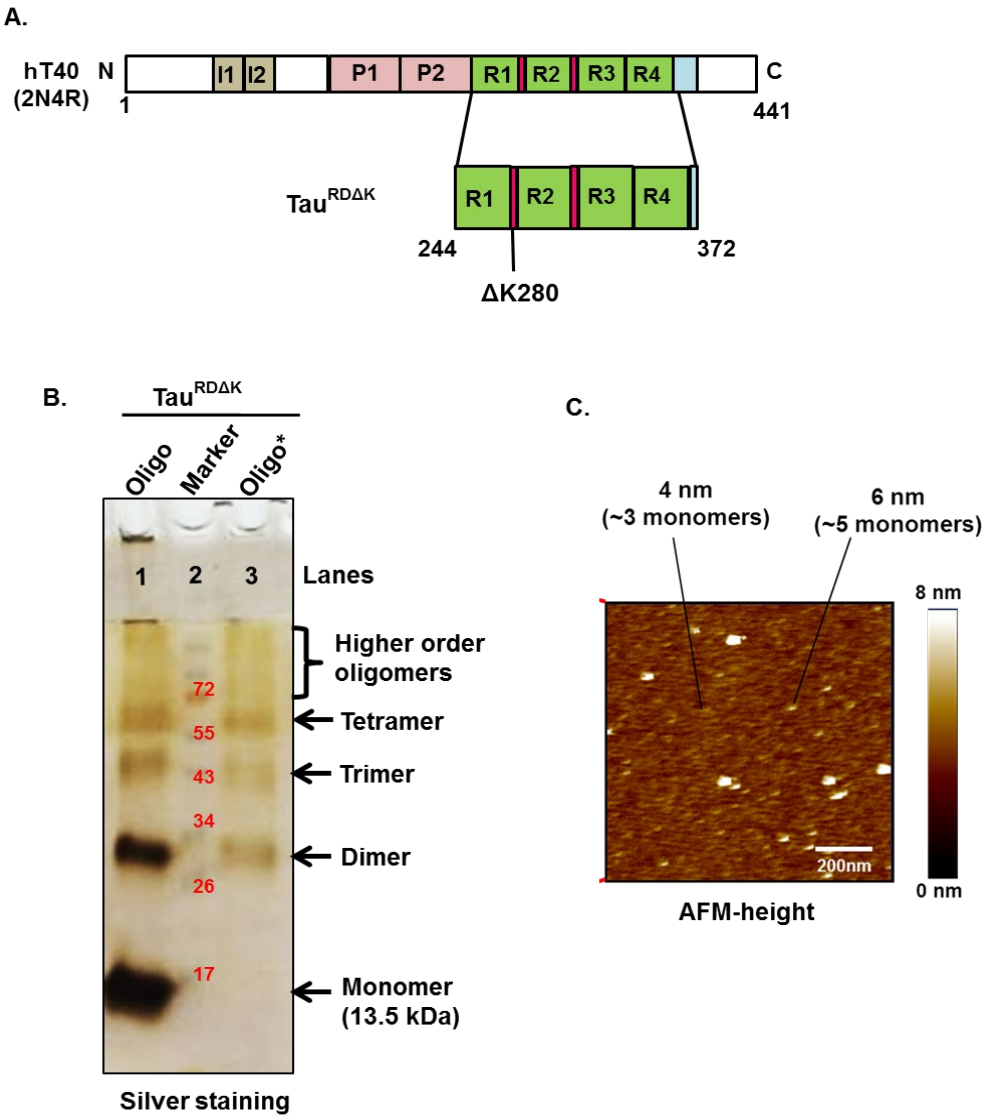


**Figure 3.1: Purified oligomers of Tau$^{RD\Delta K}$ as antigen for monoclonal antibodies.**
Purified low-n oligomers of Tau$^{RD\Delta K}$ were used as antigen to inject in mice and rat to generate different monoclonal antibodies specific to low-n oligomers of tau. **A)** The representational image of full length human tau (2N4R, 441aa) with two N-terminal inserts 1N and 2N (khaki box), two proline rich regions P1 and P2 (pink box) and repeat region with four repeats R1, R2, R3 and R4 (green box). Repeat region R2 and R3 comprises two hexapeptide motifs (red box) which promote aggregation of tau. The repeat region (K18) of tau (aa 244-372) with deletion of lysine at position 280 (ΔK280) increases the propensity of tau to form β-sheet containing aggregates. **B)** Silver staining of 17% SDS-PAGE with Tau$^{RD\Delta K}$ oligomers. Tau$^{RD\Delta K}$ was aggregated to form low-n oligomers for 30min at 37°C in TBS pH 9.0 and later cross-linked using 0.01% GA for 10min at 37°C. Unpurified oligomers run on the gel contain monomers which run at 13.5 kDa and low-n oligomers ranging from dimers to tetramers and some higher order oligomers (lane, 1). Oligomers were separated from monomers using Butyl FF 16/10 hydrophobic interaction chromatography column. The purified fractions on SDS gel confirm that oligomers were separated from monomers (lane, 3). **C)** AFM height image of purified oligomers of Tau$^{RD\Delta K}$ shows that most of the protein is comprised of low-n oligomers with heights ranging from ~4nm-6nm corresponding to 3-5 stacked monomers of tau and some higher aggregates with heights of >10nm. Abbreviation: Tau$^{RD\Delta K}$, repeat region of tau with ΔK280 mutation; Oligo, unpurified oligomers; Oligo*, purified oligomers; kDa, kilo Dalton; SDS-PAGE, sodium dodecylsulfate- poly acrylamide gel electrophoresis; GA, glutaraldehyde.

### 3.4 Specificity of antibodies against tau oligomers

Prior to in vivo testing, antibodies were extensively characterized *in vitro* and in cellular models to select potential candidates for in vivo studies. The dot blot method was employed for initial testing as this method did not use any chemical denaturing agents. It retains the antigen on the membrane in its natural conformation. To determine the specificity of the monoclonal antibodies, different mutants of tau and different species of tau were used (Figure 3.2). The polyclonal K9JA pan-tau antibody (detecting all constructs and assembly forms of tau) was used as an internal control to demonstrate that the protein was loaded in all lanes (row 1a-j). Antibodies 6H3, 8E7, 26G1 (rows 6-8) detected most forms of tau with varying affinities. Antibodies 26G1, 28D4, 29E2, 32E7 (rows 8-11) showed strong preferences for prefibrillar-aggregates of tau irrespective of mutation and domain structure (rows 8-11, columns c, g, i). Antibodies 2G9 and 6H1 had strong affinity for high molecular weight aggregates of $Tau^{RD\Delta K}$ (rows 3, 5, column d, pink boxes) as they did not detect purified low-n tau oligomers. Antibody 6B5 (row 4, columns d, i) showed high affinity for aggregates of RD/FL tau with ΔK280 mutation. Antibody 2B10 was the most specific, it showed high affinity only for $Tau^{RD\Delta K}$ purified oligomers (green box, row 2c). The anti-aggregant variants of tau (mutation ΔK280-2P) were recognized by antibodies 6H3, 8E7, and 26G1 (rows 6j, 7e, 8j). Overall, the dot blot results showed that although all antibodies were raised against the same antigen (purified oligomers of $Tau^{RD\Delta K}$) they showed different specificities and affinities for different tau constructs.

The same antibodies yielded different results when they were probed to antigens under denaturing conditions in western blots. The 2B10 antibody did not discriminate between any tau mutants and detected all forms of tau in denaturing conditions. The antibody 2B10 showed affinity for all forms of recombinant FL and RD tau (Figure 3.3 A, lanes 1-8) but it did not detect RD or FL tau in brain lysates. Non-specific binding was observed in case of brain lysates (Figure 3.3 A, lanes 10-12). Antibody 6H1 detected all forms of recombinant tau (Figure 3.3 B, lanes 1-8) and also $hTau40^{\Delta K}$ and mouse tau in brain lysates (Figure 3.3 B, lanes 10-12). These results suggest that under denaturing condition these antibodies detect tau without any specificity.

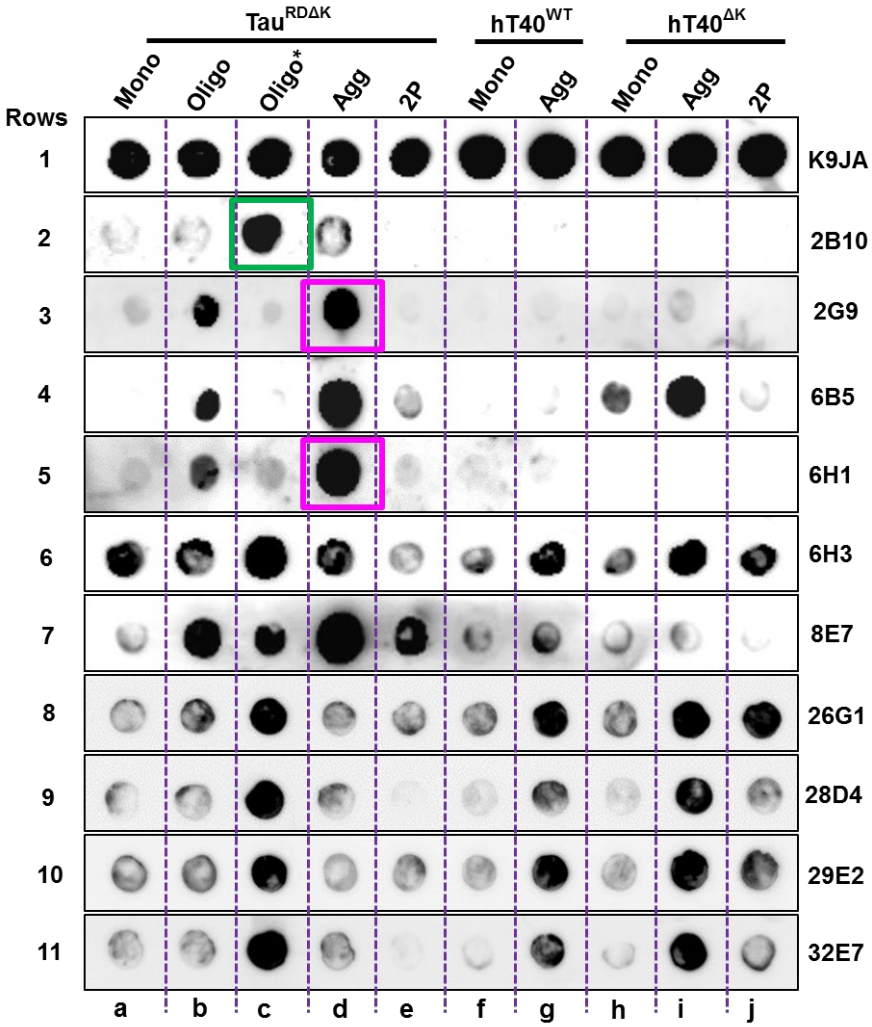


**Figure 3.2: Analysis of specificity of anti-tau oligomer antibodies by dot blot.**
Anti-tau oligomer monoclonal antibodies exhibit differential abilities to bind to different tau species or constructs. Different constructs of recombinant tau protein ($Tau^{RD\Delta K}$, $hTau40^{Wt}$ and $hTau40^{\Delta K}$) were prepared *in vitro* in monomeric form. $Tau^{RD\Delta K}$ oligomers (purified and unpurified) were prepared by incubating monomers at 37°C for 30 min in TBS pH 9.0 and cross-linked with 0.01%GA for 10 min. Aggregates of tau were prepared by incubating the tau monomers in the presence of heparin at 37°C for 120 h in BES pH 7.0. 50 ng/well of protein was loaded on PVDF membrane and immunoblotted with different anti-tau oligomer monoclonal antibodies (3 µg/blot). Row 1a-j: A representative blot (pan-tau polyclonal antibody K9JA) acts as a positive control which detects all tau constructs and assembly forms. By contrast, different monoclonal antibodies have different specificities and affinities to different constructs and assembly forms of tau. Row 2: Antibody 2B10 shows high specificity for the oligomer-enriched sample (blot 2c, green box) whereas some antibodies such as 2G9 (blot 3d), and 6H1 (blot 5d) show high affinity to aggregates (pink box) of the repeat domain (RD) of tau with the ΔK mutation. Antibody 6B5 (row 4) shows strong affinity towards aggregates of repeat domain or full length tau with the ΔK mutation (blots 4d, 4i). Rows 6-11: Further representative dot blots of different monoclonal antibodies are shown to illustrate the differential ability of antibodies to detect different tau species or constructs. Note the enhanced reaction with oligomer-enriched species of tau RD (rows 6-11, column c) and with aggregates of full-length tau (rows 6-11, column i), Abbreviations: $Tau^{RD\Delta K}$, human tau repeat domain with pro-aggregant mutation ΔK280; $hTau40^{WT}$, full length human wild type tau; $hTau40^{\Delta K}$, full length human tau with pro-aggregant mutation ΔK280; Mono, monomer; Oligo, uncross-linked and unpurified oligomers; Oligo*, cross-linked and purified oligomers; Agg, Aggregates; 2P- human tau with anti-aggregant mutation ΔK280/2P; RD, repeat domain; FL, full length.

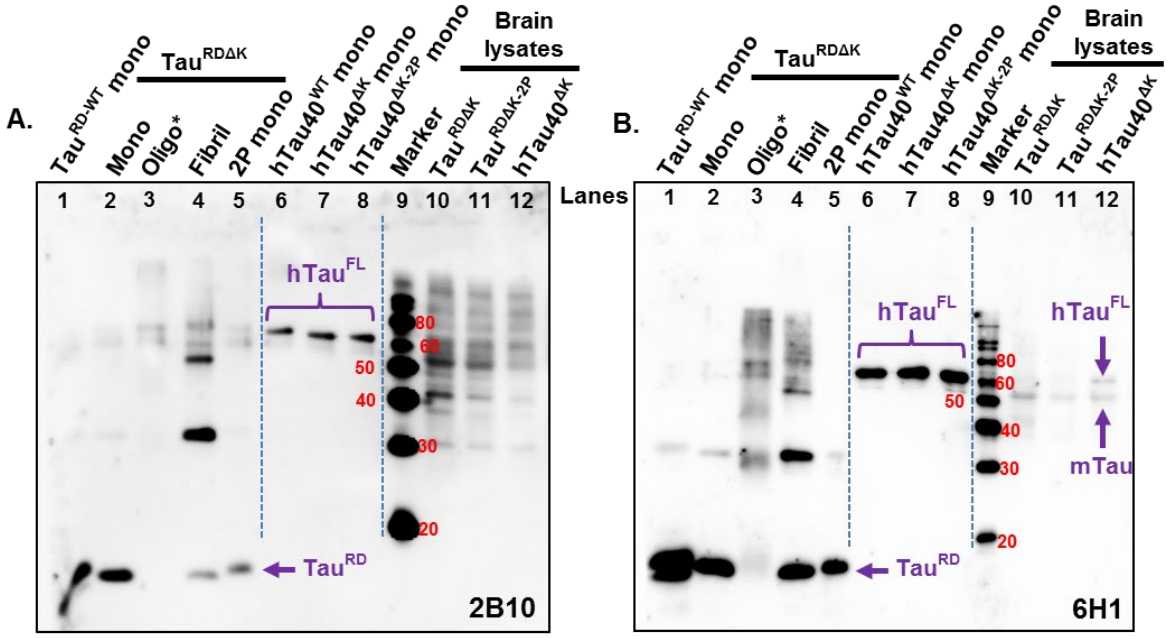


**Figure 3.3: Interactions of monoclonal antibodies in denaturing western blots.**
Recombinant protein (50 ng/well, lanes 1-8) and brain lysates (15 µg/well, lanes 10-12) were loaded on the SDS gels and immunoblotted with anti-tau oligomer monoclonal antibodies (tissue culture supernatant; 1:10 dilution). Antibody 2B10 (A) and 6H1 (B) detects all forms of RD and FL recombinant tau. Lanes: (1) $Tau^{RD\text{-}WT}$ monomer, Mr~13.8 kDa, (2) $Tau^{RD\Delta K}$ monomer, (3) $Tau^{RD\Delta K}$ oligomers ~60-80 kDa, (4) $Tau^{RD\Delta K}$ fibrils broken down into oligomers (Mr ~35-80 kDa), (5) anti-aggregant $Tau^{RD\Delta K\text{-}2P}$ (monomers and oligomers ~70 kDa), (6-8) monomers from $hTau40^{WT}$, $hTau40^{\Delta K}$, $hTau40^{\Delta K\text{-}2P}$, ~65 kDa. Antibody 2B10 (A, lanes 10-12) shows non-specific interactions in transgenic brain lysates expressing RD or FL tau. By comparison, 6H1 antibody detected the FL human tau (B, lane 12) and mouse tau (B, lane 10, 11, 12) in transgenic brain lysates. Abbreviations: Mono, monomers; Oligo*, cross-linked and purified oligomers; $Tau^{RD\Delta K}$, human tau repeat domain with pro-aggregant mutation ΔK280; $hTau40^{\Delta K}$, full length human tau with pro-aggregant mutation ΔK280; $hTau40^{WT}$, full length human wild type tau; 2P- human tau with anti-aggregant mutation ΔK280/2P; RD, repeat domain; FL, full length.

The affinity and specificity of monoclonal antibodies to their antigen was also analyzed by indirect ELISA. Different mutant and different forms of Tau proteins were coated on the plates and probed with the monoclonal antibodies. The 2B10 and 6B5 antibodies showed strong affinity to both unpurified and purified oligomers of $Tau^{RD\Delta K}$ but not to monomers or fibrils (Figure 3.4 A and C). The 6H1 antibody showed equal affinity for all forms of $Tau^{RD\Delta K}$ (mono, oligo and fibrils) and did not show preferences to any of them (Figure 3.4 B). Surprisingly, the 8E7 antibody showed stronger affinity for purified oligomers of tau than for unpurified oligomers (Figure 3.4 D) which could be due to the accessibility of the potential binding sites for 8E7 antibody in cross-linked oligomers.

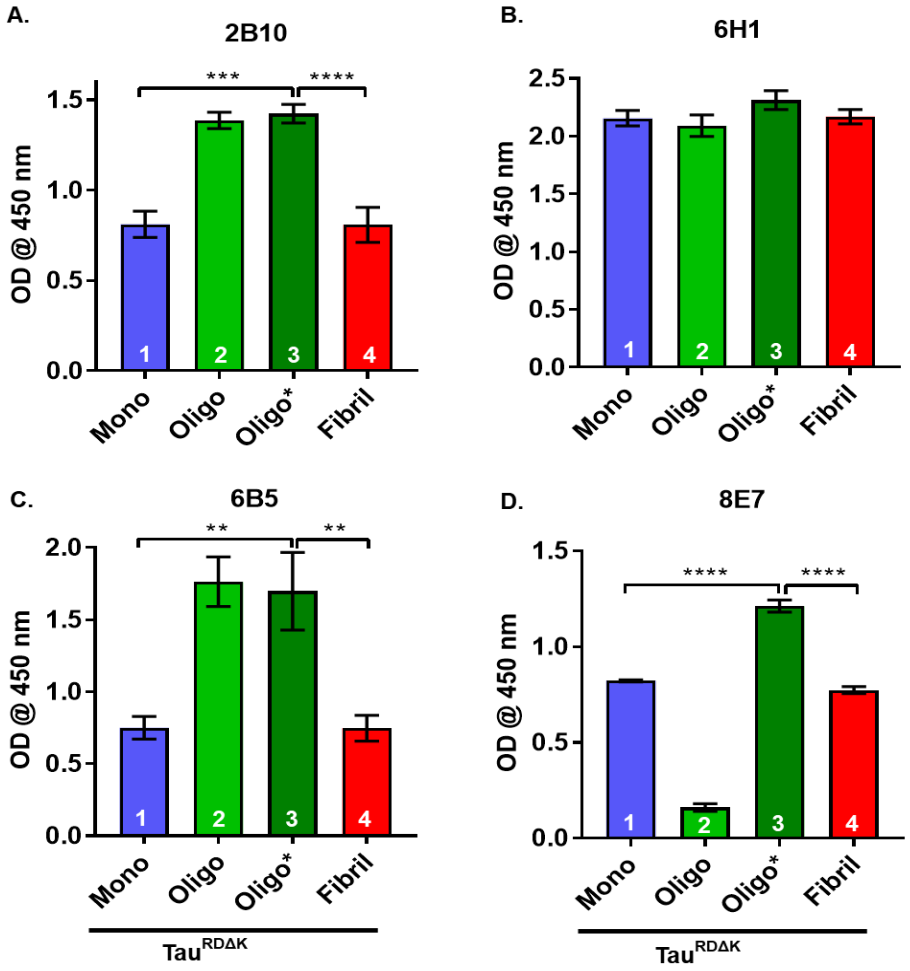


**Figure 3.4: Analysis of specificity of mAb's by indirect ELISA.**
Indirect-ELISA was used to analyse the affinity of mAb's to its antigen. 250 ng/well of antigen was coated on the 96well plates and incubated with primary anti-tau oligomer antibodies (tissue culture supernatant (1:10 dilution)) overnight at 4°C and then suitable HRPO-labelled secondary antibodies were used and detected with the ELISA kit with absorbance at 450 nm. **A)** The representative graphs of the antibodies show that 2B10 antibody has high affinity for $Tau^{RD\Delta K}$ oligomers (bars 2, 3) compared to monomer and fibrils (bars 1 and 4) (n=3; one-way ANOVA with Tukey's post hoc test; F (3, 12) = 24.51; ****$P$<0.0001 and ***$P$<0.001). **B)** Antibody 6H1 binds to all forms of $Tau^{RD\Delta K}$. It does not discriminate oligomers (bars 2, 3) from monomers and fibrils (bars 1 and 4) (n=3; one-way ANOVA with Tukey's post hoc test; F (3, 12) = 1.469; ****$P$=0.2725). **C)** Antibody 6B5 shows high affinity to oligomers (bars 2, 3) compared to monomer and fibrils (bars 1 and 4) similar to 2B10 antibody (n=3; one-way ANOVA with Tukey's post hoc test; F (3, 12) = 11.06; **$P$<0.01). **D)** Antibody 8E7 shows high affinity to purified oligomers* (bar 3) compared to un-purified oligomers (bar 2), monomers and fibrils (bars 1 and 4) (n=3; one-way ANOVA with Tukey's post hoc test; F (3, 12) = 418.6; **$P$<0.0001). Abbreviations: mAb, monoclonal antibody; ANOVA, analysis of variance; Mono, monomers; Oligo, uncross-linked and unpurified oligomers; Oligo*, cross-linked and purified oligomers; HRPO, horseradish peroxidase.

Summarizing these results (dot blot, western blot and ELISA), it appears that these anti-tau oligomer antibodies demonstrate different properties based on the method used for analysis. Since the dot blot analysis is based on non-denaturing conditions,

we selected the antibodies based on dot blot results. Interestingly, ELISA (another non-denaturing based condition) supported the dot blot results.

### 3.5 Immunocytochemistry and Immunohistochemistry

We next determined the specificity of antibodies in cell and animal models using the immunofluorescence method. Fixed N2a-wt cells and N2a cells expressing $Tau^{RD\Delta K}$ were probed with antibodies 2B10 and 6H1. Anti-tau K9JA antibody was used as total tau antibody. 2B10 and 6H1 antibodies detected human tau with high specificity in N2a-$Tau^{RD\Delta K}$ cells (Figure 3.5 A, images 4, 7). Positive control antibody K9JA detected tau strongly in N2a-$Tau^{RD\Delta K}$ cells (Figure 3.5 A, images 5, 8) and antibodies 2B10 and 6H1 showed co-localization (yellow) with the K9JA antibody (Figure 3.5 A, images 6, 9) which confirmed the specificity of 2B10 and 6H1 to human tau in cell models. Interestingly, 2B10 and 6H1 antibodies appeared also to detect other tau forms with no co-localization with K9JA. This suggests that these antibodies have affinities for oligomers as well as aggregates. All the antibodies showed little or no background fluorescence in N2a-wt cells which do not have human tau but have low amounts of mouse tau (Figure 3.5 A, images 1, 2, 3). Figure 3.5 B shows the affinity of 2B10 antibody in fixed free floating brain slices of control and KT1.K4 ($Tau^{RD\Delta K}$) mice. 2B10 antibody detected human tau in KT1.K4 animals with high specificity in the soma and in dendritic processes (Figure 3.5 B, images 3 white arrows) of the CA1 and CA3 regions of the hippocampus (Figure 3.5 B, images 3, 4) without showing any affinity to mouse tau expressed in control brains (Figure 3.5 B, images 1, 2). The immunofluorescence data suggest that 2B10 antibody shows high affinity for human tau in cell and animal models.

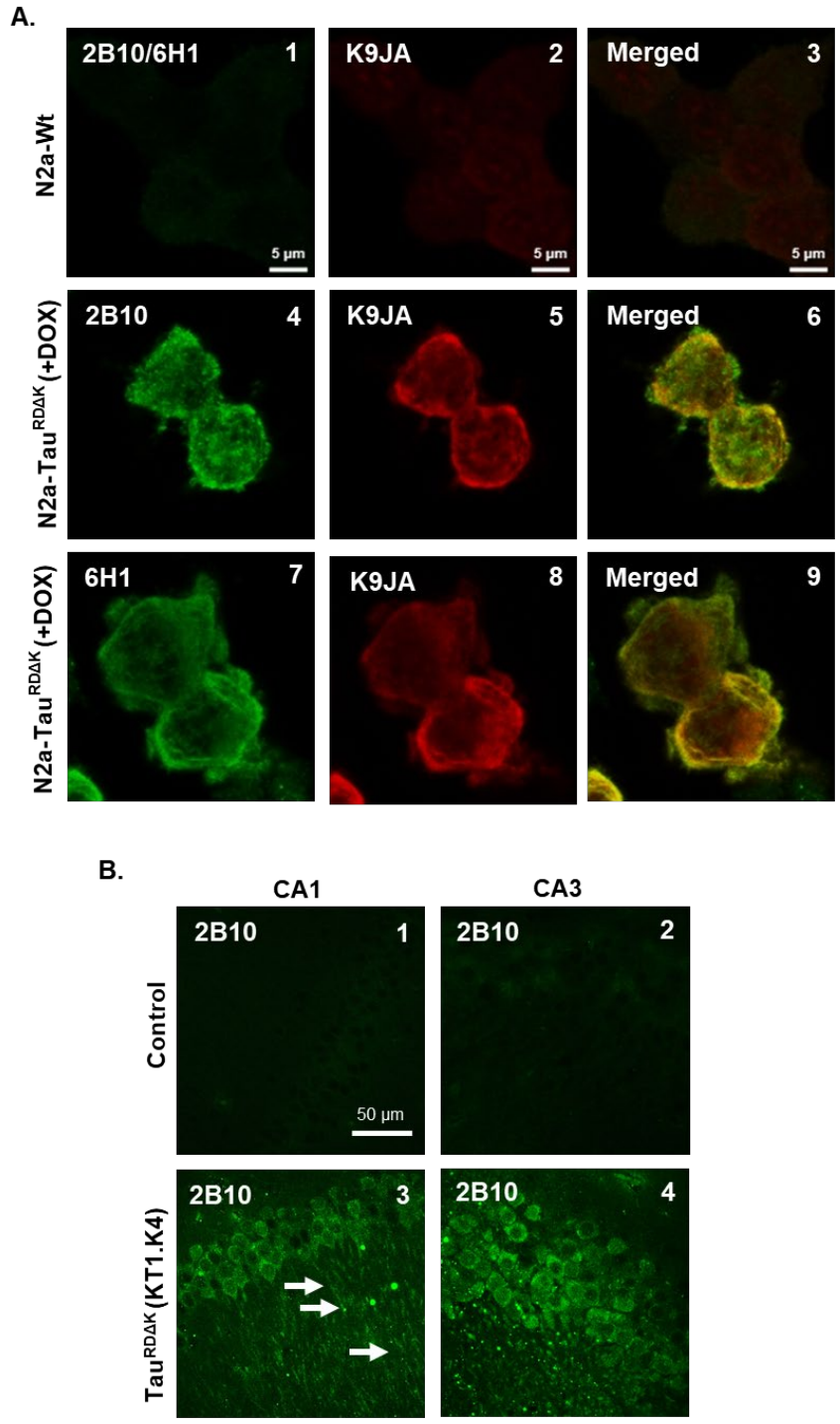


**Figure 3.5: 2B10 antibody is specific to Tau$^{RD\Delta K}$ in immunofluorescence.**
Monoclonal antibodies detected tau with high specificity in cell and animal models. **A)** 2B10 and 6H1 antibodies (green) detected tau in N2a cells expressing Tau$^{RD\Delta K}$ (image 4, 7) but with minimal or no staining in N2a-wt cells (image 1; the image 1 belongs to 2B10 antibody; since 6H1 antibody also shows similar results, it is represented as 2B10/6H1). Pan tau K9JA antibody was used as a total tau antibody (image 2, 5, 6) which co-localized with anti-tau oligomer antibodies (image 6, 9). **B)** Free floating mice brain sections probed with 2B10 antibody showed tau staining mostly in the soma and some dendritic processes (white arrows) of CA1 and CA3 neurons in the transgenic mouse expressing Tau$^{RD\Delta K}$ (image 3, 4). 2B10 antibody did not show any staining in the control brain (Image 1, 2) owing to its high specificity to Tau$^{RD\Delta K}$.

## 3.6 Analysis of affinity of the antibodies by biolayer interferometry (BLItz)

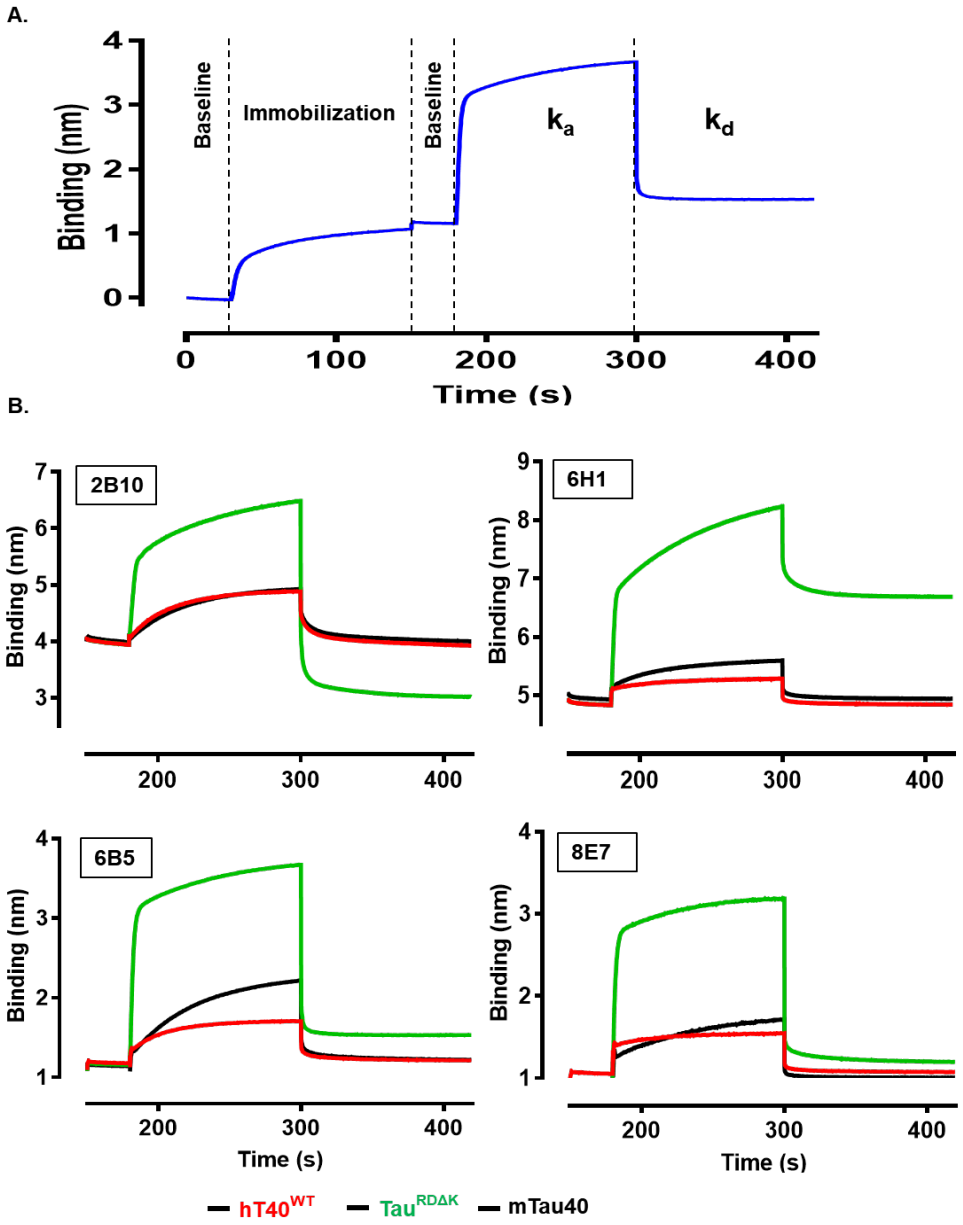


**Figure 3.6: Affinity analysis of monoclonal antibodies by BLItz.**
Bio-layer interferometry (BLItz) shows the binding affinities of immobilized monoclonal antibodies towards different constructs of human tau (FL/RD) and mouse tau. **A)** Representational image of BLItz sensogram shows the different phases of the assay. The initial phase is the buffer baseline (30 s) with the adsorption buffer. The second phase shows immobilization of different antibodies such as 2B10 (2677nM), 6H1 (866.7 nM), 6B5 (250.7 nM), 8E7 (72.67 nM) (120 s). After that the buffer baseline is run for 30 s. In the next step different constructs of FL/RD human tau and mouse tau are run to determine the association rate constant ($k_a$), dissociation rate constant ($k_d$), and binding constant ($K_D$) of each antibody towards human and mouse tau. **B)** BIItz sensograms of immobilized antibodies (2B10, 6H1, 6B5 and 8E7) towards $Tau^{RD\Delta K}$ (green), $hT40^{WT}$ (red) and mTau40 (black). The sensograms shows $k_a$ and $k_d$ values of different tau constructs towards antibodies. $K_D$ values are calculated from the obtained $k_a$ and $k_d$ values. Abbreviations: nM, nanomolar; s, seconds; nm, nanometre; RD, repeat domain tau; $k_a$, association rate constant; $k_d$, dissociation rate constant; $K_D$, dissociation constant/binding affinity.

The binding affinities of the antibodies with the different tau constructs were determined by biolayer interferometry (BLItz). Figure 3.6 A, shows a typical BLI assay sensogram, which involved four essential steps. Buffer equilibration step, immobilization of the ligand, association of the analyte ($k_a$) followed by a dissociation step ($k_d$). The association ($k_a$) and dissociation ($k_d$) rate constants were calculated by a titration series of the antigen run against an immobilized antibody. The data set was analyzed with global fitting (1:1 Langmuir interaction model), using Octet software (ForteBio), thereby producing a $k_a$, $k_d$, $K_D$. The binding affinity ($K_D$) was calculated by the ratio of the $k_d/k_a$. Sensograms in Figure 3.6 B showed association of four antibodies (2B10, 6H1, 6B5, and 8E7) with human ($hT40^{WT}$, $Tau^{RD\Delta K}$) tau and mouse tau (mTau40). 2B10 antibody showed similar rate constants for association ($k_a = 2.02 \times 10^3$ $Ms^{-1}$) and dissociation rate ($k_d = 2.68 \times 10^{-2}$ $s^{-1}$) (see Table 3.1) to $hT40^{WT}$ and mouse tau which resulted in a low dissociation constant ($K_D$ = 13.22 µM). This antibody showed moderate binding affinity to $Tau^{RD\Delta K}$ ($K_D$ = 1.21 µM) with low $k_a = 2.22 \times 10^4$ $Ms^{-1}$ and $k_d = 2.69 \times 10^{-2}$ $s^{-1}$. By contrast, 6H1 antibody showed nano molar (nM) range affinities to all three antigens with similar $k_a$ ($k_a = 2.69 \times 10^5$ Ms-1) to human tau and low $k_a$ for mouse tau. The $k_d$ value for $Tau^{RD\Delta K}$ was higher compared to the other 2 antigens (human tau and mouse tau). Therefore the affinity of the 6H1 towards $Tau^{RD\Delta K}$ ($K_D$ = 19.19 nM) was higher than to the other 2 antigens ($hT40^{WT}$ - 51.34 nM and mouse tau – 133.2 nM). Antibody

| **Sample** | | **2B10 (2677 nM)** | **6H1 (866 nM)** | **6B5 (250 nM)** | **8E7 (72 nM)** |
|---|---|---|---|---|---|
| **$hTau40^{WT}$** | **$K_D$ (M)** | 13.22 µM | 51.34 nM | 138.1 nM | 2.10 nM |
| | **$k_a$ ($Ms^{-1}$)** | $2.02 \times 10^3$ | $2.69 \times 10^5$ | $1.17 \times 10^5$ | $7.34 \times 10^6$ |
| | **$k_d$ ($s^{-1}$)** | $2.68 \times 10^{-2}$ | $1.38 \times 10^{-2}$ | $1.62 \times 10^{-2}$ | $1.54 \times 10^{-2}$ |
| **$Tau^{RD\Delta K}$** | **$K_D$ (M)** | 1.21 µM | 19.19 nM | 4.92 nM | 0.59 nM |
| | **$k_a$ ($Ms^{-1}$)** | $2.22 \times 10^4$ | $1.55 \times 10^5$ | $1.37 \times 10^5$ | $7.21 \times 10^6$ |
| | **$k_d$ ($s^{-1}$)** | $2.69 \times 10^{-2}$ | $2.97 \times 10^{-3}$ | $6.89 \times 10^{-4}$ | $4.29 \times 10^{-3}$ |
| **mTau** | **$K_D$ (M)** | 11.87 µM | 133.2 nM | 184.5 nM | 1.11 nM |
| | **$k_a$ ($Ms^{-1}$)** | $1.57 \times 10^3$ | $5.72 \times 10^4$ | $3.19 \times 10^4$ | $8.87 \times 10^6$ |
| | **$k_d$ ($s^{-1}$)** | $1.86 \times 10^{-2}$ | $7.62 \times 10^{-3}$ | $1.49 \times 10^{-4}$ | $1.00 \times 10^{-3}$ |

**Table 3.1: Affinity analysis of antibodies by BLItz.**

6B5 also showed nano molar range affinities to all FL/RD human tau constructs and mouse tau but with highest affinity for $Tau^{RD\Delta K}$. 8E7 antibody had the strongest binding affinities to $hTau40^{WT}$ ($K_D$ = 2.10 nM), $Tau^{RD\Delta K}$ ($K_D$ = 0.59 nM) and mTau40 ($K_D$ = 1.11 nM). 8E7 antibody showed similar high $k_a$ and $k_d$ values to the three antigens. Of all the tested antibodies, the 2B10 antibody showed the weakest affinities with micro molar (µM) range binding affinity. The other antibodies showed nano molar (nM) range binding affinities to human and mouse tau.

### 3.7 Antibodies eluted at acidic pH have enhanced activity

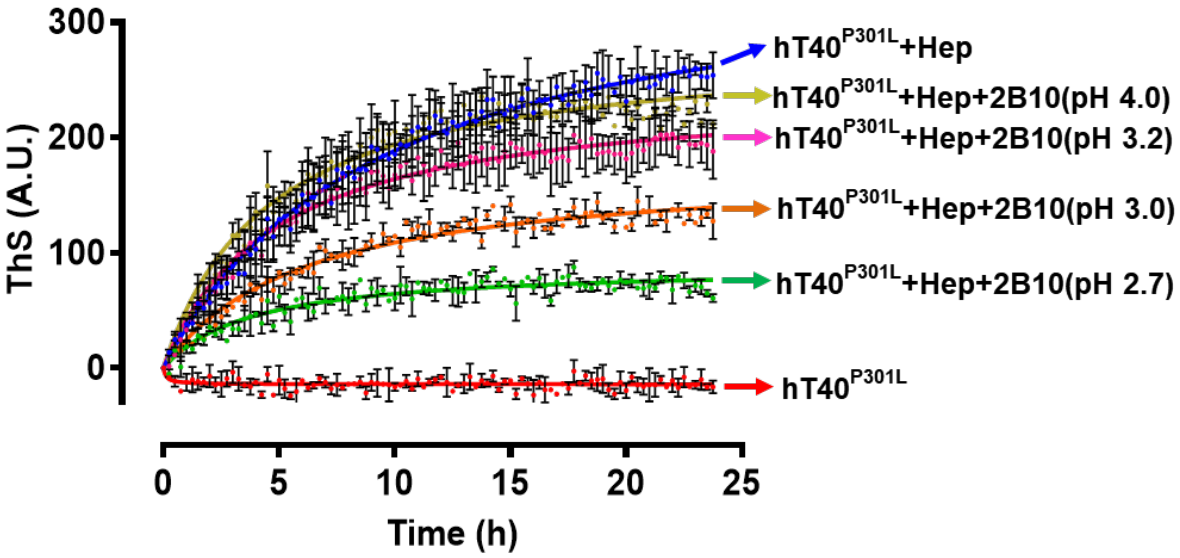


**Figure 3.7: Activity of antibodies depends on pH of elution buffer.**
10 µM of recombinant $hTau^{P301L}$ (2N4R) was incubated in the presence of heparin (2.5 µM) and 10 µM of mAb in BES pH 7.0 and the aggregation kinetics were monitored for 24 h at 37°C in the presence of the dye ThS (40 µM). Anti-tau antibody 2B10 eluted at acidic pH of 2.7 (green curve) had higher activity than the antibody eluted at lower acidic pH of 4.0 (yellow curve) compared to the control i.e. $hTau^{P301L}$ with heparin and without antibody (blue curve). As the pH of the elution buffer of the antibodies increased from more acidic (pH 2.7) to less acidic (pH 4.0) the antibodies lose their ability to block the aggregation of tau (green, orange, pink and yellow curves). Abbreviations: $hTau^{P301L}$, full length human tau with mutation of proline to leucine at the 301 position; Hep, heparin 16000; ThS, thioflavin S.

Different batches of 2B10 antibody showed differences in their ability to inhibit the aggregation (data not shown). We assumed that this was due to the differences in purification. Moreover it is known that low-pH elution buffer-exposed IgG antibodies acquire enhanced activity (Djoumerska-Alexieva et al., 2010). Therefore, 2B10 antibody purification was carried out at different acidic environments. The purified antibody was tested for its ability to block the tau-tau interaction leading to aggregation.

Usually 10 µM of antibody with 10 µM of hTau$^{P301L}$ were incubated to test aggregation in the presence of ThS and heparin in BES buffer pH 7.0. As expected, the antibodies eluted at different pH showed differences in their activity to block aggregation of tau. Figure 3.7 showed that hTau$^{P301L}$+heparin forms ThS positive aggregates (blue curve) whereas, an antibody (eluted at pH 4.0) did not inhibit the aggregation of the tau (yellow curve). In contrast, tau in the presence of antibody eluted at pH 2.7 decreased the aggregation of tau significantly (green curve). Antibody eluted at pH 3.0 and 3.2 displayed significant reduction in the aggregation of tau (brown and pink curves respectively). Taken together, we conclude that the higher the acidity (i.e. lower pH) of the elution buffer of the antibody is, the higher is the activity of the antibody to inhibit tau aggregation.

### 3.8 Anti-tau oligomer antibodies block the aggregation of tau *in vitro*

Several studies reported the close association of the NFT burden and the degree of cognitive impairment in Alzheimer disease (Arriagada et al., 1992, Spillantini and Goedert, 2013, Braak and Braak, 1991a). As the process begins at least 20 years before any clinical manifestations of Alzheimer disease are detected, targeting tau aggregation offers a rational approach to treatment and prevention (Nelson et al., 2012). The use of monoclonal antibodies is one such approach for inhibiting tau aggregation. Identification of tau aggregation inhibitors depends primarily on assays conducted *in vitro* with recombinant human tau proteins. A primary assay which detects aggregation products includes ThS dye-based fluorescence (Kumar et al., 2014). These assays depend on exogenous polyanionic inducers such as heparin or RNA (Goedert et al., 1996, Kampers et al., 1996) to increase the rate and extent of tau aggregation. In the absence of inhibitors like antibodies, tau aggregates into PHF's, whereas in the presence of antibodies tau aggregation can be inhibited. Therefore we utilized the ThS assay to test the abilities of our antibodies to inhibit tau-aggregation. 10 µM of tau (aggregation prone mutants of tau - Tau$^{RD\Delta K}$ and hTau$^{P301L}$) and 10 µM of antibody were incubated at 37°C for 24 h in the presence of 40µM ThS and 2.5 µM heparin16000 along with appropriate controls. Kinetics of ThS were measured for

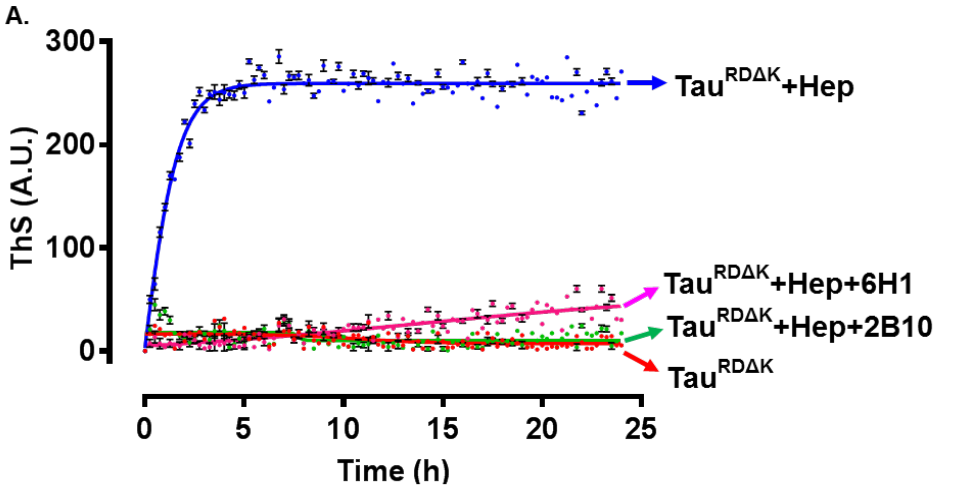


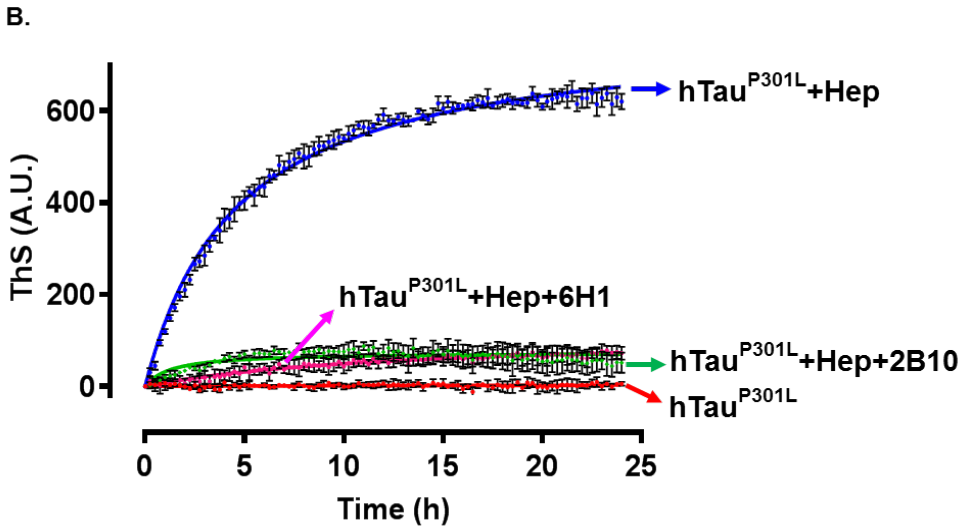


C.

| Antibody | 2B10 | 2G9 | 2H9 | 6B5 | 6H1 | 6H3 | 8E7 | 26G1 | 28D4 | 29E2 | 32E7 |
|---|---|---|---|---|---|---|---|---|---|---|---|
| % of hTau$^{P301L}$ aggregation inhibition | 90 | 44 | 12 | 18 | 89 | 21 | 64 | 73 | 58 | 70 | 48 |

**Figure 3.8: Anti-tau oligomer monoclonal antibodies block tau aggregation *in vitro*.** Monoclonal antibodies block the aggregation of tau into ThS positive aggregates. 10 µM of Tau$^{RDΔK}$ or hTau$^{P301L}$ was incubated in the presence of heparin (2.5 µM) and 10 µM of different monoclonal antibodies in BES pH 7.0 and the aggregation was monitored for 24 h at 37°C in the presence of ThS. **A)** Antibodies 2B10 (green curve) and **(B)** 6H1 (pink curve) effectively blocked the aggregation of Tau$^{RDΔK}$ and hTau$^{P301L}$ compared to their respective controls (blue curves). In the presence of antibodies the protein was restricted mostly to its monomeric form. **C)** Quantification of the ability of different mAb's blocking the aggregation of hTau$^{P301L}$ was summarized in the table. The number denotes the percentage of aggregation inhibition by the respective antibodies. Antibodies like 2B10 and 6H1 (green) are very robust in blocking the aggregation of tau by 90 & 89% respectively. Some antibodies like 8E7, 26G1, 28D4 and 29E2 block the aggregation by >50% whereas the antibodies like 2G9, 2H9, 6B5, 6H3 and 32E7 partially block the aggregation by <50%. Abbreviations: ThS, thioflavin S; Hep, heparin; h, hours. A.U., arbitrary units.

every 15 min. In the presence of heparin tau aggregated and reached saturation in 3 h for $Tau^{RD\Delta K}$ (blue curves in Figure 3.8 A) and 15 h in $hTau^{P301L}$ (blue curve in Figure 3.8 B) compared to tau monomers in the absence of heparin (red curves in Figure 3.8 A, B) which did not show any increase in ThS fluorescence even after 24 h. Antibodies 2B10 (green curve) and 6H1 (pink curve) inhibited the formation of ThS positive aggregates of tau dramatically (~90%).

Quantification of the aggregation inhibition of $hTau^{P301L}$ (tau:antibodies = 1:1 molar ratio concentration) showed that some antibodies like 2B10 and 6H1 were able to inhibit the aggregation of tau up to 90%, whereas some antibodies like 8E7, 26G1, 28D4 and 29E2 were able to inhibit aggregation up to>50% (Figure 3.8 B). Antibodies 2H9, 6B5 inhibited aggregation poorly (<20%).

This result confirms that anti-tau oligomer antibodies are able to inhibit the tau aggregation with different efficiencies.

### 3.9 Antibodies reduce tau aggregation by blocking the low-n oligomeric state

Fluorescence-based aggregation assays allow high throughput screening, so they are well suited for primary screens, whereas DLS and AFM microscopy approaches provide detailed insights regarding quantity, composition and morphology of aggregation species (Wegmann et al., 2012). The size of the tau species in the presence of antibodies after 24 h of aggregation in the presence of heparin at 37°C was measured by the DLS method. Figure 3.9 A shows the average hydrodynamic radius ($R_H$) of $hTau^{P301L}$ aggregates (blue curve) as ~60-100 nm in diameter, whereas the monomer (red curve) shows $R_H$ ~2-5 nm. The $R_H$ of aggregates was >20 fold higher than $R_H$ of monomers. This represents the presence of high molecular weight aggregates or fibrils in the $hTau^{P301L}$+heparin sample (blue curve). In the presence of antibody 2B10 (green curve) and 6H1 (pink curve) the average $R_H$ was ~10 nm and 25 nm diameter respectively. Thus, the average $R_H$ values of antibody treated samples corresponds to the low-n and high-n oligomers of tau. From the above observation, it is evident that antibody 2B10 binds to low-n oligomers (~2-5 monomers) and prevents the tau aggregation thereafter. Similarly 6H1 antibody binds to low-n and high-n (>10 mers) oligomers and prevents further aggregation.

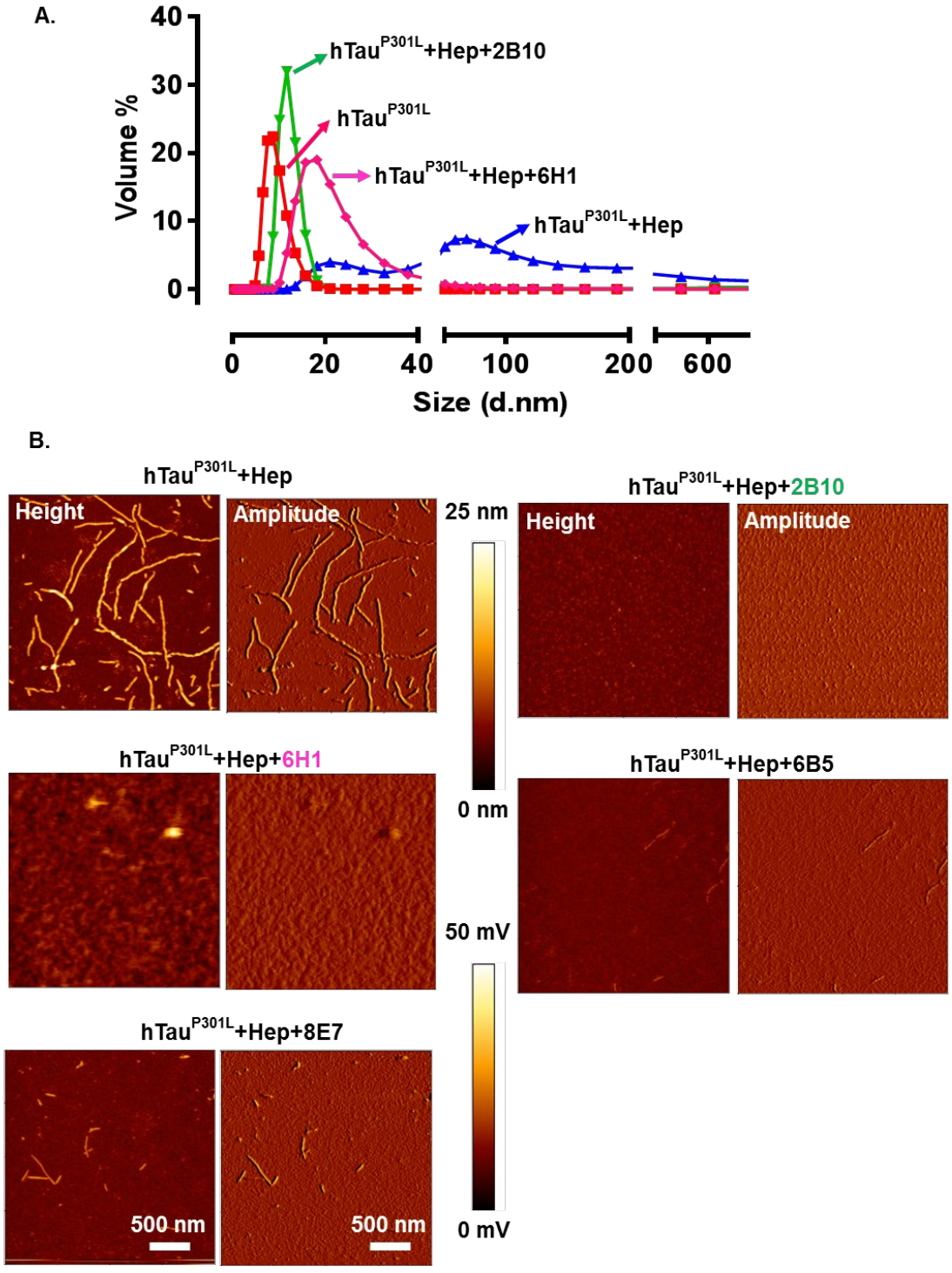


**Figure 3.9: Structural forms of tau in the presence of monoclonal antibodies.**
10 µM of hTau$^{P301L}$ was incubated in the presence of heparin (2.5 µM) with or without different antibodies (10 µM) in BES pH 7.0 for 24 h at 37°C. **A)** The hydrodynamic radius (measured by dynamic light scattering) of hTau$^{P301L}$ in the presence of antibodies 2B10 (green) and 6H1 (pink) was mostly in the range of low-n oligomers i.e. <20nm compared to that of the control (blue), which was in the range of 10-200nm. **B)** Height and amplitude images of atomic force microscopy revealed that antibody treated hTau$^{P301L}$ was mostly in the form of oligomers (2B10 and 6H1). Antibodies like 6B5 and 8E7 showed few aggregated forms of tau.Abbreviation: d. nm, diameter in nanometer; nm, nanometer; mV, milli volt.

Structural analysis is necessary to determine the nature of aggregates. We performed AFM analysis that revealed the morphology of the tau in the presence and absence of the antibodies. Figure 3.9 B shows the height and amplitude images of the tau. In the absence of antibodies, hTau$^{P301L}$ formed lengthy PHF's which are clearly visible in height and amplitude images. The height of the hTau$^{P301L}$ PHF's were broadly in the range of 10-18 nm. In the presence of the antibody 2B10, tau aggregation was restricted up to low-n oligomers that were characterized by their globular shape with an average height of 2-3 nm that corresponded to the dimer-tetramer of tau oligomers (Kaniyappan et al., 2017). In the presence of the antibody 6H1, tau was restricted to low-n oligomers and some bigger aggregates. In both cases, no tau filaments were observed. Antibodies 6B5 and 8E7 also inhibited the tau aggregation, but to a lesser extent. In the presence of 6B5 and 8E7 antibodies, short tau-filaments were observed on mica by AFM.

Taken together, we conclude that anti-tau oligomer monoclonal antibodies are active in inhibiting the aggregation of tau *in vitro* and halt the growth at the oligomer state.

### 3.10 Concentration dependent activity of antibodies to block tau aggregation

For any inhibitor (antibody) that binds reversibly to a single site on a target molecule (i.e., a 1:1 binding stoichiometry), one expects that binding, hence inhibition, will be saturable leaving no traces of active target (aggregation-competent tau). To determine the concentration of antibody required to diminish the aggregation of tau protein, different stoichiometric concentrations of antibodies were employed to inhibit tau aggregation. Based on the previous observations (Figure 3.8 C) regarding the ability of antibodies to inhibit the tau aggregation in ThS fluorescence kinetics, low concentrations of 2B10, 6H1, 8E7 and high concentrations of 6B5 antibodies were tested against 10 µM of hTau$^{P301L}$. Figure 3.10 A shows hTau$^{P301L}$+heparin aggregated effectively (blue curve). Tau protein in the presence of antibody at 1:1 ratio inhibited tau aggregation by 3-4 ~fold (green curve). Reducing the concentration of antibody (Tau:Antibody = 1:0.5 (orange curve) and 1:0.25 (pink curve)), showed the aggregation inhibition in a concentration dependent manner. In Figure 3.10 B 6H1 antibody at 10 µM (pink curve) and 5 µM (orange curve) concentrations decreased the aggregation propensity of tau by ~3-4 fold. At 2.5 µM (green curve) concentration also showed a

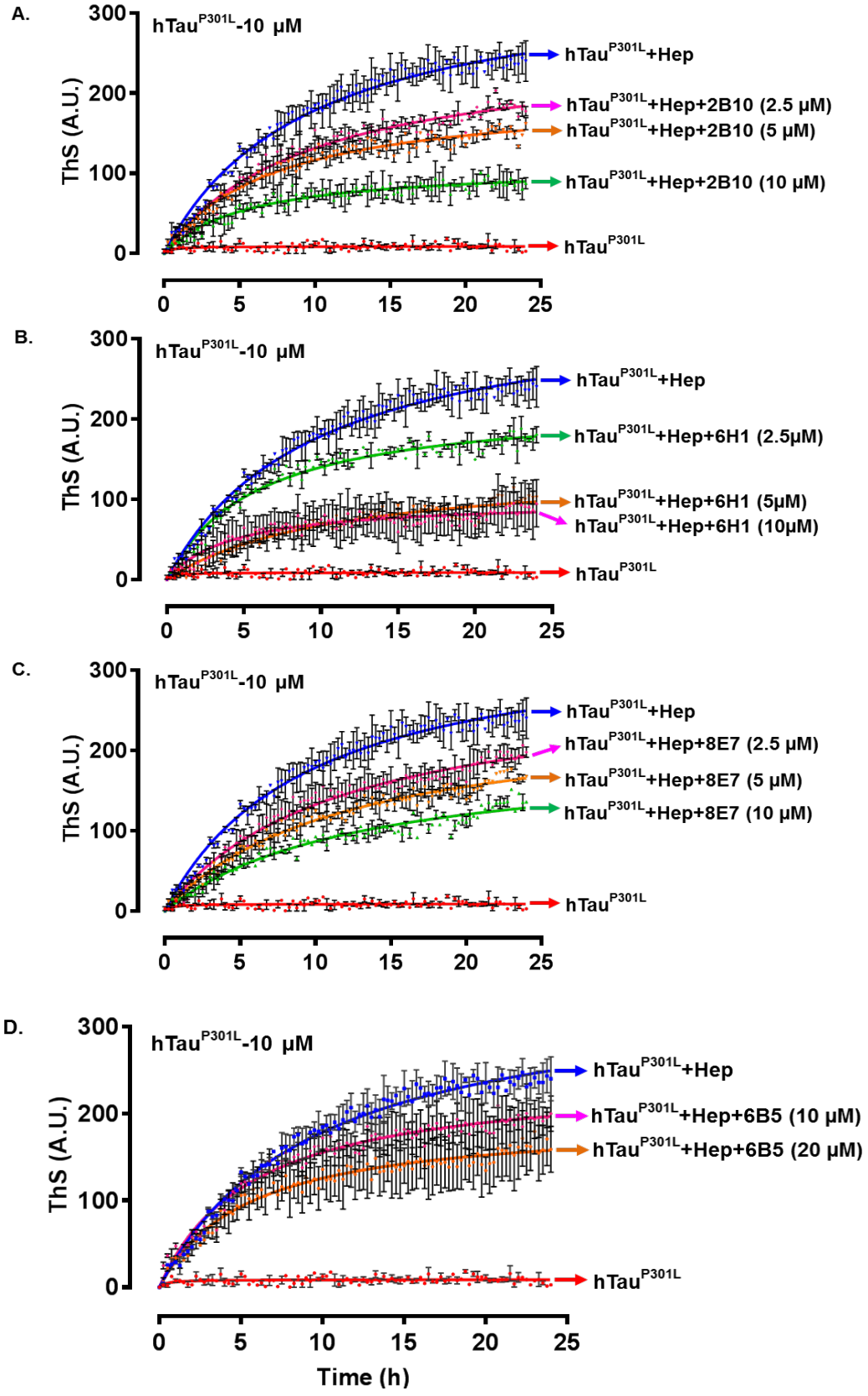


**Figure 3.10: Antibody dependent inhibition of tau aggregation.**
Inhibition of aggregation of tau by anti-tau antibodies is dependent on the molar ratio of antibody to tau concentration. 10 µM of hTau$^{P301L}$ was incubated with different concentrations of antibody in the

presence of heparin. **A)** 2B10 antibody at 10 µM (green curve) was able to inhibit tau aggregation better than 5 µM (orange curve) and 2.5 µM (pink curve) **B)** 6H1 antibody at 10 µM (pink curve) and 5 µM (orange curve) concentrations showed similar activity at inhibiting tau aggregation but at lower concentrations of 2.5 µM (green curve) it showed decreased ability to inhibit tau aggregation. **C)** 8E7 antibody showed concentration dependent inhibition of tau aggregation. 10 µM (green curve) of antibody showed better inhibition compared to 5 µM (orange curve) and 2.5 µM (pink curve). **D)** 6B5 antibody did not show any significant difference in inhibiting tau aggregation even after increasing the antibody concentration from 10 µM (pink curve) to 20 µM (orange curve). Abbreviation: ThS, thioflavin S; A.U., arbitrary unit; Hep, heparin 16,000.

decrease in tau aggregation, however the effect was smaller. Similarly in Figure 3.10 C the antibody 8E7 showed concentration dependent inhibitory activity. As the concentration of antibody increased from 2.5 µM (pink curve) to 5 µM (orange curve) and 10 µM (green curve), there was an increase in the antibody's ability to inhibit tau aggregation.

Figure 3.10 D, 10 µM (pink curve) of 6B5 antibody did not inhibit the aggregation whereas increasing the concentration up to 2 fold i.e. 20 µM (orange curve) had a noticeable effect. The results demonstrate that antibodies 2B10 and 6H1 are able to inhibit tau aggregation at approximately equal stoichiometric ratios of tau to antibody whereas other antibodies such as 6B5 were not able to inhibit the aggregation even at higher concentration.

## 3.11 Intracellular delivery of antibodies has no effect on aggregation of tau and early apoptosis in N2a cells expressing Tau$^{RD\Delta K}$

Inhibition of tau aggregation within the neurons is one of the major targets in the field of tauopathies. Since the experimental results of tau aggregation inhibition by monoclonal antibodies *in vitro* was successful we further subjected them to test in cell culture models. N2a cells with inducible expression of Tau$^{RD\Delta K}$ forms fibrous aggregates (Khlistunova et al., 2006) and the population of cells with aggregates can be measured by the dye ThS. ThS is cell permeable when added to the cell culture medium and its fluorescence can be recorded in live cells using flow cytometry (Pickhardt et al., 2017).

Since tau aggregation takes place intracellularly, the antibodies have to be delivered into the cells to combat tau aggregation. Antibodies can be internalized via bulk endocytosis or via receptor Fc mediated endocytosis (Congdon et al., 2013). However,

for experimental purposes we used the Xfect protein transfection reagent to deliver antibodies directly into the cells. The representative image Figure 3.11A shows that anti-tau antibodies were delivered into the N2a-cells expressing $Tau^{RD\Delta K}$ using Xfect transfection reagent. After 2 h N2a cells were incubated with 1 µg/ml of doxycycline and 0.0005% ThS for 96 h and ThS positive cells were measured using flow cytometry. ThS fluorescence was detected in the green-channel (y-axis) and diffracted light around the cell (intensity proportional to cell diameter) is measured as forward scatter (x-axis). In Figure 3.11B, antibodies 2B10 (3.40%), 6H1 (3.73%) and 6B5 (3.48%) treated cells at 15 µg/well (166.6 nM) concentration did not show any significant differences in ThS+ cell population compared to the control (3.38%). This indicates that these antibodies were inefficient at blocking the aggregation of tau in the cells. By contrast, cells treated with antibody 8E7 showed a slight (4.02%) increase in ThS+ cell population compared to control, suggesting some enhancement of aggregation. None of the other antibodies reduced ThS positive cells. Taken together we conclude that antibodies at this concentration are ineffective in inhibiting the aggregation in cells.

Annexin V (AnnV) is an indicator of early steps in apoptosis, which can be measured by incubating the cell with fluorescent AnnV (AnnV-APC for red fluorescence). Allophycocyanin (APC) is an intensely bright phycobili protein that exhibits far-red fluorescence. AnnV binds to the cells that display phosphatidylserine (PS) on the cell surface during the event of early apoptosis. AnnV positive cells can be measured in flow cytometer by using APC conjugated AnnV. N2a cells over-expressing $Tau^{RD\Delta K}$ in the presence of doxycycline show moderate cell death due to expression and aggregation of $Tau^{RD\Delta K}$. Therefore we further investigated whether the antibodies can rescue the cells from toxic effects induced by $Tau^{RD\Delta K}$. Anti-tau antibodies were delivered into the cells using Xfect transfection reagent as before and AnnV positive cells were measured after the antibody treatment (96h in cells). In Figure 3.11 C, antibodies 2B10 (1.02%), 6H1 (1.22%), 6B5 (1.64%) and 8E7 (1.50%) treated cells did not show any significant differences in AnnV population compared to the control (1.18%). None of the antibodies have shown any decrease in the early apoptosis caused by $Tau^{RD\Delta K}$. Overall, the intracellular delivery of anti-tau antibodies did not

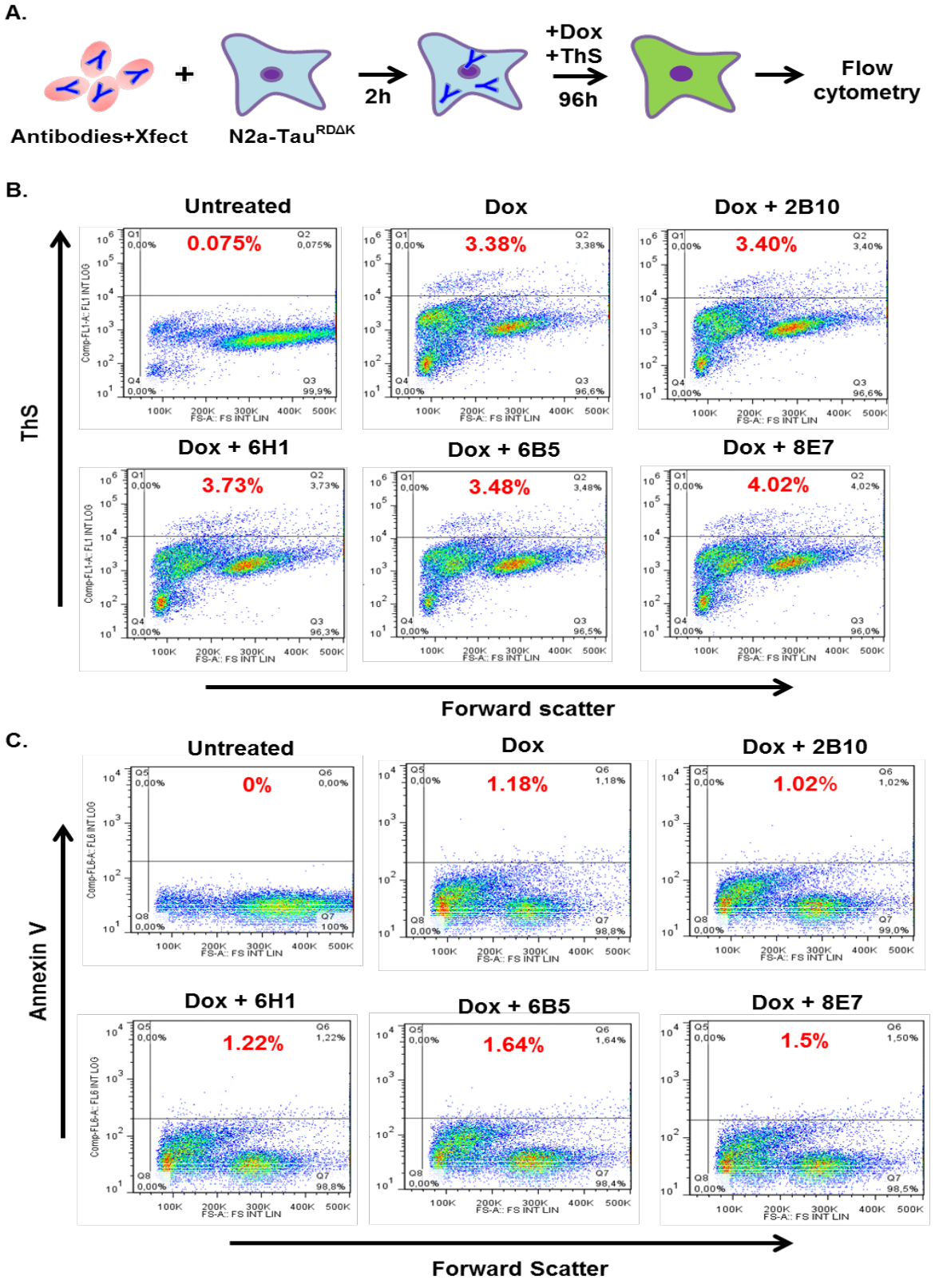


**Figure 3.11: Intracellular delivery of antibodies has no effect on tau aggregation.**
15 µg/well (25 µg/ml) of anti-tau oligomer antibodies were delivered into the cells (N2a-Tau$^{RD\Delta K}$) using Xfect reagent to combat the aggregation of tau in cells (as judged by decrease in ThS+ cells) and rescue the cells from apoptosis (by decreasing APC-Annexin V staining- a pre-apoptotic marker).

**A)** Diagram of the Xfect protein transfection procedure: antibodies encapsulated in Xfect reagent (pink) were incubated with N2a-Tau$^{RD\Delta K}$ for 2 h. Later N2a cells were incubated with 1 µg/ml of doxycycline and 0.0005% ThS for 96 h (stained with Annexin V after 96 h). ThS/Annexin V positive cells were counted using flow cytometry and plotted in a graph of forward scatter (cell diameter, x-axis) versus fluorescence (ThS/Annexin V fluorescence intensity, y-axis). **B)** Forward scatter plot (cell volume, x-axis) versus "green" channel (ThS fluorescence, y-axis). Area II (Q2) represents the ThS positive cell population. Dox induced cells showed 3.38% ThS positive cells. None of the antibodies have reduced ThS positive cell population. **C)** Forward scatter plot (cell volume, x-axis) versus "red" channel (APC Annexin V fluorescence, y-axis). Area II (Q2) represents the AnnV positive cell population. Dox induced cells showed 1.18% AnnV positive cells. None of the antibodies rescued the cells from pathological effects caused by Tau$^{RD\Delta K}$. Abbreviations: AnnV, Annexin V; ThS, thioflavin S; Q2, quadrant 2.

show any significant effects in blocking the tau aggregation or decreasing the early apoptosis caused by the pro-aggregant tau.

### 3.12 Tau split-luciferase protein-fragment complementation assay

Data from experiments described above suggests that antibodies were effective at blocking tau aggregation *in vitro* but not in N2a cells expressing Tau$^{RD\Delta K}$, as judged by ThS fluorescence assay (reflecting the end products of aggregation/high molecular weight aggregates). Therefore antibodies were further tested to explore whether they can inhibit the initial stages of tau aggregation, i.e., dimerization or oligomerization. For this purpose, we adopted a well-characterized macromolecular interaction platform i.e. split-luciferase complementation assay (Villalobos et al., 2010). Tau$^{RD\Delta K}$ was fused with either N-terminal (Luc-N) or C-terminal (Luc-C) fragments of click beetle green luciferase. N2a wildtype cells were used to interrogate the interaction of Tau$^{RD\Delta K}$ monomers which was monitored by luciferase protein fragment complementation and analyzed by bioluminescence imaging of live cells (Wang et al., 2017). After 15 h of co-transfection of tau constructs (Tau$^{RD\Delta K}$-Luc-N+ Tau$^{RD\Delta K}$-Luc-C) in N2a cells, the dimerization of tau can be measured by bioluminescence of luciferin (Figure 3.12, first well and bar 1). But in case of cells transfected either with Tau$^{RD\Delta K}$-Luc-N or Tau$^{RD\Delta K}$-Luc-C did not show any bioluminescence signal which shows that without the presence of two complement luciferase constructs there is no bioluminescence signal detected (Figure 3.12, bar 2, 3). To rule out the possibility of a bioluminescence signal without tau, we co-transfected the N2a cells with Luc-N and Luc-C constructs without any tau. In this case there was no luminescence signal detectable (Figure 3.12, well 4 and bar 4). These results confirm that bioluminescence based on tau-split luciferase

protein-fragment complementation assay is an ideal assay to detect initial a key early step in tau aggregation.

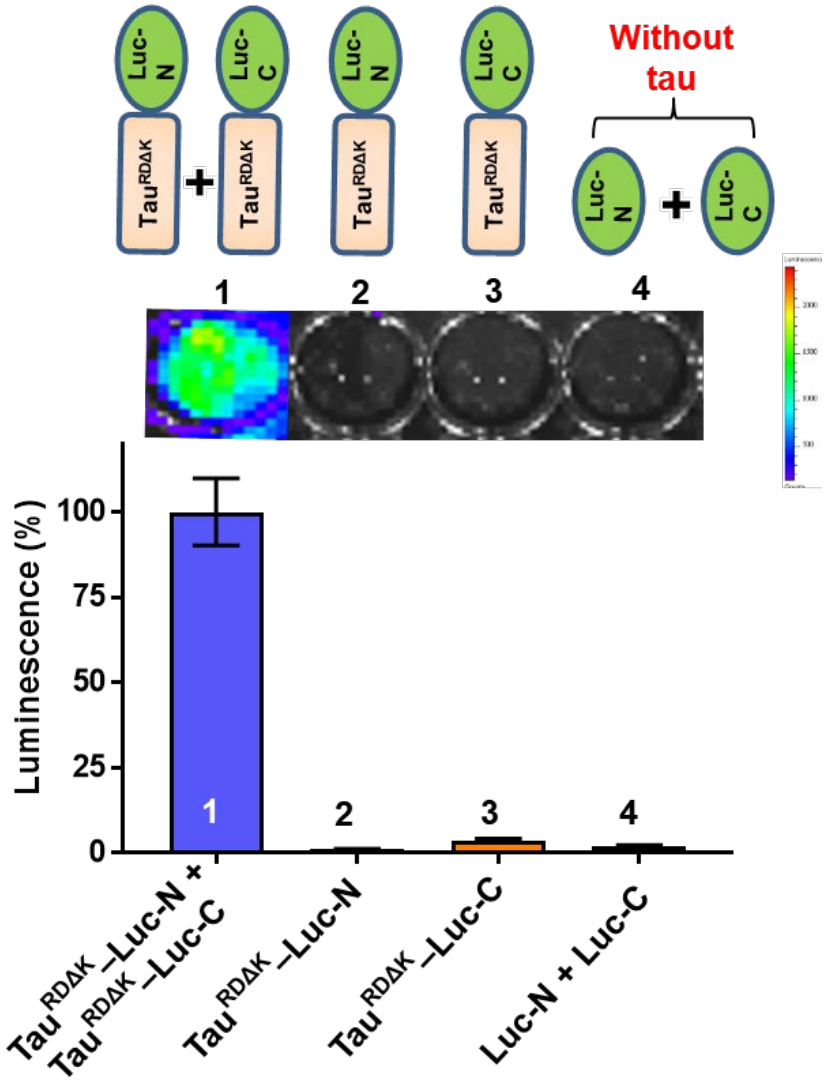


**Figure 3.12: Tau-luciferase protein-fragment complementation assay.**
Click-beetle green luciferase gene was split in to two complementary units containing N-terminal (Luc-N) and C-terminal (Luc-C) parts. These two complementary fragments are fused to the C-terminal end of Tau$^{RD\Delta K}$. The diagram at top shows the luciferase bioluminescence in N2a cells expressing tau constructs (Tau$^{RD\Delta K}$-Luc-N+ Tau$^{RD\Delta K}$-Luc-C) (bar 1). No bioluminescence was observed in cells expressing controls (Tau$^{RD\Delta K}$-Luc-N, bar 2), (Tau$^{RD\Delta K}$-Luc-C, bar 3), (Luc-N + Luc-C, bar 4). Tau$^{RD\Delta K}$, pro-aggregant repeat domain tau; Luc-N, luciferase N-terminal part; Luc-C, Luciferase C-terminal part. (n=3; one-way ANOVA with Tukey's post hoc test; F (3, 8) = 98.08; ****$P$=<0.0001).

## 3.13 Antibodies inhibit tau dimerization in tau-luciferase protein-fragment complementation assay

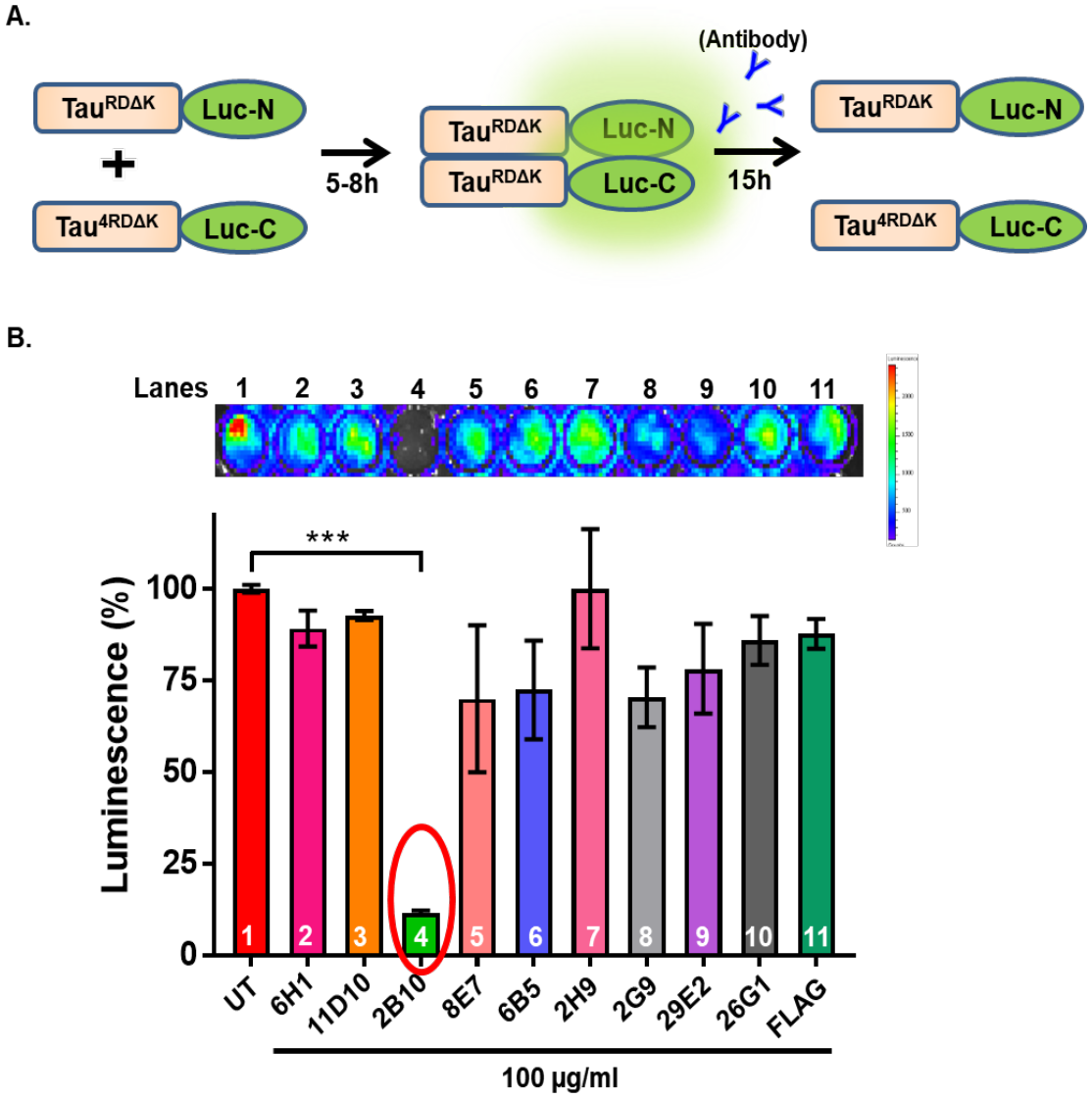


**Figure 3.13: Effect of antibodies on dimerization of tau monitored by tau-luciferase protein-fragment complementation assay.**
**A)** Graphical representation showing tau-luciferase protein-fragment complementation assay. N2a cells were co-transfected with Tau$^{RD\Delta K}$-Luc-N and Tau$^{RD\Delta K}$-Luc-C. Affinity of tau molecules (dimerization or oligomerization) will lead to complementation of both split luciferase fragments resulting in measurable bioluminescence signal. Bioluminescence signal indicates tau dimerization and hence aggregation. Antibody treatment blocks tau dimerization and decreases the bioluminescence signal intensity. **B)** N2a cells expressing these constructs were treated with 100 µg/ml of various antibodies. Representational image of 96 well plate showing ability of antibodies in blocking tau aggregation was recorded by capturing the bioluminescence intensity. Histogram was plotted based on the recorded bioluminescence intensity values. 2B10 antibody (bar 4, red oval) shows significant decrease in bioluminescence signal compared to untreated N2a cells (n=3; one-way ANOVA with Tukey's post hoc test; F (10, 22) = 5.755; ****P*=0.0003.

Monoclonal antibodies are further tested to explore their ability to attenuate the tau aggregation process at the stage of dimerization. N2a cells were co-transfected with tau-luciferase constructs ($Tau^{RD\Delta K}$-Luc-N + $Tau^{RD\Delta K}$-Luc-C) and after 5-8 h of DNA-transfection, antibodies were incubated for 15 h in the extracellular medium (without any transfection reagent) followed by imaging (Figure 3.13 A). Figure 3.13 B shows that treatment with antibodies has shown significant differences in bioluminescence signal which relates to changes in tau dimerization in cells. 2B10 antibody (bar 4, red oval) dramatically decreased tau dimerization, as it has shown only ~10% bioluminescence intensity (lane 4) compared to the untreated (bar 1; lane 1) and control non-specific FLAG antibody treated cells (bar 11; lane 11). Some antibodies like 8E7 (bar 5; lane 5), 6B5 (bar 6; lane 6) and 2G9 (bar 8; lane 8) showed ~60% bioluminescence signal compared to control but the result was not statistically significant. By contrast, antibodies like 6H1 (bar 2; lane 2), 11D10 (bar 3; lane 3), 2H9 (bar 7; lane 7), 29E2 (bar 9; lane 9), and 26G1 (bar 10; lane 10) did not show any significant difference compared with controls. From these results, we conclude that antibody 2B10 efficiently blocks the dimerization/oligomerization of tau.

## 3.14 Antibody 2B10 blocks the dimerization in a concentration dependent manner

Antibody 2B10 was further tested to search for the lowest concentration of the antibody which reproduces the inhibition of dimerization or oligomerization in cells (Figure 3.13). N2a cells transfected with tau-luciferase constructs were incubated (extracellularly) with various concentrations of 2B10 antibody ranging from 6.25-100 µg/ml (Figure 3.14). Concentrations of the 2B10 antibody as low as 6.25 µg/ml (41 nM) (bar 2; lane 2) were able decrease the bioluminescence intensity to ~75% compared to the untreated (bar1; lane 1) and control antibody treated (bar 7; lane 7) samples. Higher amounts of 2B10 antibody like 12.5 µg/ml (83 nM) (bar 3; lane 3), 25 µg/ml (166 nM) (bar 4; lane 4) and 50 µg/ml (333 nM) (bar 5; lane 5) were able to decrease the bioluminescence intensity to ~60%. 2B10 antibody showed significant decrease in the bioluminescence intensity to ~40% at the highest concentration of 100 µg/ml (666 nM) (bar 6; lane 6). 2B10 antibody decreased the bioluminescence in a concentration-dependent manner.

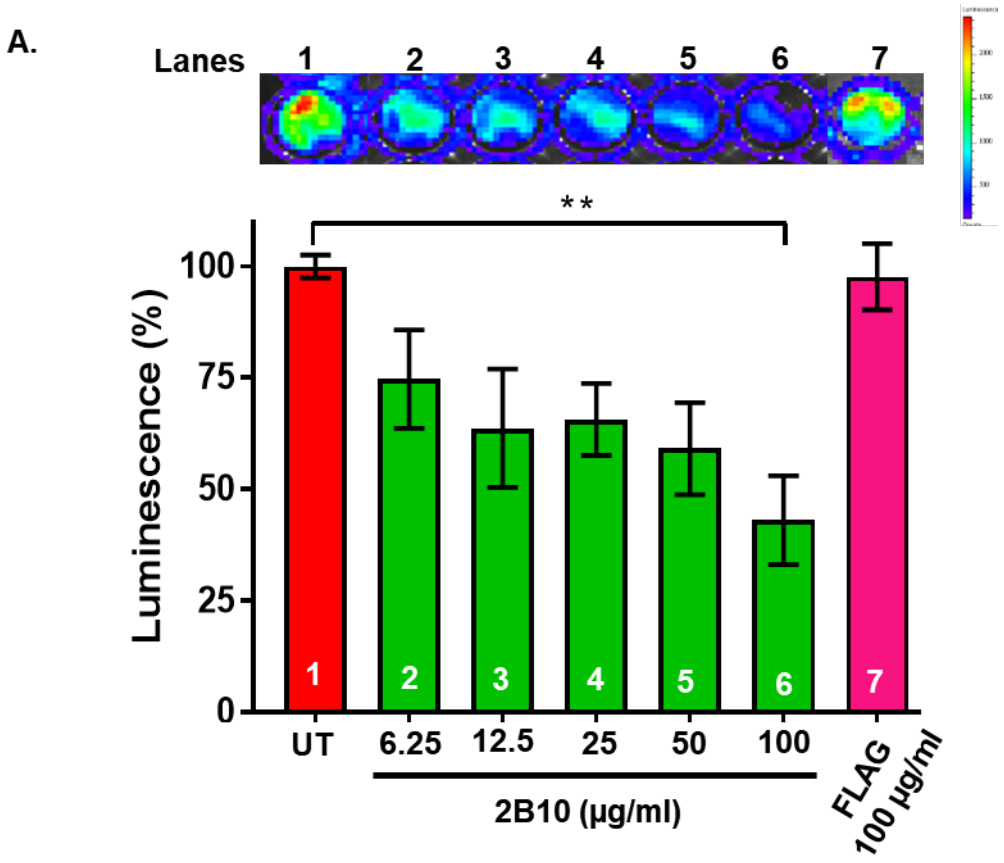


**Figure 3.14: 2B10 antibody inhibits the dimerization of tau.**
**A)** N2a cells were co-transfected with Tau$^{RD\Delta K}$-Luc-N and Tau$^{RD\Delta K}$-Luc-C constructs. Cells were treated with various concentrations (6.25, 12.5, 25, 50, 100 µg/ml) of 2B10 and control antibodies for 15h. Representative images illustrating the decrease in bioluminescence intensity are shown on top and quantified in the histogram. 100 µg/ml (bar 7) of 2B10 antibody showed significant decrease in bioluminescence compared with the controls (bars 1, 2). By contrast, 100 µg/ml (bar 7) of control FLAG antibody did not show any significant difference with the controls (bars 1, 2) (n=3; one-way ANOVA with Tukey's post hoc test; F (7, 16) = 4.481; ***P*=0.0062).

## 3.15 Uptake of antibodies by N2a cells

From the results described above, it is evident that antibodies which are applied extracellularly are able to inhibit the intracellular oligomerization of tau (fragment complementation assay). But the question remains how these extracellular antibodies are acting on intracellular tau aggregation? We therefore explored whether the antibodies enter the cells, using published procedures (Shamir et al., 2016). Antibody uptake assay was done with the A647 fluorophore tagged 2B10 antibody and non-specific FLAG antibodies. Different concentrations of antibodies ranging from 10-60 µg/ml (66-400 nM) were added to N2a wildtype cells and N2a cells expressing

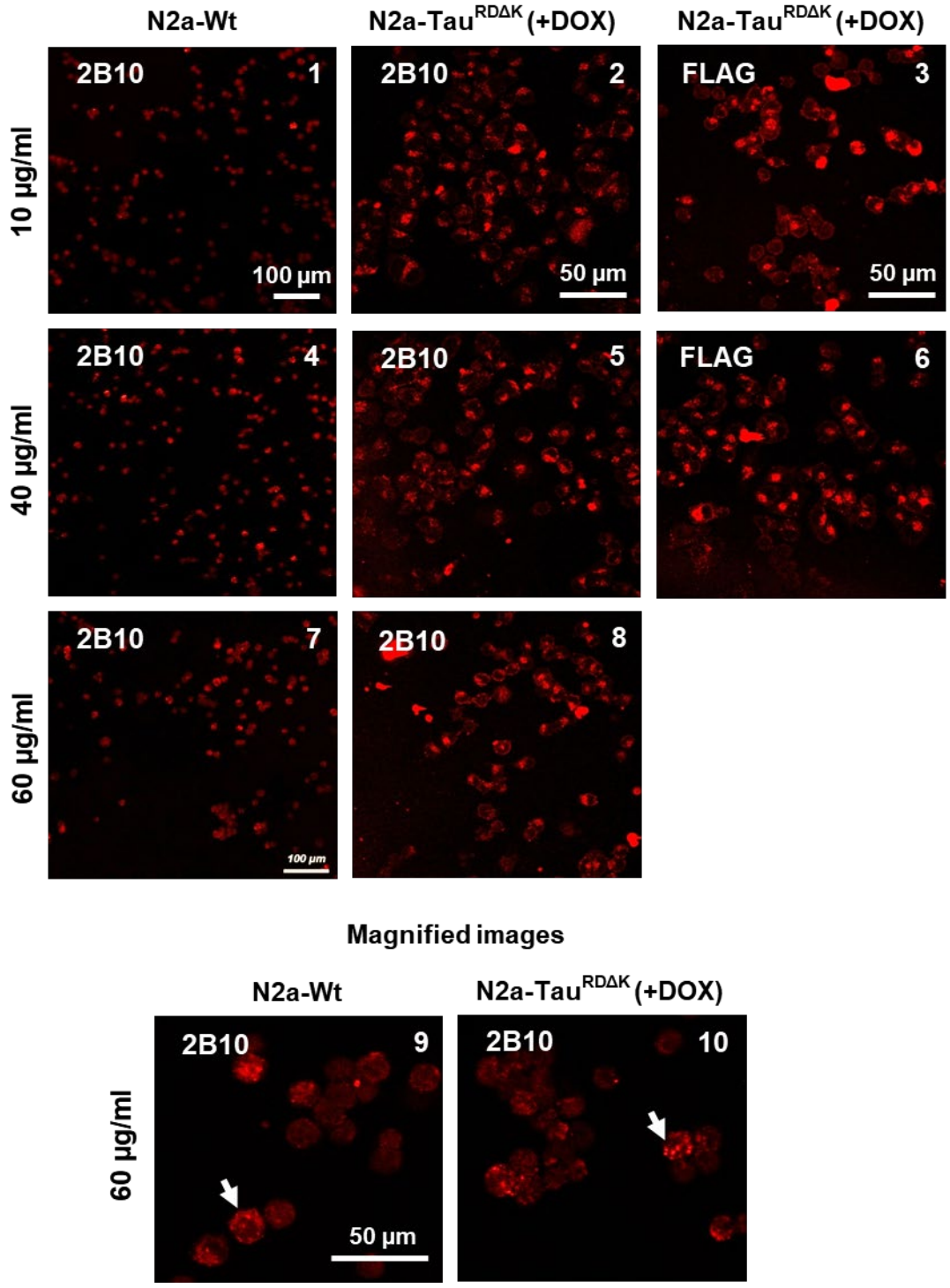


**Figure 3.15: Internalization of tau antibodies.**
Uptake of antibodies by cells was monitored by immunofluorescence. N2a- wt cells or N2a cells expressing Tau$^{RD\Delta K}$ were treated extracellularly with 10-60 µg/ml of Alexa647 tagged 2B10 (red) and non-specific FLAG (red) antibodies for 24 h. Cells were then fixed for immunocytochemistry. Alexa tagged 2B10 antibody showed uptake both in N2a-wt (images 1, 4, 7) and N2a-Tau$^{RD\Delta K}$ (images 2, 5, 8) cells. Non-specific FLAG antibodies were also taken up by N2a-Tau$^{RD\Delta K}$ cells (images 3, 6). Magnified images of 2B10 antibody (images 9, 10) showed localization of antibody as punctate structures (white arrows) in the cells. Abbreviations: Wt, wild type; Tau$^{RD\Delta K}$, pro-aggregant repeat domain tau; DOX, doxycycline.

$Tau^{RD\Delta K}$ in the extracellular medium for 24 h, then cells were fixed to observe the antibody uptake. After 24 h, uptake of 2B10 antibody was observed in both cells types (N2a-wt, N2a- $Tau^{RD\Delta K}$) irrespective of the presence or absence of the tau inside the cell. Antibody uptake was observed at all concentrations (10, 40 and 60 µg/ml of 2B10 antibody) in both the N2a-wt cells (Figure 3.15, images 1, 4, 7) and N2a- $Tau^{RD\Delta K}$ cells (Figure 3.15, images 2, 5, 8). Surprisingly, non-specific FLAG antibody was also taken up by N2a- $Tau^{RD\Delta K}$ cells (Figure 3.15, images 3, 6). We also noticed at higher magnification that the antibodies in cells were not distributed homogeneously in the cytoplasm, but rather were localized as punctate dots (Figure 3.15, image 9, 10-arrowhead).

## 3.16 Localization of internalized antibodies in lysosomes of N2a cells

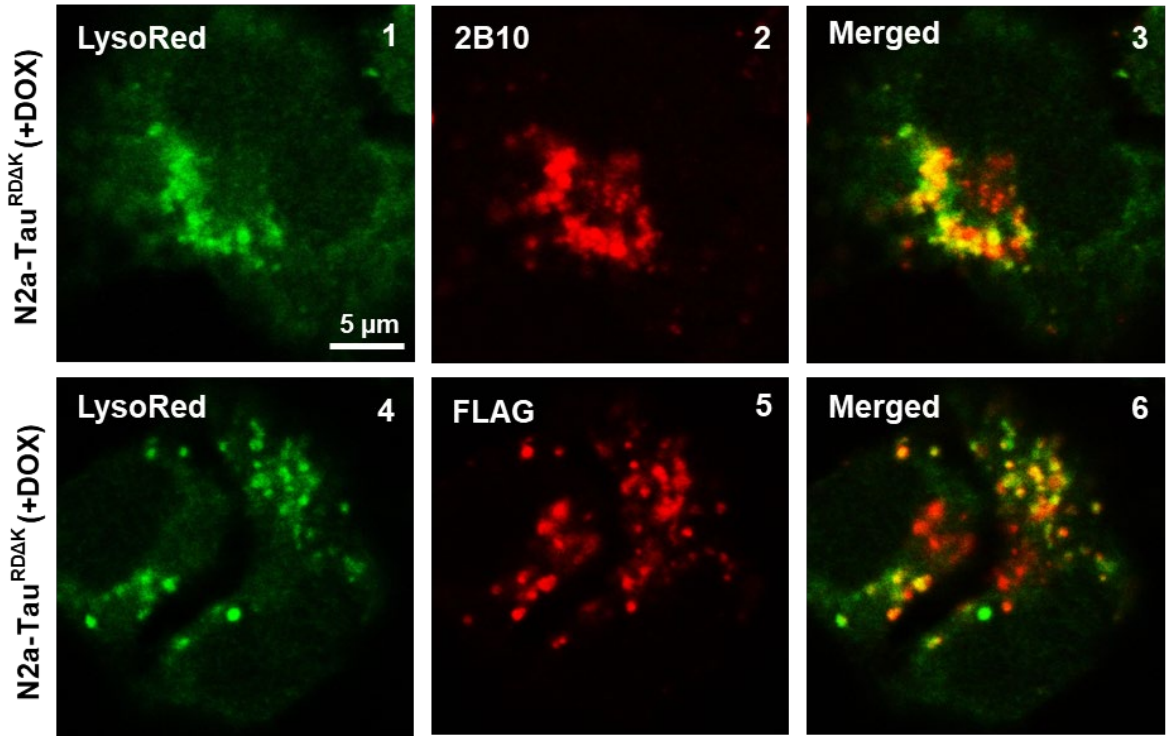


**Figure 3.16: Localization of antibodies in lysosomes.**
60 µg/ml of A647 labelled 2B10 (red) and FLAG (red) antibodies were applied extracellularly for 24 h with 75 nM of Lysotracker dye (green) on N2a-$Tau^{RD\Delta K}$ cells induced with doxycycline. Lysotracker dye stained the lysosomes (image 1, 4). 2B10 and FLAG antibodies were taken up by cells and localized as punctate structures (images 2, 5). These antibodies showed co-localization (yellow) with lysosomes (images 3, 6). Abbreviations: $Tau^{RD\Delta K}$, pro-aggregant repeat domain tau; DOX, doxycycline.

The above results (Figure 3.15, image 9, 10) suggest that the extracellular antibodies are internalized by N2a cells and are localized in punctate structures. In order to

understand the specific nature of these punctate structures in which antibodies are sorted we stained the cells with fluorescent dyes which label and track acidic organelles in living cells (LysotrackerRed DND 99). This dye is cell permeable and binds to lysosomes. 24 h of incubation of fluorophore labelled 2B10 (red) and non-specific FLAG (red) antibodies on N2a-Tau$^{RD\Delta K}$ cells showed a significant uptake of antibodies by cells and the antibody was compartmentalized in to punctate structures (Figure 3.16, images 2, 5). Lysotracker dye (green) stained the acidic organells with low pH in the cytoplasm (Figure 3.16, images 1, 4). Antibodies 2B10 and FLAG showed co-localization (yellow) with the lysotracker dye (Figure 3.16, images 3, 6) which confirms that the tau specific antibody 2B10 and non-specific antibody FLAG were internalized by the cells and were sorted to the lysosomes by an unknown mechanism.

### 3.17 Antibodies promote tau entry to lysosomes for its clearance

The antibodies added extracellularly were internalized by the cells and are sorted to lysosomes (Figure 3.16), however it is unknown whether the antibodies in lysosomes are bound to tau or antibodies promote sorting of tau to lysosomes. To test this we incubated N2a-Tau$^{RD\Delta K}$ cells (doxycycline, 48 h) with lysotracker dye (green) and fluorophore labelled 2B10 (red) or FLAG (red) antibodies (extracellularly) for 24 h followed by cell fixation and probing with K9JA antibody (blue). Lysotracker dye stained the lysosomes (green) (Figure 3.17, images 1, 5). Antibodies 2B10 (red) and FLAG (red) were taken up by the cells and compartmentalized as punctate structures (Figure 3.17, images 2, 6). K9JA antibody (blue) detected Tau$^{RD\Delta K}$ in N2a cells (Figure 3.17, images 3, 7). N2a Tau$^{RD\Delta K}$ cells treated with 2B10 antibody showed clear co-localization (white) with lysotracker dye and pan tau antibody K9JA (Figure 3.17, image 4, white arrows) whereas cells treated with control FLAG antibody cells did not show co-localization with the pan tau antibody (Figure 3.17, image 8). It is evident that tau was compartmentalized in 2B10 antibody treated cells (Figure 3.17, image 3) but in FLAG antibody treated cells tau was distributed all over the cell (Figure 3.17, image 7). This result shows that 2B10 antibody recruits the tau to lysosomes presumably for its clearance.

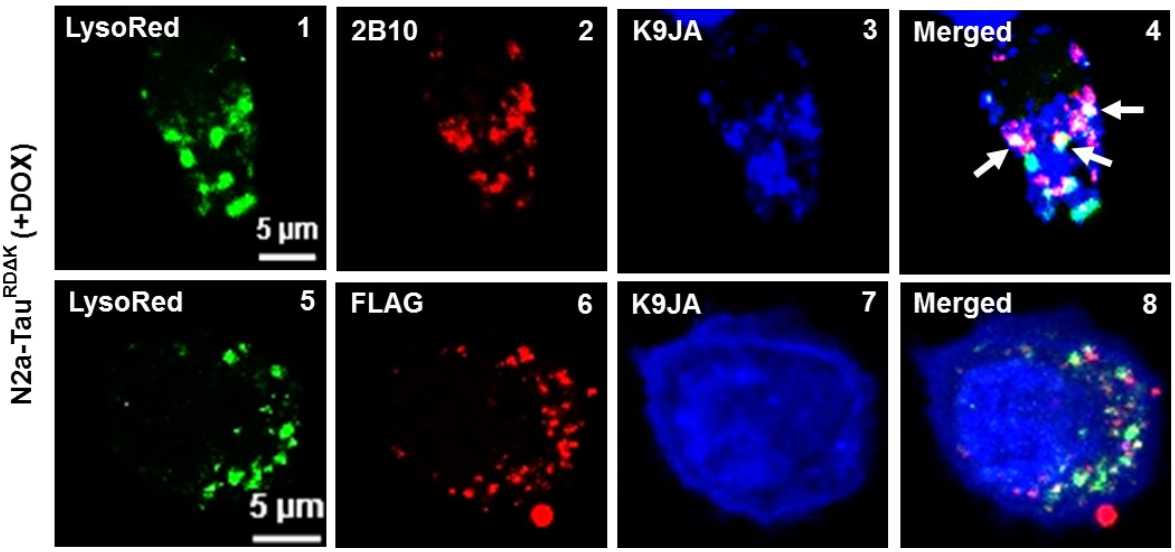


**Figure 3.17: Antibodies promote tau clearance via lysosomes**
60 µg/ml of Alexa647 labelled 2B10 (red) or FLAG (red) antibodies were applied extracellularly for 24 h with 75 nM of Lysotracker dye (green) on N2a-Tau$^{RD\Delta K}$ cells induced with doxycycline. Cells were fixed and probed with K9JA antibody (blue) which detected Tau$^{RD\Delta K}$ (image 3, 7). Lysotracker dye stained lysosomes (images 1, 5). 2B10 and FLAG antibodies were taken up by cells and compartmentalized (images 2, 6). 2B10 antibody shows co-localization with tau and lysosomes (image 4, white arrows) whereas FLAG antibody shows co-localization only with lysosomes but not with tau (image 8). Abbreviations: Tau$^{RD\Delta K}$, pro-aggregant repeat domain tau.

In conclusion, the monoclonal antibody 2B10 binds specifically to low-n oligomers of tau (dot blot, ELISA, IC and IHC) with weak affinity (BLI). Antibody 2B10 blocks the aggregation of tau *invitro* (ThS, DLS, and AFM) but fails to do so in N2a cells expressing Tau$^{RD\Delta K}$ (flow cytometry-ThS). Interestingly, 2B10 antibody added extracellularly is able to block the dimerization of tau in an antibody concentration dependent manner (split luciferase complement assay). Moreover, extracellularly added antibody enters the cells, binds to cytosolic tau (Tau$^{RD\Delta K}$) and recruits tau (presumably toxic oligomers) to lysosomes for degradation.

# 4 Discussion

## 4.1 Amyloid-β and tau in AD

Extracellular amyloid plaques comprising amyloid beta peptides and intracellular neurofibrillary tangles composed of tau in brain tissue represent the two major pathological hallmarks of AD (Fu et al., 2018). Therefore most therapeutic approaches have focussed on the reduction of these aggregates, either directly by inhibiting their formation, or indirectly by modulating the pathways that lead to aggregate deposition. Aβ-targeted approaches were initially (early 1990's) more favored because genetic evidence pointed to a causal role of APP cleavage leading to Aβ accumulation in familial AD (Hardy and Selkoe, 2002). Under normal physiological conditions, the transmembrane protein APP is cleaved by α and γ-secretases. During disease condition, improper cleavage of APP by "β secretase" releases Aβ peptides that aggregate into filaments in the extracellular matrix and cause synaptic degeneration. Thus attempts were made to inhibit β- or γ-secretases or to enhance α-secretases to lower the production of amyloid beta. These attempts have been discontinued for lack of efficacy or toxic side effects (Hampel et al., 2015). Other drugs were designed to inhibit Aβ aggregates to improve memory in transgenic mice. However, these approaches have not generated disease-modifying drugs so far, even though animal models showed promising results (Cummings et al., 2018).

As an alternative, the focus shifted to tau protein and its aggregates, particularly since mutations in the tau gene were recognized to cause different types of neurodegenerative tauopathies closely related to AD (e.g. frontotemporal dementia, Pick disease (Lee et al., 2001, Orr et al., 2017). Unlike APP and Aβ, tau is a highly soluble cytosolic protein which primarily binds to microtubules and stabilizes them in neuronal axons, thus enabling axonal transport or neurite outgrowth (Mandelkow and Mandelkow, 2012). Under pathological conditions, tau becomes post-translationally modified (e.g. by phosphorylation, proteolysis, acetylation, glycosylation, ubiquitinylation), and the corresponding enzymatic pathways served as entry points for drug developments (Holtzman et al., 2016). Other approaches included the lowering of tau in neurons (by drugs or antisense oligonucleotides), or interference with the spreading of tau pathology between brain regions (DeVos et al., 2018). As in the case

of Aβ, these approaches have not yet generated disease-modifying drugs for humans, in spite of promising results with animal models and in clinical trials up to phase II (Medina, 2018).

## 4.2 Immunotherapy for AD

An alternative treatment strategy is immunotherapy. The rationale for this approach is that antibodies against aggregating proteins (generated by passive or active immunization) can scavenge their targets and deliver them for destruction, for example in microglia or in lysosomes of neurons (Funk et al., 2015, Krishnamurthy et al., 2011). However, thus far Aβ targeted immunotherapy was not successful, and studies had to be halted because of inflammation and other side effects (Honig et al., 2018). Moreover Aβ targeted immunotherapy had low or no impact on tau pathology (Boche et al., 2010, Nelson et al., 2012, Congdon and Sigurdsson, 2018). Currently several tau-targeted immunotherapy studies (both active and passive immunotherapy) are underway. In animal models they led to reduction in tau aggregation, phosphorylation and cognitive decline in transgenic mice (Castillo-Carranza et al., 2014b, Castillo-Carranza et al., 2014a, Zilka et al., 2012, Kontsekova et al., 2014, Sigurdsson, 2014, Sankaranarayanan et al., 2015, Yanamandra et al., 2013).

Some of these studies targeted tau protein in general, i.e. all isoforms or assembly states (Yanamandra et al., 2013). The main advantage of focusing on total tau was that a larger pool of tau can be targeted. However, there was concern about potential toxicity associated with clearance of physiologically functional tau protein, and about the lack of distinction between diverse modified forms of tau (fragments, phosphorylation states etc.) (Pedersen and Sigurdsson, 2015). Alternatively other approaches targeted sites in the tau molecule involved in aggregation, or early forms of assembly (oligomers) considered to be the most toxic species. Examples are (1) antibody DC8E8 against an epitope in the repeat domain which prevents aggregation of tau (Kontsekova et al., 2014), (2) antibody TOMA against tau oligomers which prevents tau induced toxicity (Castillo-Carranza et al., 2014b).

## 4.3 Characterization of anti-tau low-n oligomeric antibodies

Our earlier study had shown that low-n oligomers of tau (prepared in a highly pure fashion, see below) do not affect cell viability as such. This was in contrast to other reports describing pronounced cytotoxicity of oligomer preparations as observed by MTT and LDH assays (Flach et al., 2012, Lasagna-Reeves et al., 2011). However, our low-n oligomers caused severe synaptotoxicity (Kaniyappan et al., 2017). These observations were consistent with early stages of AD pathology where synapses become impaired long before neurons decay (Yoshiyama et al., 2007, Conforti et al., 2007, Van der Jeugd et al., 2012). Since synapses are key regulators of learning and memory, we decided to target the species that destroys the synapses and therefore raised monoclonal antibodies against low-n oligomers of tau.

The antigen consisted predominantly of low-n oligomers with sizes ranging from dimers to hexamers, roughly globular in shape and purified by a hydrophobic interaction chromatography (Figure 3.1). Monoclonal antibodies (mAb's) raised against these tau oligomers were analyzed by biophysical, biochemical and cell biological methods. Based on the results from the first characterization of the monoclonal antibodies (tissue culture supernatants), we selected the clones that strongly detected tau oligomers and aggregates. Antibodies were then tested for their specificity against monomers and aggregates (low-n oligomers or fibrils) of wildtype and mutant (ΔK, ΔK-2P) tau (repeat domain and full-length). We observed that in dot blot analysis, only the 2B10 antibody was specific to purified low-n oligomers of $Tau^{RD\Delta K}$ (Figure 3.2). Other antibodies such as 6H1, 2G9 detected both oligomers and aggregates of $Tau^{RD\Delta K}$. Antibodies 26G1, 28D4, 29E2, 32E7 showed strong preferences for prefibrillar-aggregates of tau irrespective of mutation and domain structure (Figure 3.2). However the results were different when western blotting methods were applied. All mAb's detected all forms of recombinant tau proteins in western blots (Figure 3.3). The discrepancy was due to the fact that dot blots kept the protein in a native conformation whereas western blotting required denaturation by SDS in the sample buffer. This confirmed that some of the antibodies were conformation dependent and recognized tau only under specific conditions. These results are reminiscent of the outcomes of experiments with monoclonal antibodies specific for Aβ aggregates (Hatami et al., 2014). ELISA analysis

confirmed that 2B10 has higher affinity for $Tau^{RD\Delta K}$ oligomers than for monomers (Figure 3.4). Immunocytochemistry and immunohistochemistry data revealed that antibody 2B10 detects tau protein only in the pro-aggregant tau repeat domain in a cellular model of tauopathy and in transgenic mice (Figure 3.5). Since the 2B10 antibody provides similar results in dot blots and ELISA we consider antibody 2B10 to be specific for low-n oligomers of $Tau^{RD\Delta K}$. We also determined the affinity of the antibodies using biolayer interferometry analysis (BLI). The 2B10 antibody specific for low-n oligomers of $Tau^{RD\Delta K}$ had the lowest affinity to tau compared to other antibodies. Affinity analysis was performed using monomers, as aggregated tau failed to immobilize on the chip. This could explain the low affinity for 2B10 antibody (Table 3.1).

If an antibody would target a toxic or aggregation prone conformation of tau it would be a promising asset for a therapeutical intervention in AD and other tauopathies. From the preliminary antibody characterization we concluded that several antibodies have a conformational epitope, which can be characterized further to use as a therapeutic antibody. Earlier monoclonal antibodies were directly tested on tau transgenic animals. This type of approach will restrict the researcher to explore off targets and on targets of the antibodies in the animals. However, the mechanism of reduction of tau aggregation by antibodies is not understood in transgenic mice (Yanamandra et al., 2013, Castillo-Carranza et al., 2014b). It would therefore be advisable to perform a systematic approach to characterize the antibody before entering animal studies. For this reason we performed *in vitro* tau aggregation inhibition assays with tau constructs K19, K18 (3-repeat, 4-repeat domain respectively, data not shown), $Tau^{RD\Delta K}$ and $hTau^{P301L}$ protein in the presence of heparin and antibodies. This revealed that several antibodies inhibit tau aggregation dramatically. More specifically, antibodies 2B10 and 6H1 strongly (~90%) inhibited the aggregation (Figure 3.8) even at a 1:1 (antibody:tau) molar ratio. Similar studies were performed with the antibodies raised against amyloid beta peptides (Solomon et al., 1996, Liu et al., 2004). In their conditions aggregation of amyloid beta was inhibited either only at a 4:1 (antibody:amyloid beta) molar ratio (Solomon et al., 1996) or at 20 µM equimolar concentrations (Liu et al., 2004). Such *in vitro* studies on inhibition of tau aggregation were not reported prior to our study. Therefore we conclude that some of our antibodies at 1:1 (antibody:tau) molar ratio inhibit tau aggregation strongly and could be used as potential therapeutic antibodies.

In our case, different batches of antibodies from the same clone displayed differences in their biological activity (tau aggregation inhibition). It is known that IgG antibodies exposed to low-pH elution buffer acquire enhanced activity (Djoumerska-Alexieva et al., 2010). Therefore we explored a different purification strategy especially by varying the pH of the elution buffer. Indeed, a low pH of the elution buffer (HCl, pH-2.7) yielded a substantial increase (~70%) in their biological activity (inhibiting $hTau^{P301L}$ aggregation) compared to antibodies eluted at pH-4.0 (Figure 3.7).

We next characterized the tau aggregates that were formed in the presence of antibodies after 24 h by DLS and AFM. These techniques are commonly used to characterize protein assemblies in solution (Liu et al., 2004). Dynamic light scattering yielded an average hydrodynamic radius of aggregates (formed in the absence of antibody) as $R_H$~60-100 nm (equivalent to ~240-400 molecules of $hTau^{P301L}$). By comparison, aggregates formed in presence of antibody 2B10 or 6H1 resulted in substantially smaller $R_H$ values of ~10nm and 25 nm, respectively. (equivalent to low-n oligomers). AFM revealed that in the presence of antibodies the tau protein did not form filamentous aggregates. In presence of antibody 2B10 the aggregates had sizes of 2-3 nm, equivalent to trimers and tetramers, in the case of antibody 6H1 the sizes (2-15 nm) were in the range of dimers up to ~20mers. This means that antibody 2B10 bound to low-n oligomers, antibody 6H1 to high-n oligomers, and both antibodies inhibited tau protein aggregation. Antibody 6B5 did not inhibit tau aggregation significantly *in vitro*, even at higher concentration (1:2 = tau:antibody ratio) (Figure 3.10). By contrast, antibodies 2B10, 6H1 and 8E7 retained their inhibitory activity even at low concentrations (1:0.5 and 0.25 = tau:antibody ratio), making them suitable for further translational studies (Figure 3.10).

Tau is an intracellular protein which aggregates inside the neurons. Abnormal tau inside cells can cause microtubule disruption, transport inhibition and dysregulation of signaling or degradation pathways (Stamer et al., 2002, Wang and Mandelkow, 2016). One of the major questions in the field of tauopathies is the nature of the toxic species of tau and their mechanism of toxicity. Several studies suggested that pre-fibrillar forms or tau oligomers are the major toxic species (Lasagna-Reeves et al., 2010, Flach et al., 2012, Kaniyappan et al., 2017, Yoshiyama et al., 2007, Van der Jeugd et al., 2012,

Haass and Selkoe, 2007). One would expect that clearance of cytosolic tau from cells by therapeutic antibodies (active or passive immunotherapy) can only be achieved when the antibodies enter the cells at the required concentration and inhibit the tau aggregation or neutralize the activity of the toxic tau conformation.

On the other hand a small fraction of tau is also found extracellularly and is thought to enable the spreading of tau pathology from cell to cell (Figure 4.1) (Fuster-Matanzo et al., 2018, Gibbons et al., 2018). In support of this view, tau is also present at nanomolar concentrations in the ISF (Yamada et al., 2011). Therefore it is necessary to inhibit the intracellular and extracellular tau to prevent the spreading of tau pathology to other brain regions which in turn decrease the overall tau pathology in AD patients. This can be achieved by immunotherapy, where an antibody can bind intra or extracellularly to pathological tau to degrade it.

For these reasons tau-immunotherapy gained considerable interest in AD research. Several recent studies suggested that intravenous or intraperitoneal injection of tau specific antibodies like PHF6, PHF13 (Sankaranarayanan et al., 2015), pSer413, pSer396 specific antibodies (Umeda et al., 2015), TOMA antibody against tau oligomers (Castillo-Carranza et al., 2014b), N-terminal tau specific antibodies (Dai et al., 2015) and human tau specific antibody HJ8.5 (Yanamandra et al., 2013) into transgenic animals showed improvement in memory and reduction in intracellular tau pathology, especially tau aggregation.

We therefore investigated whether a specific low-n tau oligomer antibody can inhibit the formation of ThS positive cells in an inducible N2a cell model expressing $Tau^{RD\Delta K}$. Extracellular application of the antibodies to N2a cells did not reduce the number of ThS positive cells (data not shown). Although different modes (receptor dependent and independent) of antibody entry into the cells (SHSY5Y cells and primary neurons) to combat intracellular tau pathology had been reported (Congdon et al., 2013, Shamir et al., 2016), in our case it appears that the cells did not take up the antibody at the required concentration to reduce tau aggregation. We therefore delivered the antibodies directly into the cells before the expression of tau was induced, using the Xfect transfection reagent. We used 25 µg/ml of antibody to inhibit intracellular tau aggregation. Despite such huge concentration, intracellularly delivered antibodies

failed to inhibit the tau aggregation (ThS positive cells) in the N2a cell model of tauopathy (Figure 3.11). A possible explanation is that the concentration of antibodies applied (extra and intracellularly) was very low (167 nM) compared to the high concentration (~95 µM) of the tau expressed in N2a cells which was recently reported (Pickhardt et al., 2017).

An important aspect of antibody mediated improvement in tau pathology is neutralizing the effects of the toxic tau conformation. Studies performed so far tried to explore the antibodies ability to neutralize tau toxicity by incubating the cells with tau-antibody complex (tau pre-incubated with antibody) extracellularly and perform toxicity assay (MTT) (Lasagna-Reeves et al., 2012). In our case we addressed the toxicity of intracellular tau oligomers, using the N2a cell model expressing $Tau^{RD\Delta K}$. As reported previously, the cell death observed in this model is due to the oligomers (Pickhardt et al., 2017) whose effect could be presumably eliminated by an antibody specific to tau-oligomers. Therefore we exposed the N2a cells to antibodies and tested by FACS whether this reduced the fraction of Annexin V-labeled cells (a marker of incipient apoptosis); however, the treatment had no effect (Figure 3.11).

There are several reasons possible for these observations on antibody 2B10.

1) There was insufficient uptake of 2B10 antibody into the N2a cells (expressing ~95 µM of $Tau^{RD\Delta K}$ (Pickhardt et al., 2017)). The *in vitro* data show that antibody 2B10 inhibits tau aggregation at equimolar concentration, but such a high concentration (100 µM) of antibody could not be reached in the cell culture system.

2) The antibody was present in the cell for 96 h. During this time it could have been degraded by the cell system (Press et al., 1989).

3) Selection of the assay: In N2a cells, the ThS dye robustly labels filamentous tau aggregates assembled with β-structure, but incipient forms of aggregation (oligomers) are not labeled reliably. Therefore reduction of oligomers by antibodies might not have been detectable. This would require a more sensitive assay where the initial stages of tau aggregation (oligomerization) can be monitored.

In order to achieve this we developed a tau-split luciferase complementation assay (Villalobos et al., 2010) to monitor the oligomerization of $Tau^{RD\Delta K}$. This assay monitors the early changes that occur during tau dimerization using the interaction of N- or C-terminal luciferase fragments fused to tau molecules, respectively, which can be visualized by the bioluminescence of luciferin (Wegmann et al., 2016). We co-expressed $Tau^{RD\Delta K}$-Luc-N and $Tau^{RD\Delta K}$-Luc-C plasmids in N2a cells and applied antibodies extracellularly for 15h. Interestingly, antibody 2B10 (specific for low-n oligomers) inhibited the tau dimerization completely in a concentration dependent manner (Figure 3.14), whereas others had no effect (Figure 3.13). The results were intriguing, considering that the antibody with lowest affinity when applied extracellularly inhibited the tau-dimerization better than antibodies with higher affinity. Analogous observations were made by others (Congdon et al., 2016). Thus the mode of activity of antibodies applied extracellularly to inhibit the dimerization of tau inside the cells requires further investigation.

### 4.4 Entry of antibodies into cells

We hypothesized that antibody 2B10 must have been internalized by the N2a cells. There are contradictory evidences about internalization of antibodies by neurons and the mechanism of entry (Yanamandra et al., 2013, Funk et al., 2015, Congdon et al., 2013). We therefore investigated whether our antibodies are internalized by neurons using fluorescent labelling. Alexa 647-tagged 2B10 antibody could be shown to enter both N2a wild type cells and transgenic N2a-$Tau^{RD\Delta K}$ cells in a concentration dependent manner. All cells were able to take the antibody up but to different degrees (Figure 3.15). Surprisingly, we observed that the cells took up all antibodies tested including the control antibodies (secondary antibody, FLAG non-specific antibody). We also observed that the antibody (2B10) uptake by N2a cells was not dependent on the concentration of tau inside the neurons. These observations are contrary to previous reports that the cells take up only specific antibodies and the uptake of antibodies is dependent on the concentration of the pathological tau inside the neurons (Gu et al., 2013, Shamir et al., 2016).

The internalized antibodies were detected as puncta in the cytoplasm (Figure 3.15). Since it is known that antibodies are localized in endosomes or lysosomes (Shamir et

al., 2016), we checked the localization of the 2B10 antibody. We observed that our antibody clearly co-localized with lysosomal markers. All other internalized antibodies also co-localized with the lysosomes (Figure 3.16). A likely reason is that the internalized antibodies are degraded in the lysosomes whether they are specific to tau protein or not. We observed that only the 2B10 antibody was able to bind to tau ($Tau^{RD\Delta K}$) in the cytosol and in the lysosomes but the control antibody did not bind to tau (Figure 3.17). The 2B10 antibody bound to tau was localized in lysosomes presumably for degradation. This data is consistent with the previous findings that the endosomal–lysosomal pathway is involved in antibody-mediated clearance of tau aggregates (Gu et al., 2013, Krishnamurthy et al., 2011). The mechanism of entry of our antibodies into N2a cells is not known yet. In our hands, the blockers used to inhibit different modes of endocytosis were toxic to our N2a cell model. Therefore, the mechanism of antibody uptake is currently under investigation in other cell systems.

In spite of the different effects of the antibody actions, it is important to understand the mechanism of antibody mediated reduction and clearance of tau aggregates. In general tau antibodies could use different mechanisms to eliminate or reduce tau protein and hence aggregation. One possibility is that extracellular tau binds to the antibodies which can get internalized by microglia cell surface receptors (FcγRII and FcγRIII). This could inhibit spreading of tau pathology (Funk et al., 2015). Another possibility is the internalization of antibodies by neurons and guiding tau to lysosomes for degradation which could reduce intracellular tau and therefore tau aggregation (Gu et al., 2013) (Figure 4.1). Anti-tau antibodies (produced by active immunization with tau) immobilize extracellular tau to prevent its entry into healthy neurons and engage microglia for tau clearance via their effector functions (Novak et al., 2018). Anti-tau antibodies can also prevent cell-cell spreading of tau pathology by binding to extracellular monomeric or aggregated tau and prevent their entry into neurons (Evans et al., 2018).

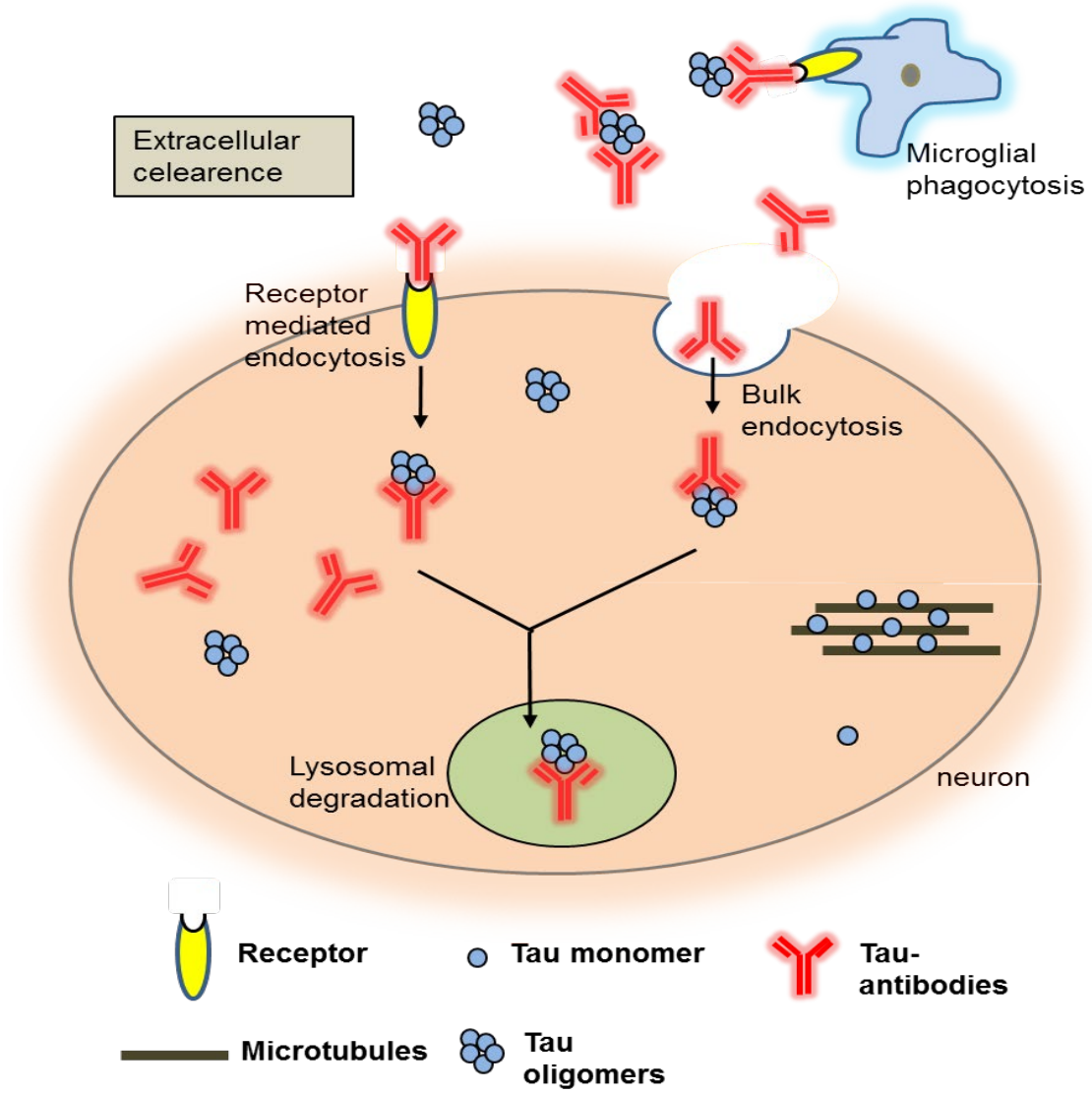


**Figure 4.1: Proposed mechanisms of activity of anti-tau antibodies**
Cartoon representation of the proposed mechanistic roles of tau antibodies in combating tau pathology *in vitro* and *in vivo* models. Intraperitoneally (I.P) injected antibodies cross the blood brain barrier and interact with the extra and intracellular tau. Antibodies can bind to the extracellular tau aggregates (small fraction) and promote the microglial phagocytosis via the Fcγ receptors for extracellular clearance of tau aggregates and thereby preventing the spread of pathological tau. Some antibodies are readily taken up by the neurons via the receptor mediated (Fcγ II/III) or receptor independent (bulk endocytosis) pathways and are released into the cytosol, where they interact with the pathological tau and promote their clearance via endosomal-lysosomal pathway.

In conclusion, this study focussed on the generation of tau oligomer-specific antibodies and their uptake into neurons. Different types of antibody can be taken up by cells, but only oligomer-specific antibodies bind to tau and form clusters in lysosomes. This would be the basis for reducing cytoplasmic tau and thus reducing aggregation. The mechanistic details of antibody mediated inhibition of tau-aggregation and clearance still has to be elucidated.

# 5 References

ALONSO., A. D. C., MEDERLYOVA, A., NOVAK, M., GRUNDKE-IQBAL, I. & IQBAL, K. 2004. Promotion of hyperphosphorylation by frontotemporal dementia tau mutations. *J Biol Chem,* 279**,** 34873-81.

ANDORFER, C., ACKER, C. M., KRESS, Y., HOF, P. R., DUFF, K. & DAVIES, P. 2005. Cell-cycle reentry and cell death in transgenic mice expressing nonmutant human tau isoforms. *J Neurosci,* 25**,** 5446-54.

ANDREADIS, A. 2005. Tau gene alternative splicing: expression patterns, regulation and modulation of function in normal brain and neurodegenerative diseases. *Biochim Biophys Acta,* 1739**,** 91-103.

ANDREADIS, A. 2006. Misregulation of tau alternative splicing in neurodegeneration and dementia. *Prog Mol Subcell Biol,* 44**,** 89-107.

ANDREADIS, A., BRODERICK, J. A. & KOSIK, K. S. 1995. Relative exon affinities and suboptimal splice site signals lead to non-equivalence of two cassette exons. *Nucleic Acids Res,* 23**,** 3585-93.

ARRIAGADA, P. V., GROWDON, J. H., HEDLEY-WHYTE, E. T. & HYMAN, B. T. 1992. Neurofibrillary tangles but not senile plaques parallel duration and severity of Alzheimer's disease. *Neurology,* 42**,** 631-9.

ASUNI, A. A., BOUTAJANGOUT, A., QUARTERMAIN, D. & SIGURDSSON, E. M. 2007. Immunotherapy targeting pathological tau conformers in a tangle mouse model reduces brain pathology with associated functional improvements. *J Neurosci,* 27**,** 9115-29.

AVILA, J. 2006. Tau phosphorylation and aggregation in Alzheimer's disease pathology. *FEBS Lett,* 580**,** 2922-7.

AVILA, J., LUCAS, J. J., PEREZ, M. & HERNANDEZ, F. 2004. Role of tau protein in both physiological and pathological conditions. *Physiol Rev,* 84**,** 361-84.

BARGHORN, S., DAVIES, P. & MANDELKOW, E. 2004. Tau paired helical filaments from Alzheimer's disease brain and assembled in vitro are based on beta-structure in the core domain. *Biochemistry,* 43**,** 1694-703.

BARGHORN, S., ZHENG-FISCHHOFER, Q., ACKMANN, M., BIERNAT, J., VON BERGEN, M., MANDELKOW, E. M. & MANDELKOW, E. 2000. Structure, microtubule interactions, and paired helical filament aggregation by tau mutants of frontotemporal dementias. *Biochemistry,* 39**,** 11714-21.

BIERNAT, J., GUSTKE, N., DREWES, G., MANDELKOW, E. M. & MANDELKOW, E. 1993. Phosphorylation of Ser262 strongly reduces binding of tau to microtubules: distinction between PHF-like immunoreactivity and microtubule binding. *Neuron,* 11**,** 153-63.

BLAIR, L. J., SABBAGH, J. J. & DICKEY, C. A. 2014. Targeting Hsp90 and its co-chaperones to treat Alzheimer's disease. *Expert Opin Ther Targets,* 18**,** 1219-32.

BOCHE, D., DONALD, J., LOVE, S., HARRIS, S., NEAL, J. W., HOLMES, C. & NICOLL, J. A. 2010. Reduction of aggregated Tau in neuronal processes but not in the cell bodies after Abeta42 immunisation in Alzheimer's disease. *Acta Neuropathol,* 120**,** 13-20.

BOUTAJANGOUT, A., INGADOTTIR, J., DAVIES, P. & SIGURDSSON, E. M. 2011. Passive immunization targeting pathological phospho-tau protein in a mouse model reduces functional decline and clears tau aggregates from the brain. *J Neurochem,* 118**,** 658-67.

BOUTAJANGOUT, A. & WISNIEWSKI, T. 2014. Tau-based therapeutic approaches for Alzheimer's disease - a mini-review. *Gerontology,* 60**,** 381-5.

BRAAK, H. & BRAAK, E. 1991a. Demonstration of amyloid deposits and neurofibrillary changes in whole brain sections. *Brain Pathol,* 1**,** 213-6.

BRAAK, H. & BRAAK, E. 1991b. Neuropathological stageing of Alzheimer-related changes. *Acta Neuropathol,* 82**,** 239-59.

BRAAK, H. & DEL TREDICI, K. 2016. Potential Pathways of Abnormal Tau and alpha-Synuclein Dissemination in Sporadic Alzheimer's and Parkinson's Diseases. *Cold Spring Harb Perspect Biol,* 8.

BROOKMEYER, R., GRAY, S. & KAWAS, C. 1998. Projections of Alzheimer's disease in the United States and the public health impact of delaying disease onset. *Am J Public Health,* 88**,** 1337-42.

BUDUR, K., WEST, T., BRAUNSTEIN, J. B., FOGELMAN, I., BORDELON, Y. M., LITVAN, I., ROBERSON, E. D., HU, H., VERGHESE, P. B., BATEMAN, R. J., FLORIAN, H., WANG, D., RYMAN, D., GAULT, L., GOSS, S., MENDONCA, N., RENDENBACH-MUELLER, B., KERWIN, D. R., BOXER, A. L. & HOLTZMAN, D. M. 2017. Results of a Phase 1, Single Ascending Dose, Placebo-Controlled Study of Abbv-8e12 in Patients with Progressive Supranuclear Palsy and Phase 2 Study Design in Early Alzheimer's Disease. *Alzheimer's & Dementia,* 13**,** P599-P600.

BULIC, B., PICKHARDT, M. & MANDELKOW, E. 2013. Progress and developments in tau aggregation inhibitors for Alzheimer disease. *J Med Chem,* 56**,** 4135-55.

CABRALES FONTELA, Y., KADAVATH, H., BIERNAT, J., RIEDEL, D., MANDELKOW, E. & ZWECKSTETTER, M. 2017. Multivalent cross-linking of actin filaments and microtubules through the microtubule-associated protein Tau. *Nat Commun,* 8**,** 1981.

CASTILLO-CARRANZA, D. L., GERSON, J. E., SENGUPTA, U., GUERRERO-MUNOZ, M. J., LASAGNA-REEVES, C. A. & KAYED, R. 2014a. Specific targeting of tau oligomers in Htau mice prevents cognitive impairment and tau toxicity following injection with brain-derived tau oligomeric seeds. *J Alzheimers Dis,* 40 Suppl 1**,** S97-S111.

CASTILLO-CARRANZA, D. L., SENGUPTA, U., GUERRERO-MUNOZ, M. J., LASAGNA-REEVES, C. A., GERSON, J. E., SINGH, G., ESTES, D. M., BARRETT, A. D., DINELEY, K. T., JACKSON, G. R. & KAYED, R. 2014b. Passive immunization with Tau

oligomer monoclonal antibody reverses tauopathy phenotypes without affecting hyperphosphorylated neurofibrillary tangles. *J Neurosci,* 34**,** 4260-72.

CHAI, X., WU, S., MURRAY, T. K., KINLEY, R., CELLA, C. V., SIMS, H., BUCKNER, N., HANMER, J., DAVIES, P., O'NEILL, M. J., HUTTON, M. L. & CITRON, M. 2011. Passive immunization with anti-Tau antibodies in two transgenic models: reduction of Tau pathology and delay of disease progression. *J Biol Chem,* 286**,** 34457-67.

CONFORTI, L., ADALBERT, R. & COLEMAN, M. P. 2007. Neuronal death: where does the end begin? *Trends Neurosci,* 30**,** 159-66.

CONGDON, E. E., GU, J., SAIT, H. B. & SIGURDSSON, E. M. 2013. Antibody uptake into neurons occurs primarily via clathrin-dependent Fcgamma receptor endocytosis and is a prerequisite for acute tau protein clearance. *J Biol Chem,* 288**,** 35452-65.

CONGDON, E. E., LIN, Y., RAJAMOHAMEDSAIT, H. B., SHAMIR, D. B., KRISHNASWAMY, S., RAJAMOHAMEDSAIT, W. J., RASOOL, S., GONZALEZ, V., LEVENGA, J., GU, J., HOEFFER, C. & SIGURDSSON, E. M. 2016. Affinity of Tau antibodies for solubilized pathological Tau species but not their immunogen or insoluble Tau aggregates predicts in vivo and ex vivo efficacy. *Mol Neurodegener,* 11**,** 62.

CONGDON, E. E. & SIGURDSSON, E. M. 2018. Tau-targeting therapies for Alzheimer disease. *Nat Rev Neurol*.

CUMMINGS, J. & FOX, N. 2017. Defining Disease Modifying Therapy for Alzheimer's Disease. *J Prev Alzheimers Dis,* 4**,** 109-115.

CUMMINGS, J., LEE, G., RITTER, A. & ZHONG, K. 2018. Alzheimer's disease drug development pipeline: 2018. *Alzheimers Dement (N Y),* 4**,** 195-214.

DAI, C. L., CHEN, X., KAZIM, S. F., LIU, F., GONG, C. X., GRUNDKE-IQBAL, I. & IQBAL, K. 2015. Passive immunization targeting the N-terminal projection domain of tau decreases tau pathology and improves cognition in a transgenic mouse model of Alzheimer disease and tauopathies. *J Neural Transm (Vienna),* 122**,** 607-17.

DAI, C. L., TUNG, Y. C., LIU, F., GONG, C. X. & IQBAL, K. 2017. Tau passive immunization inhibits not only tau but also Abeta pathology. *Alzheimers Res Ther,* 9**,** 1.

DECKER, J. M., KRUGER, L., SYDOW, A., DENNISSEN, F. J., SISKOVA, Z., MANDELKOW, E. & MANDELKOW, E. M. 2016. The Tau/A152T mutation, a risk factor for frontotemporal-spectrum disorders, leads to NR2B receptor-mediated excitotoxicity. *EMBO Rep,* 17**,** 552-69.

DEVOS, S. L., CORJUC, B. T., COMMINS, C., DUJARDIN, S., BANNON, R. N., CORJUC, D., MOORE, B. D., BENNETT, R. E., JORFI, M., GONZALES, J. A., DOOLEY, P. M., ROE, A. D., PITSTICK, R., IRIMIA, D., FROSCH, M. P., CARLSON, G. A. & HYMAN, B. T. 2018. Tau reduction in the presence of amyloid-beta prevents tau pathology and neuronal death in vivo. *Brain,* 141**,** 2194-2212.

DICKEY, C. A., KAMAL, A., LUNDGREN, K., KLOSAK, N., BAILEY, R. M., DUNMORE, J., ASH, P., SHORAKA, S., ZLATKOVIC, J., ECKMAN, C. B., PATTERSON, C., DICKSON, D. W., NAHMAN, N. S., JR., HUTTON, M., BURROWS, F. & PETRUCELLI,

L. 2007. The high-affinity HSP90-CHIP complex recognizes and selectively degrades phosphorylated tau client proteins. *J Clin Invest,* 117**,** 648-58.

DJOUMERSKA-ALEXIEVA, I. K., DIMITROV, J. D., VOYNOVA, E. N., LACROIX-DESMAZES, S., KAVERI, S. V. & VASSILEV, T. L. 2010. Exposure of IgG to an acidic environment results in molecular modifications and in enhanced protective activity in sepsis. *FEBS J,* 277**,** 3039-50.

DREWES, G., EBNETH, A., PREUSS, U., MANDELKOW, E. M. & MANDELKOW, E. 1997. MARK, a novel family of protein kinases that phosphorylate microtubule-associated proteins and trigger microtubule disruption. *Cell,* 89**,** 297-308.

ECKERMANN, K., MOCANU, M. M., KHLISTUNOVA, I., BIERNAT, J., NISSEN, A., HOFMANN, A., SCHONIG, K., BUJARD, H., HAEMISCH, A., MANDELKOW, E., ZHOU, L., RUNE, G. & MANDELKOW, E. M. 2007. The beta-propensity of Tau determines aggregation and synaptic loss in inducible mouse models of tauopathy. *J Biol Chem,* 282**,** 31755-65.

ENGEL, T., GONI-OLIVER, P., LUCAS, J. J., AVILA, J. & HERNANDEZ, F. 2006. Chronic lithium administration to FTDP-17 tau and GSK-3beta overexpressing mice prevents tau hyperphosphorylation and neurofibrillary tangle formation, but pre-formed neurofibrillary tangles do not revert. *J Neurochem,* 99**,** 1445-55.

EVANS, L. D., WASSMER, T., FRASER, G., SMITH, J., PERKINTON, M., BILLINTON, A. & LIVESEY, F. J. 2018. Extracellular Monomeric and Aggregated Tau Efficiently Enter Human Neurons through Overlapping but Distinct Pathways. *Cell Rep,* 22**,** 3612-3624.

FALCON, B., ZHANG, W., MURZIN, A. G., MURSHUDOV, G., GARRINGER, H. J., VIDAL, R., CROWTHER, R. A., GHETTI, B., SCHERES, S. H. W. & GOEDERT, M. 2018. Structures of filaments from Pick's disease reveal a novel tau protein fold. *Nature,* 561**,** 137-140.

FATOUROS, C., PIR, G. J., BIERNAT, J., KOUSHIKA, S. P., MANDELKOW, E., MANDELKOW, E. M., SCHMIDT, E. & BAUMEISTER, R. 2012. Inhibition of tau aggregation in a novel Caenorhabditis elegans model of tauopathy mitigates proteotoxicity. *Hum Mol Genet,* 21**,** 3587-603.

FISCHER, D., MUKRASCH, M. D., VON BERGEN, M., KLOS-WITKOWSKA, A., BIERNAT, J., GRIESINGER, C., MANDELKOW, E. & ZWECKSTETTER, M. 2007. Structural and microtubule binding properties of tau mutants of frontotemporal dementias. *Biochemistry,* 46**,** 2574-82.

FITZPATRICK, A. W. P., FALCON, B., HE, S., MURZIN, A. G., MURSHUDOV, G., GARRINGER, H. J., CROWTHER, R. A., GHETTI, B., GOEDERT, M. & SCHERES, S. H. W. 2017. Cryo-EM structures of tau filaments from Alzheimer's disease. *Nature,* 547**,** 185-190.

FLACH, K., HILBRICH, I., SCHIFFMANN, A., GARTNER, U., KRUGER, M., LEONHARDT, M., WASCHIPKY, H., WICK, L., ARENDT, T. & HOLZER, M. 2012. Tau oligomers impair artificial membrane integrity and cellular viability. *J Biol Chem,* 287**,** 43223-33.

FU, H., HARDY, J. & DUFF, K. E. 2018. Selective vulnerability in neurodegenerative diseases. *Nat Neurosci,* 21**,** 1350-1358.

FUNK, K. E., MIRBAHA, H., JIANG, H., HOLTZMAN, D. M. & DIAMOND, M. I. 2015. Distinct Therapeutic Mechanisms of Tau Antibodies: Promoting Microglial Clearance Versus Blocking Neuronal Uptake. *J Biol Chem,* 290**,** 21652-62.

FUSTER-MATANZO, A., HERNANDEZ, F. & AVILA, J. 2018. Tau Spreading Mechanisms; Implications for Dysfunctional Tauopathies. *Int J Mol Sci,* 19.

GAUTHIER, S., FELDMAN, H. H., SCHNEIDER, L. S., WILCOCK, G. K., FRISONI, G. B., HARDLUND, J. H., MOEBIUS, H. J., BENTHAM, P., KOOK, K. A., WISCHIK, D. J., SCHELTER, B. O., DAVIS, C. S., STAFF, R. T., BRACOUD, L., SHAMSI, K., STOREY, J. M., HARRINGTON, C. R. & WISCHIK, C. M. 2016. Efficacy and safety of tau-aggregation inhibitor therapy in patients with mild or moderate Alzheimer's disease: a randomised, controlled, double-blind, parallel-arm, phase 3 trial. *Lancet,* 388**,** 2873-2884.

GIBBONS, G. S., LEE, V. M. Y. & TROJANOWSKI, J. Q. 2018. Mechanisms of Cell-to-Cell Transmission of Pathological Tau: A Review. *JAMA Neurol*.

GOEDERT, M., JAKES, R., SPILLANTINI, M. G., HASEGAWA, M., SMITH, M. J. & CROWTHER, R. A. 1996. Assembly of microtubule-associated protein tau into Alzheimer-like filaments induced by sulphated glycosaminoglycans. *Nature,* 383**,** 550-3.

GOEDERT, M., SPILLANTINI, M. G. & CROWTHER, R. A. 1992. Cloning of a big tau microtubule-associated protein characteristic of the peripheral nervous system. *Proc Natl Acad Sci U S A,* 89**,** 1983-7.

GOODE, B. L., CHAU, M., DENIS, P. E. & FEINSTEIN, S. C. 2000. Structural and functional differences between 3-repeat and 4-repeat tau isoforms. Implications for normal tau function and the onset of neurodegenetative disease. *J Biol Chem,* 275**,** 38182-9.

GREENBERG, S. G., DAVIES, P., SCHEIN, J. D. & BINDER, L. I. 1992. Hydrofluoric acid-treated tau PHF proteins display the same biochemical properties as normal tau. *J Biol Chem,* 267**,** 564-9.

GU, J., CONGDON, E. E. & SIGURDSSON, E. M. 2013. Two novel Tau antibodies targeting the 396/404 region are primarily taken up by neurons and reduce Tau protein pathology. *J Biol Chem,* 288**,** 33081-95.

GUSTKE, N., TRINCZEK, B., BIERNAT, J., MANDELKOW, E. M. & MANDELKOW, E. 1994. Domains of tau protein and interactions with microtubules. *Biochemistry,* 33**,** 9511-22.

HAASS, C. & SELKOE, D. J. 2007. Soluble protein oligomers in neurodegeneration: lessons from the Alzheimer's amyloid beta-peptide. *Nat Rev Mol Cell Biol,* 8**,** 101-12.

HAMPEL, H., EWERS, M., BURGER, K., ANNAS, P., MORTBERG, A., BOGSTEDT, A., FROLICH, L., SCHRODER, J., SCHONKNECHT, P., RIEPE, M. W., KRAFT, I., GASSER, T., LEYHE, T., MOLLER, H. J., KURZ, A. & BASUN, H. 2009. Lithium trial

in Alzheimer's disease: a randomized, single-blind, placebo-controlled, multicenter 10-week study. *J Clin Psychiatry,* 70**,** 922-31.

HAMPEL, H., SCHNEIDER, L. S., GIACOBINI, E., KIVIPELTO, M., SINDI, S., DUBOIS, B., BROICH, K., NISTICO, R., AISEN, P. S. & LISTA, S. 2015. Advances in the therapy of Alzheimer's disease: targeting amyloid beta and tau and perspectives for the future. *Expert Rev Neurother,* 15**,** 83-105.

HANGER, D. P., ANDERTON, B. H. & NOBLE, W. 2009. Tau phosphorylation: the therapeutic challenge for neurodegenerative disease. *Trends Mol Med,* 15**,** 112-9.

HARDY, J. & SELKOE, D. J. 2002. The amyloid hypothesis of Alzheimer's disease: progress and problems on the road to therapeutics. *Science,* 297**,** 353-6.

HATAMI, A., ALBAY, R., 3RD, MONJAZEB, S., MILTON, S. & GLABE, C. 2014. Monoclonal antibodies against Abeta42 fibrils distinguish multiple aggregation state polymorphisms in vitro and in Alzheimer disease brain. *J Biol Chem,* 289**,** 32131-43.

HO, S. W., TSUI, Y. T., WONG, T. T., CHEUNG, S. K., GOGGINS, W. B., YI, L. M., CHENG, K. K. & BAUM, L. 2013. Effects of 17-allylamino-17-demethoxygeldanamycin (17-AAG) in transgenic mouse models of frontotemporal lobar degeneration and Alzheimer's disease. *Transl Neurodegener,* 2**,** 24.

HOCHGRAFE, K., SYDOW, A., MATENIA, D., CADINU, D., KONEN, S., PETROVA, O., PICKHARDT, M., GOLL, P., MORELLINI, F., MANDELKOW, E. & MANDELKOW, E. M. 2015. Preventive methylene blue treatment preserves cognition in mice expressing full-length pro-aggregant human Tau. *Acta Neuropathol Commun,* 3**,** 25.

HOLTZMAN, D. M., CARRILLO, M. C., HENDRIX, J. A., BAIN, L. J., CATAFAU, A. M., GAULT, L. M., GOEDERT, M., MANDELKOW, E., MANDELKOW, E. M., MILLER, D. S., OSTROWITZKI, S., POLYDORO, M., SMITH, S., WITTMANN, M. & HUTTON, M. 2016. Tau: From research to clinical development. *Alzheimers Dement,* 12**,** 1033-1039.

HONIG, L. S., VELLAS, B., WOODWARD, M., BOADA, M., BULLOCK, R., BORRIE, M., HAGER, K., ANDREASEN, N., SCARPINI, E., LIU-SEIFERT, H., CASE, M., DEAN, R. A., HAKE, A., SUNDELL, K., POOLE HOFFMANN, V., CARLSON, C., KHANNA, R., MINTUN, M., DEMATTOS, R., SELZLER, K. J. & SIEMERS, E. 2018. Trial of Solanezumab for Mild Dementia Due to Alzheimer's Disease. *N Engl J Med,* 378**,** 321-330.

HOSOKAWA, M., ARAI, T., MASUDA-SUZUKAKE, M., NONAKA, T., YAMASHITA, M., AKIYAMA, H. & HASEGAWA, M. 2012. Methylene blue reduced abnormal tau accumulation in P301L tau transgenic mice. *PLoS One,* 7**,** e52389.

HOWLETT, D. R. 2001. A beta oligomerization A Therapeutic Target for Alzheimers Disease. *Current Medicinal Chemistry - Immunology, Endocrine & Metabolic Agents,* 1**,** 25-38.

HUBER, C. M., YEE, C., MAY, T., DHANALA, A. & MITCHELL, C. S. 2018. Cognitive Decline in Preclinical Alzheimer's Disease: Amyloid-Beta versus Tauopathy. *J Alzheimers Dis,* 61**,** 265-281.

HUNG, S. Y. & FU, W. M. 2017. Drug candidates in clinical trials for Alzheimer's disease. *J Biomed Sci,* 24**,** 47.

ITTNER, A., BERTZ, J., SUH, L. S., STEVENS, C. H., GOTZ, J. & ITTNER, L. M. 2015. Tau-targeting passive immunization modulates aspects of pathology in tau transgenic mice. *J Neurochem,* 132**,** 135-45.

JEGANATHAN, S., VON BERGEN, M., BRUTLACH, H., STEINHOFF, H. J. & MANDELKOW, E. 2006. Global hairpin folding of tau in solution. *Biochemistry,* 45**,** 2283-93.

JEGANATHAN, S., VON BERGEN, M., MANDELKOW, E. M. & MANDELKOW, E. 2008. The natively unfolded character of tau and its aggregation to Alzheimer-like paired helical filaments. *Biochemistry,* 47**,** 10526-39.

JENSEN-JAROLIM, E. & SINGER, J. 2011. Cancer vaccines inducing antibody production: more pros than cons. *Expert Rev Vaccines,* 10**,** 1281-9.

KAMPERS, T., FRIEDHOFF, P., BIERNAT, J., MANDELKOW, E. M. & MANDELKOW, E. 1996. RNA stimulates aggregation of microtubule-associated protein tau into Alzheimer-like paired helical filaments. *FEBS Lett,* 399**,** 344-9.

KANIYAPPAN, S., CHANDUPATLA, R. R., MANDELKOW, E. M. & MANDELKOW, E. 2017. Extracellular low-n oligomers of tau cause selective synaptotoxicity without affecting cell viability. *Alzheimers Dement,* 13**,** 1270-1291.

KHLISTUNOVA, I., BIERNAT, J., WANG, Y., PICKHARDT, M., VON BERGEN, M., GAZOVA, Z., MANDELKOW, E. & MANDELKOW, E. M. 2006. Inducible expression of Tau repeat domain in cell models of tauopathy: aggregation is toxic to cells but can be reversed by inhibitor drugs. *J Biol Chem,* 281**,** 1205-14.

KONTSEKOVA, E., ZILKA, N., KOVACECH, B., NOVAK, P. & NOVAK, M. 2014. First-in-man tau vaccine targeting structural determinants essential for pathological tau-tau interaction reduces tau oligomerisation and neurofibrillary degeneration in an Alzheimer's disease model. *Alzheimers Res Ther,* 6**,** 44.

KRISHNAMURTHY, P. K., DENG, Y. & SIGURDSSON, E. M. 2011. Mechanistic Studies of Antibody-Mediated Clearance of Tau Aggregates Using an ex vivo Brain Slice Model. *Front Psychiatry,* 2**,** 59.

KUMAR, S., TEPPER, K., KANIYAPPAN, S., BIERNAT, J., WEGMANN, S., MANDELKOW, E. M., MULLER, D. J. & MANDELKOW, E. 2014. Stages and conformations of the Tau repeat domain during aggregation and its effect on neuronal toxicity. *J Biol Chem,* 289**,** 20318-32.

LAI, A. Y. & MCLAURIN, J. 2012. Inhibition of amyloid-beta peptide aggregation rescues the autophagic deficits in the TgCRND8 mouse model of Alzheimer disease. *Biochim Biophys Acta,* 1822**,** 1629-37.

LASAGNA-REEVES, C. A., CASTILLO-CARRANZA, D. L., GUERRERO-MUOZ, M. J., JACKSON, G. R. & KAYED, R. 2010. Preparation and characterization of neurotoxic tau oligomers. *Biochemistry,* 49**,** 10039-41.

LASAGNA-REEVES, C. A., CASTILLO-CARRANZA, D. L., SENGUPTA, U., CLOS, A. L., JACKSON, G. R. & KAYED, R. 2011. Tau oligomers impair memory and induce synaptic and mitochondrial dysfunction in wild-type mice. *Mol Neurodegener,* 6**,** 39.

LASAGNA-REEVES, C. A., CASTILLO-CARRANZA, D. L., SENGUPTA, U., SARMIENTO, J., TRONCOSO, J., JACKSON, G. R. & KAYED, R. 2012. Identification of oligomers at early stages of tau aggregation in Alzheimer's disease. *FASEB J,* 26**,** 1946-59.

LEE, G., COWAN, N. & KIRSCHNER, M. 1988. The primary structure and heterogeneity of tau protein from mouse brain. *Science,* 239**,** 285-8.

LEE, V. M., GOEDERT, M. & TROJANOWSKI, J. Q. 2001. Neurodegenerative tauopathies. *Annu Rev Neurosci,* 24**,** 1121-59.

LEROY, K., YILMAZ, Z. & BRION, J. P. 2007. Increased level of active GSK-3beta in Alzheimer's disease and accumulation in argyrophilic grains and in neurones at different stages of neurofibrillary degeneration. *Neuropathol Appl Neurobiol,* 33**,** 43-55.

LIU, E., WANG, D., SPERLING, R., SALLOWAY, S., FOX, N. C., BLENNOW, K., SCHELTENS, P., SCHMIDT, M. E., STREFFER, J., NOVAK, G., EINSTEIN, S., BOOTH, K., KETTER, N., BRASHEAR, H. R. & GROUP, E. L. N. I. 2018. Biomarker pattern of ARIA-E participants in phase 3 randomized clinical trials with bapineuzumab. *Neurology,* 90**,** e877-e886.

LIU, R., YUAN, B., EMADI, S., ZAMEER, A., SCHULZ, P., MCALLISTER, C., LYUBCHENKO, Y., GOUD, G. & SIERKS, M. R. 2004. Single chain variable fragments against beta-amyloid (Abeta) can inhibit Abeta aggregation and prevent abeta-induced neurotoxicity. *Biochemistry,* 43**,** 6959-67.

MA, Q. L., ZUO, X., YANG, F., UBEDA, O. J., GANT, D. J., ALAVERDYAN, M., TENG, E., HU, S., CHEN, P. P., MAITI, P., TETER, B., COLE, G. M. & FRAUTSCHY, S. A. 2013. Curcumin suppresses soluble tau dimers and corrects molecular chaperone, synaptic, and behavioral deficits in aged human tau transgenic mice. *J Biol Chem,* 288**,** 4056-65.

MANDELKOW, E. M. & MANDELKOW, E. 2012. Biochemistry and cell biology of tau protein in neurofibrillary degeneration. *Cold Spring Harb Perspect Med,* 2**,** a006247.

MARTIN, L., LATYPOVA, X. & TERRO, F. 2011. Post-translational modifications of tau protein: implications for Alzheimer's disease. *Neurochem Int,* 58**,** 458-71.

MEDINA, M. 2018. An Overview on the Clinical Development of Tau-Based Therapeutics. *Int J Mol Sci,* 19.

MESSING, L., DECKER, J. M., JOSEPH, M., MANDELKOW, E. & MANDELKOW, E. M. 2013. Cascade of tau toxicity in inducible hippocampal brain slices and prevention by aggregation inhibitors. *Neurobiol Aging,* 34**,** 1343-1354.

MILLER, D. W., COOKSON, M. R. & DICKSON, D. W. 2004. Glial cell inclusions and the pathogenesis of neurodegenerative diseases. *Neuron Glia Biol,* 1**,** 13-21.

MOCANU, M. M., NISSEN, A., ECKERMANN, K., KHLISTUNOVA, I., BIERNAT, J., DREXLER, D., PETROVA, O., SCHONIG, K., BUJARD, H., MANDELKOW, E., ZHOU, L., RUNE, G. & MANDELKOW, E. M. 2008. The potential for beta-structure in the repeat domain of tau protein determines aggregation, synaptic decay, neuronal loss, and coassembly with endogenous Tau in inducible mouse models of tauopathy. *J Neurosci,* 28**,** 737-48.

MUKRASCH, M. D., BIBOW, S., KORUKOTTU, J., JEGANATHAN, S., BIERNAT, J., GRIESINGER, C., MANDELKOW, E. & ZWECKSTETTER, M. 2009. Structural polymorphism of 441-residue tau at single residue resolution. *PLoS Biol,* 7**,** e34.

MUKRASCH, M. D., BIERNAT, J., VON BERGEN, M., GRIESINGER, C., MANDELKOW, E. & ZWECKSTETTER, M. 2005. Sites of tau important for aggregation populate {beta}-structure and bind to microtubules and polyanions. *J Biol Chem,* 280**,** 24978-86.

NELSON, P. T., ALAFUZOFF, I., BIGIO, E. H., BOURAS, C., BRAAK, H., CAIRNS, N. J., CASTELLANI, R. J., CRAIN, B. J., DAVIES, P., DEL TREDICI, K., DUYCKAERTS, C., FROSCH, M. P., HAROUTUNIAN, V., HOF, P. R., HULETTE, C. M., HYMAN, B. T., IWATSUBO, T., JELLINGER, K. A., JICHA, G. A., KOVARI, E., KUKULL, W. A., LEVERENZ, J. B., LOVE, S., MACKENZIE, I. R., MANN, D. M., MASLIAH, E., MCKEE, A. C., MONTINE, T. J., MORRIS, J. C., SCHNEIDER, J. A., SONNEN, J. A., THAL, D. R., TROJANOWSKI, J. Q., TRONCOSO, J. C., WISNIEWSKI, T., WOLTJER, R. L. & BEACH, T. G. 2012. Correlation of Alzheimer disease neuropathologic changes with cognitive status: a review of the literature. *J Neuropathol Exp Neurol,* 71**,** 362-81.

NEVE, R. L., HARRIS, P., KOSIK, K. S., KURNIT, D. M. & DONLON, T. A. 1986. Identification of cDNA clones for the human microtubule-associated protein tau and chromosomal localization of the genes for tau and microtubule-associated protein 2. *Brain Res,* 387**,** 271-80.

NISBET, R. M. & GOTZ, J. 2018. Amyloid-beta and Tau in Alzheimer's Disease: Novel Pathomechanisms and Non-Pharmacological Treatment Strategies. *J Alzheimers Dis,* 64**,** S517-S527.

NOBLE, W., HANGER, D. P., MILLER, C. C. & LOVESTONE, S. 2013. The importance of tau phosphorylation for neurodegenerative diseases. *Front Neurol,* 4**,** 83.

NOVAK, P., SCHMIDT, R., KONTSEKOVA, E., KOVACECH, B., SMOLEK, T., KATINA, S., FIALOVA, L., PRCINA, M., PARRAK, V., DAL-BIANCO, P., BRUNNER, M., STAFFEN, W., RAINER, M., ONDRUS, M., ROPELE, S., SMISEK, M., SIVAK, R., ZILKA, N., WINBLAD, B. & NOVAK, M. 2018. FUNDAMANT: an interventional 72-week phase 1 follow-up study of AADvac1, an active immunotherapy against tau protein pathology in Alzheimer's disease. *Alzheimers Res Ther,* 10**,** 108.

NOVAK, P., SCHMIDT, R., KONTSEKOVA, E., ZILKA, N., KOVACECH, B., SKRABANA, R., VINCE-KAZMEROVA, Z., KATINA, S., FIALOVA, L., PRCINA, M., PARRAK, V., DAL-BIANCO, P., BRUNNER, M., STAFFEN, W., RAINER, M., ONDRUS, M., ROPELE, S., SMISEK, M., SIVAK, R., WINBLAD, B. & NOVAK, M. 2017. Safety and immunogenicity of the tau vaccine AADvac1 in patients with Alzheimer's disease: a randomised, double-blind, placebo-controlled, phase 1 trial. *The Lancet Neurology,* 16**,** 123-134.

ORR, M. E., SULLIVAN, A. C. & FROST, B. 2017. A Brief Overview of Tauopathy: Causes, Consequences, and Therapeutic Strategies. *Trends Pharmacol Sci,* 38**,** 637-648.

PANZA, F., SOLFRIZZI, V., IMBIMBO, B. P. & LOGROSCINO, G. 2014. Amyloid-directed monoclonal antibodies for the treatment of Alzheimer's disease: the point of no return? *Expert Opin Biol Ther,* 14**,** 1465-76.

PATTERSON, K. R., REMMERS, C., FU, Y., BROOKER, S., KANAAN, N. M., VANA, L., WARD, S., REYES, J. F., PHILIBERT, K., GLUCKSMAN, M. J. & BINDER, L. I. 2011. Characterization of prefibrillar Tau oligomers in vitro and in Alzheimer disease. *J Biol Chem,* 286**,** 23063-76.

PEDERSEN, J. T. & SIGURDSSON, E. M. 2015. Tau immunotherapy for Alzheimer's disease. *Trends Mol Med,* 21**,** 394-402.

PEI, J. J., TANAKA, T., TUNG, Y. C., BRAAK, E., IQBAL, K. & GRUNDKE-IQBAL, I. 1997. Distribution, levels, and activity of glycogen synthase kinase-3 in the Alzheimer disease brain. *J Neuropathol Exp Neurol,* 56**,** 70-8.

PICKHARDT, M., BIERNAT, J., HUBSCHMANN, S., DENNISSEN, F. J. A., TIMM, T., AHO, A., MANDELKOW, E. M. & MANDELKOW, E. 2017. Time course of Tau toxicity and pharmacologic prevention in a cell model of Tauopathy. *Neurobiol Aging,* 57**,** 47-63.

PICKHARDT, M., BIERNAT, J., KHLISTUNOVA, I., WANG, Y. P., GAZOVA, Z., MANDELKOW, E. M. & MANDELKOW, E. 2007a. N-phenylamine derivatives as aggregation inhibitors in cell models of tauopathy. *Curr Alzheimer Res,* 4**,** 397-402.

PICKHARDT, M., GAZOVA, Z., VON BERGEN, M., KHLISTUNOVA, I., WANG, Y., HASCHER, A., MANDELKOW, E. M., BIERNAT, J. & MANDELKOW, E. 2005. Anthraquinones inhibit tau aggregation and dissolve Alzheimer's paired helical filaments in vitro and in cells. *J Biol Chem,* 280**,** 3628-35.

PICKHARDT, M., LARBIG, G., KHLISTUNOVA, I., COKSEZEN, A., MEYER, B., MANDELKOW, E. M., SCHMIDT, B. & MANDELKOW, E. 2007b. Phenylthiazolyl-hydrazide and its derivatives are potent inhibitors of tau aggregation and toxicity in vitro and in cells. *Biochemistry,* 46**,** 10016-23.

PICKHARDT, M., NEUMANN, T., SCHWIZER, D., CALLAWAY, K., VENDRUSCOLO, M., SCHENK, D., ST GEORGE-HYSLOP, P., MANDELKOW, E. M., DOBSON, C. M., MCCONLOGUE, L., MANDELKOW, E. & TOTH, G. 2015. Identification of Small Molecule Inhibitors of Tau Aggregation by Targeting Monomeric Tau As a Potential Therapeutic Approach for Tauopathies. *Curr Alzheimer Res,* 12**,** 814-28.

PIR, G. J., CHOUDHARY, B., MANDELKOW, E. & MANDELKOW, E. M. 2016. Tau mutant A152T, a risk factor for FTD/PSP, induces neuronal dysfunction and reduced lifespan independently of aggregation in a C. elegans Tauopathy model. *Mol Neurodegener,* 11**,** 33.

PRESS, O. W., FARR, A. G., BORROZ, K. I., ANDERSON, S. K. & MARTIN, P. J. 1989. Endocytosis and degradation of monoclonal antibodies targeting human B-cell malignancies. *Cancer Res,* 49**,** 4906-12.

PRZEDBORSKI, S., VILA, M. & JACKSON-LEWIS, V. 2003. Series Introduction: Neurodegeneration: What is it and where are we? *Journal of Clinical Investigation,* 111**,** 3-10.

RAMSDEN, M., KOTILINEK, L., FORSTER, C., PAULSON, J., MCGOWAN, E., SANTACRUZ, K., GUIMARAES, A., YUE, M., LEWIS, J., CARLSON, G., HUTTON, M. & ASHE, K. H. 2005. Age-dependent neurofibrillary tangle formation, neuron loss, and memory impairment in a mouse model of human tauopathy (P301L). *J Neurosci,* 25**,** 10637-47.

RANE, J. S., BHAUMIK, P. & PANDA, D. 2017. Curcumin Inhibits Tau Aggregation and Disintegrates Preformed Tau Filaments in vitro. *J Alzheimers Dis,* 60**,** 999-1014.

REAS, E. T. 2017. Amyloid and Tau Pathology in Normal Cognitive Aging. *J Neurosci,* 37**,** 7561-7563.

REITZ, C. & MAYEUX, R. 2014. Alzheimer disease: epidemiology, diagnostic criteria, risk factors and biomarkers. *Biochem Pharmacol,* 88**,** 640-51.

SANKARANARAYANAN, S., BARTEN, D. M., VANA, L., DEVIDZE, N., YANG, L., CADELINA, G., HOQUE, N., DECARR, L., KEENAN, S., LIN, A., CAO, Y., SNYDER, B., ZHANG, B., NITLA, M., HIRSCHFELD, G., BARREZUETA, N., POLSON, C., WES, P., RANGAN, V. S., CACACE, A., ALBRIGHT, C. F., MEREDITH, J., JR., TROJANOWSKI, J. Q., LEE, V. M., BRUNDEN, K. R. & AHLIJANIAN, M. 2015. Passive immunization with phospho-tau antibodies reduces tau pathology and functional deficits in two distinct mouse tauopathy models. *PLoS One,* 10**,** e0125614.

SCHWALBE, M., BIERNAT, J., BIBOW, S., OZENNE, V., JENSEN, M. R., KADAVATH, H., BLACKLEDGE, M., MANDELKOW, E. & ZWECKSTETTER, M. 2013. Phosphorylation of human Tau protein by microtubule affinity-regulating kinase 2. *Biochemistry,* 52**,** 9068-79.

SCHWEERS, O., MANDELKOW, E. M., BIERNAT, J. & MANDELKOW, E. 1995. Oxidation of cysteine-322 in the repeat domain of microtubule-associated protein tau controls the in vitro assembly of paired helical filaments. *Proc Natl Acad Sci U S A,* 92**,** 8463-7.

SCHWEERS, O., SCHONBRUNN-HANEBECK, E., MARX, A. & MANDELKOW, E. 1994. Structural studies of tau protein and Alzheimer paired helical filaments show no evidence for beta-structure. *J Biol Chem,* 269**,** 24290-7.

SHAMIR, D. B., ROSENQVIST, N., RASOOL, S., PEDERSEN, J. T. & SIGURDSSON, E. M. 2016. Internalization of tau antibody and pathological tau protein detected with a flow cytometry multiplexing approach. *Alzheimers Dement,* 12**,** 1098-1107.

SHELTON, L. B., BAKER, J. D., ZHENG, D., SULLIVAN, L. E., SOLANKI, P. K., WEBSTER, J. M., SUN, Z., SABBAGH, J. J., NORDHUES, B. A., KOREN, J., 3RD, GHOSH, S., BLAGG, B. S. J., BLAIR, L. J. & DICKEY, C. A. 2017. Hsp90 activator Aha1 drives production of pathological tau aggregates. *Proc Natl Acad Sci U S A,* 114**,** 9707-9712.

SHYTLE, R. D., TAN, J., BICKFORD, P. C., REZAI-ZADEH, K., HOU, L., ZENG, J., SANBERG, P. R., SANBERG, C. D., ALBERTE, R. S., FINK, R. C. & ROSCHEK, B., JR. 2012. Optimized turmeric extract reduces beta-Amyloid and phosphorylated Tau protein burden in Alzheimer's transgenic mice. *Curr Alzheimer Res,* 9**,** 500-6.

SIGURDSSON, E. M. 2014. Tau immunotherapy and imaging. *Neurodegener Dis,* 13**,** 103-6.

SKOVRONSKY, D. M., LEE, V. M. & TROJANOWSKI, J. Q. 2006. Neurodegenerative diseases: new concepts of pathogenesis and their therapeutic implications. *Annu Rev Pathol,* 1**,** 151-70.

SOLOMON, B., KOPPEL, R., HANAN, E. & KATZAV, T. 1996. Monoclonal antibodies inhibit in vitro fibrillar aggregation of the Alzheimer beta-amyloid peptide. *Proc Natl Acad Sci U S A,* 93**,** 452-5.

SPILLANTINI, M. G. & GOEDERT, M. 2013. Tau pathology and neurodegeneration. *Lancet Neurol,* 12**,** 609-22.

SPILLANTINI, M. G., MURRELL, J. R., GOEDERT, M., FARLOW, M. R., KLUG, A. & GHETTI, B. 1998. Mutation in the tau gene in familial multiple system tauopathy with presenile dementia. *Proc Natl Acad Sci U S A,* 95**,** 7737-41.

SPILLANTINI, M. G., VAN SWIETEN, J. C. & GOEDERT, M. 2000. Tau gene mutations in frontotemporal dementia and parkinsonism linked to chromosome 17 (FTDP-17). *Neurogenetics,* 2**,** 193-205.

STAMER, K., VOGEL, R., THIES, E., MANDELKOW, E. & MANDELKOW, E. M. 2002. Tau blocks traffic of organelles, neurofilaments, and APP vesicles in neurons and enhances oxidative stress. *J Cell Biol,* 156**,** 1051-63.

STOOTHOFF, W. H. & JOHNSON, G. V. 2005. Tau phosphorylation: physiological and pathological consequences. *Biochim Biophys Acta,* 1739**,** 280-97.

SYDOW, A., HOCHGRAFE, K., KONEN, S., CADINU, D., MATENIA, D., PETROVA, O., JOSEPH, M., DENNISSEN, F. J. & MANDELKOW, E. M. 2016. Age-dependent neuroinflammation and cognitive decline in a novel Ala152Thr-Tau transgenic mouse model of PSP and AD. *Acta Neuropathol Commun,* 4**,** 17.

SYDOW, A., VAN DER JEUGD, A., ZHENG, F., AHMED, T., BALSCHUN, D., PETROVA, O., DREXLER, D., ZHOU, L., RUNE, G., MANDELKOW, E., D'HOOGE, R., ALZHEIMER, C. & MANDELKOW, E. M. 2011. Tau-induced defects in synaptic plasticity, learning, and memory are reversible in transgenic mice after switching off the toxic Tau mutant. *J Neurosci,* 31**,** 2511-25.

TELL, V. & HILGEROTH, A. 2013. Recent developments of protein kinase inhibitors as potential AD therapeutics. *Front Cell Neurosci,* 7**,** 189.

TEPPER, K., BIERNAT, J., KUMAR, S., WEGMANN, S., TIMM, T., HUBSCHMANN, S., REDECKE, L., MANDELKOW, E. M., MULLER, D. J. & MANDELKOW, E. 2014. Oligomer formation of tau protein hyperphosphorylated in cells. *J Biol Chem,* 289**,** 34389-407.

THEUNIS, C., CRESPO-BIEL, N., GAFNER, V., PIHLGREN, M., LOPEZ-DEBER, M. P., REIS, P., HICKMAN, D. T., ADOLFSSON, O., CHUARD, N., NDAO, D. M., BORGHGRAEF, P., DEVIJVER, H., VAN LEUVEN, F., PFEIFER, A. & MUHS, A. 2013. Efficacy and safety of a liposome-based vaccine against protein Tau, assessed in tau.P301L mice that model tauopathy. *PLoS One,* 8**,** e72301.

TIMM, T., VON KRIES, J. P., LI, X., ZEMPEL, H., MANDELKOW, E. & MANDELKOW, E. M. 2011. Microtubule affinity regulating kinase activity in living neurons was examined by a genetically encoded fluorescence resonance energy transfer/fluorescence lifetime imaging-based biosensor: inhibitors with therapeutic potential. *J Biol Chem,* 286**,** 41711-22.

TROQUIER, L., CAILLIEREZ, R., BURNOUF, S., FERNANDEZ-GOMEZ, F. J., GROSJEAN, M. E., ZOMMER, N., SERGEANT, N., SCHRAEN-MASCHKE, S., BLUM, D. & BUEE, L. 2012. Targeting phospho-Ser422 by active Tau Immunotherapy in the THYTau22 mouse model: a suitable therapeutic approach. *Curr Alzheimer Res,* 9**,** 397-405.

UMEDA, T., EGUCHI, H., KUNORI, Y., MATSUMOTO, Y., TANIGUCHI, T., MORI, H. & TOMIYAMA, T. 2015. Passive immunotherapy of tauopathy targeting pSer413-tau: a pilot study in mice. *Ann Clin Transl Neurol,* 2**,** 241-55.

VAN DER JEUGD, A., HOCHGRAFE, K., AHMED, T., DECKER, J. M., SYDOW, A., HOFMANN, A., WU, D., MESSING, L., BALSCHUN, D., D'HOOGE, R. & MANDELKOW, E. M. 2012. Cognitive defects are reversible in inducible mice expressing pro-aggregant full-length human Tau. *Acta Neuropathol,* 123**,** 787-805.

VILLALOBOS, V., NAIK, S., BRUINSMA, M., DOTHAGER, R. S., PAN, M. H., SAMRAKANDI, M., MOSS, B., ELHAMMALI, A. & PIWNICA-WORMS, D. 2010. Dual-color click beetle luciferase heteroprotein fragment complementation assays. *Chem Biol,* 17**,** 1018-29.

VON BERGEN, M., BARGHORN, S., BIERNAT, J., MANDELKOW, E. M. & MANDELKOW, E. 2005. Tau aggregation is driven by a transition from random coil to beta sheet structure. *Biochim Biophys Acta,* 1739**,** 158-66.

VON BERGEN, M., BARGHORN, S., LI, L., MARX, A., BIERNAT, J., MANDELKOW, E. M. & MANDELKOW, E. 2001. Mutations of tau protein in frontotemporal dementia promote aggregation of paired helical filaments by enhancing local beta-structure. *J Biol Chem,* 276**,** 48165-74.

VON BERGEN, M., FRIEDHOFF, P., BIERNAT, J., HEBERLE, J., MANDELKOW, E. M. & MANDELKOW, E. 2000. Assembly of tau protein into Alzheimer paired helical filaments depends on a local sequence motif ((306)VQIVYK(311)) forming beta structure. *Proc Natl Acad Sci U S A,* 97**,** 5129-34.

WANG, Y., BALAJI, V., KANIYAPPAN, S., KRUGER, L., IRSEN, S., TEPPER, K., CHANDUPATLA, R., MAETZLER, W., SCHNEIDER, A., MANDELKOW, E. & MANDELKOW, E. M. 2017. The release and trans-synaptic transmission of Tau via exosomes. *Mol Neurodegener,* 12**,** 5.

WANG, Y. & MANDELKOW, E. 2016. Tau in physiology and pathology. *Nat Rev Neurosci,* 17**,** 5-21.

WANG, Y. P., BIERNAT, J., PICKHARDT, M., MANDELKOW, E. & MANDELKOW, E. M. 2007. Stepwise proteolysis liberates tau fragments that nucleate the Alzheimer-like aggregation of full-length tau in a neuronal cell model. *Proc Natl Acad Sci U S A,* 104**,** 10252-7.

WARD, S. M., HIMMELSTEIN, D. S., LANCIA, J. K., FU, Y., PATTERSON, K. R. & BINDER, L. I. 2013. TOC1: characterization of a selective oligomeric tau antibody. *J Alzheimers Dis,* 37**,** 593-602.

WEGMANN, S., MULLER, D. J. & MANDELKOW, E. 2012. Investigating fibrillar aggregates of Tau protein by atomic force microscopy. *Methods Mol Biol,* 849**,** 169-83.

WEGMANN, S., NICHOLLS, S., TAKEDA, S., FAN, Z. & HYMAN, B. T. 2016. Formation, release, and internalization of stable tau oligomers in cells. *J Neurochem,* 139**,** 1163-1174.

WEINGARTEN, M. D., LOCKWOOD, A. H., HWO, S. Y. & KIRSCHNER, M. W. 1975. A protein factor essential for microtubule assembly. *Proc Natl Acad Sci U S A,* 72**,** 1858-62.

WEST, T., HU, Y., VERGHESE, P. B., BATEMAN, R. J., BRAUNSTEIN, J. B., FOGELMAN, I., BUDUR, K., FLORIAN, H., MENDONCA, N. & HOLTZMAN, D. M. 2017. Preclinical and Clinical Development of ABBV-8E12, a Humanized Anti-Tau Antibody, for Treatment of Alzheimer's Disease and Other Tauopathies. *J Prev Alzheimers Dis,* 4**,** 236-241.

WILSON, D. M. & BINDER, L. I. 1997. Free fatty acids stimulate the polymerization of tau and amyloid beta peptides. In vitro evidence for a common effector of pathogenesis in Alzheimer's disease. *Am J Pathol,* 150**,** 2181-95.

WISCHIK, C. M., EDWARDS, P. C., LAI, R. Y., ROTH, M. & HARRINGTON, C. R. 1996. Selective inhibition of Alzheimer disease-like tau aggregation by phenothiazines. *Proc Natl Acad Sci U S A,* 93**,** 11213-8.

YAMADA, K., CIRRITO, J. R., STEWART, F. R., JIANG, H., FINN, M. B., HOLMES, B. B., BINDER, L. I., MANDELKOW, E. M., DIAMOND, M. I., LEE, V. M. & HOLTZMAN, D. M. 2011. In vivo microdialysis reveals age-dependent decrease of brain interstitial fluid tau levels in P301S human tau transgenic mice. *J Neurosci,* 31**,** 13110-7.

YANAMANDRA, K., KFOURY, N., JIANG, H., MAHAN, T. E., MA, S., MALONEY, S. E., WOZNIAK, D. F., DIAMOND, M. I. & HOLTZMAN, D. M. 2013. Anti-tau antibodies that block tau aggregate seeding in vitro markedly decrease pathology and improve cognition in vivo. *Neuron,* 80**,** 402-414.

YOSHIYAMA, Y., HIGUCHI, M., ZHANG, B., HUANG, S. M., IWATA, N., SAIDO, T. C., MAEDA, J., SUHARA, T., TROJANOWSKI, J. Q. & LEE, V. M. 2007. Synapse loss and microglial activation precede tangles in a P301S tauopathy mouse model. *Neuron,* 53**,** 337-51.

ZILKA, N., STOZICKA, Z., CENTE, M., KAZMEROVA, Z., KOVACECH, B. & NOVAK, M. 2012. Immunomodulation of memory-impairing protein tau in Alzheimer's disease. *Neurodegener Dis,* 10**,** 242-5.

# 6 Publications

1. Pir GJ, Choudhary B, Kaniyappan S, **Chandupatla RR**, Mandelkow E, Mandelkow EM, Wang Y. Suppressing Tau Aggregation and Toxicity by an Anti-Aggregant Tau Fragment. ***Molecular Neurobiology.*** 2018 Sep 8; doi: 10.1007/s12035-018-1326-z

2. Kaniyappan S, **Chandupatla RR,** Mandelkow EM and Mandelkow E. Purification and Characterization of low-n Tau oligomers. ***Methods Mol Biol.*** 2018;1779:99-111. doi: 10.1007/978-1-4939-7816-8_8.

3. Kaniyappan S, **Chandupatla RR,** Mandelkow EM and Mandelkow E. Extracellular low-n pro-aggregant Tau repeat domain oligomers cause synaptotoxicity accompanied by elevated calcium and reactive oxygen species. ***Alzheimer's & Dementia****,* 2017 May 18. pii: S1552-5260(17)30183-8. doi: 10.1016/j.jalz.2017.04.002.

4. Wang Y, Balaji V, Kaniyappan S, Krüger L, Irsen S, Tepper K, **Chandupatla R**, Maetzler W, Schneider A, Mandelkow E, Mandelkow EM . The release and trans-synaptic transmission of Tau via exosomes. ***Mol Neurodegener.*** 2017 Jan 13;12(1):5. doi: 10.1186/s13024-016-0143-y.

5. **Chandupatla RR,** Kaniyappan S, Feederle R, Kremmer E, Mandelkow EM. Antibody mediated inhibition of tau aggregation *in vitro* and in neuronal cells. Abstract, ADPD conference, Vienna, 2017 **(Poster presentation)**.

## Appendix

### Chemical composition

### Protein purification chemicals:

**10 X CB Buffer**

| Chemical | Weight | Stock | Volume |
|---|---|---|---|
| 0.2 M Na-Mes | 42.646 g | - | - |
| 10 mM Na-EGTA | 3.804 g | 0.5 M | 20 ml |
| 10 mM $MgCl_2$ | 2 g | | 1 ml |

Make up to 1 liter with double distilled water, pH 6.8. Store at 4°C**.** Prepare the whole solution once or prepare it from stock.

**Re Suspension Buffer Composition: For 100 ml**

| Chemical | Stock | Volume |
|---|---|---|
| CB Buffer | 10 X | 10 ml |
| DTT | 1 M | 0.5 ml |
| PMSF | 0.1 M | 2 ml |
| Leupeptin | 10 mg/ml | 100 µl |
| Pepstatin A | 5 mg/ml | 200 µl |
| benzamidine | 1 M | 200 µl |
| MQ $H_2O$ | | 87 ml |

**Mono S A Buffer 10 X**

| Chemical | 10X Stock | Volume for 1X |
|---|---|---|
| 20 mM Na-MES | 0.2 M | 100 ml |
| 50 mM NaCl | 5 M | 10 ml |
| 2 mM DTT | 1 M | 2 ml |
| 1 mM Na-EGTA | 0.5 M | 2 ml |
| 1 mM $MgSO_4$ | 1 M | 1 ml |
| 0.1 mM PMSF | 0.1 M | 1 ml |

Make up to 1Liter; pH 6.8; sterilize; PMSF and DTT should be added fresh.

**Mono S B Buffer (250 ml suffices for a single run)**

| Chemical | Stock | Volume |
|---|---|---|
| 20 mM Na-MES | 0.2 M | 100 ml |
| 1 M NaCl | 5 M | 200 ml |
| 2 mM DTT | 1 M | 2 ml |
| 1 mM Na-EGTA | 0.5 M | 2 ml |
| 1 mM $MgSO_4$ | 1 M | 1 ml |
| 0.1 mM PMSF | 0.1 M | 1 ml |

Make up to 1Liter; pH 6.8; Sterilize; PMSF and DTT should be added fresh.

**SDS gel composition**

| Ingredients | 10% resolving gel | 17% resolving gel | 4% stacking gel |
|---|---|---|---|
| 40% Acrylamide | 15 ml | 25.6 ml | 5.4 ml |
| 1 M Tris HCl pH 8.8 | 22 ml | 22 ml | - |
| 0.25 M Tris HCl pH 6.8 | - | - | 27 ml |
| $H_2O$ | 22 ml | 11.5 ml | - |
| $H_2O$ + bromophenol blue | - | - | 20.9 ml |
| 10 % SDS | 600 µl | 600 µl | 540 µl |
| TEMED | 120 µl | 120 µl | 108 µl |
| 10% APS | 65 µl | 65 µl | 150 µl |

**5X SDS sample buffer**

0.32 M Tris-HCl, pH 6.8; 10% SDS; 50% glycerol; 1.43 M ß-ME; and $10^{-2}$% bromophenol blue

**1X SDS running buffer**

0.25 M Tris; 0.192 M glycine; 0.1% SDS; Make the volume up to 10 liters with doubly distilled water.

**10X blotting buffer or Transfer buffer**

390 mM Glycine; 480 mM Tris; 0.3% SDS;

Make up to 1 liter with doubly distilled water.

**1X blotting buffer or Transfer buffer**

100 ml of 10X blotting buffer; 50 ml 100% methanol;

Make up to 1 liter with doubly distilled water.

**10X TBST**

100 mM Tris; 1.5 M NaCl; 0.5% Tween 20; Make up to 2.5 liters with doubly distilled water. Adjust the pH to 7.5

**Stripping buffer**

0.2 M glycine; 1 mM EDTA-Na; 0.5 M NaCl, pH 2.5.

**Coomassie Stain**

25% isopropanol; 10% acetic acid; 0.05% coomassie R-250;

Make up to 200 ml with doubly distilled water.

**Coomassie destaining solution**

**Intensive**

2.5 L ethanol; 2.0 L doubly distilled water; and 0.5 L acetic acid

**Normal:**

250 ml ethanol; 375 ml acetic acid; and 4375 ml doubly distilled water

**Silver staining:**

**Fixative:** 30% ethanol and 10% acetic acid

**Cross-linking reagent:** 30% ethanol; 0.5 M sodium acetate; 0.2% sodium thiocyanate and 0.5% glutaraldehyde

**Silver nitrate staining solution:** 0.1% silver nitrate; and 0.02% formaldehyde

**Developing solution:** 2.5% sodium carbonate; 0.01% formaldehyde.

**Reaction ending solution:** 50 mM EDTA, pH 8.0

**AFM**

**Adsorption buffer** (**PBS)**

137 mM NaCl; 8 mM $NH_2PO_4$, 2.7 mM KCl; and 1.5 mM $KH_2PO_4$ adjusted to pH 7.4.

**Imaging buffer:**

10 mM Tris–HCl; 50 mM KCl; adjusted to pH 7.4.

**Cell culture chemicals**

**N2a cells culture medium**

15% FBS; 1% penicillin and streptomycin; 1% NEAA; diluted in MEME medium followed by filter sterilization.

**N2a cells freezing medium:**

50% FBS; 40% MEME; 10% DMSO;

Preparation and sterilization using syringe filters.

**2X Lysis buffer**

100 mM Tris-HCl, pH 7.4; 20% glycerol ; 2% NP 40 detergent; 10 mM DTT; 2 mM EGTA; 40 mM NaF and 2 mM $Na_3VO_4$.

**Working lysis buffer**

2X lysis buffer; 150 mM NaCl; 1X complete protease mini; 1X PhosSTOP; 5 mM CHAPS. Make up these chemicals with distilled water to the desired volume.

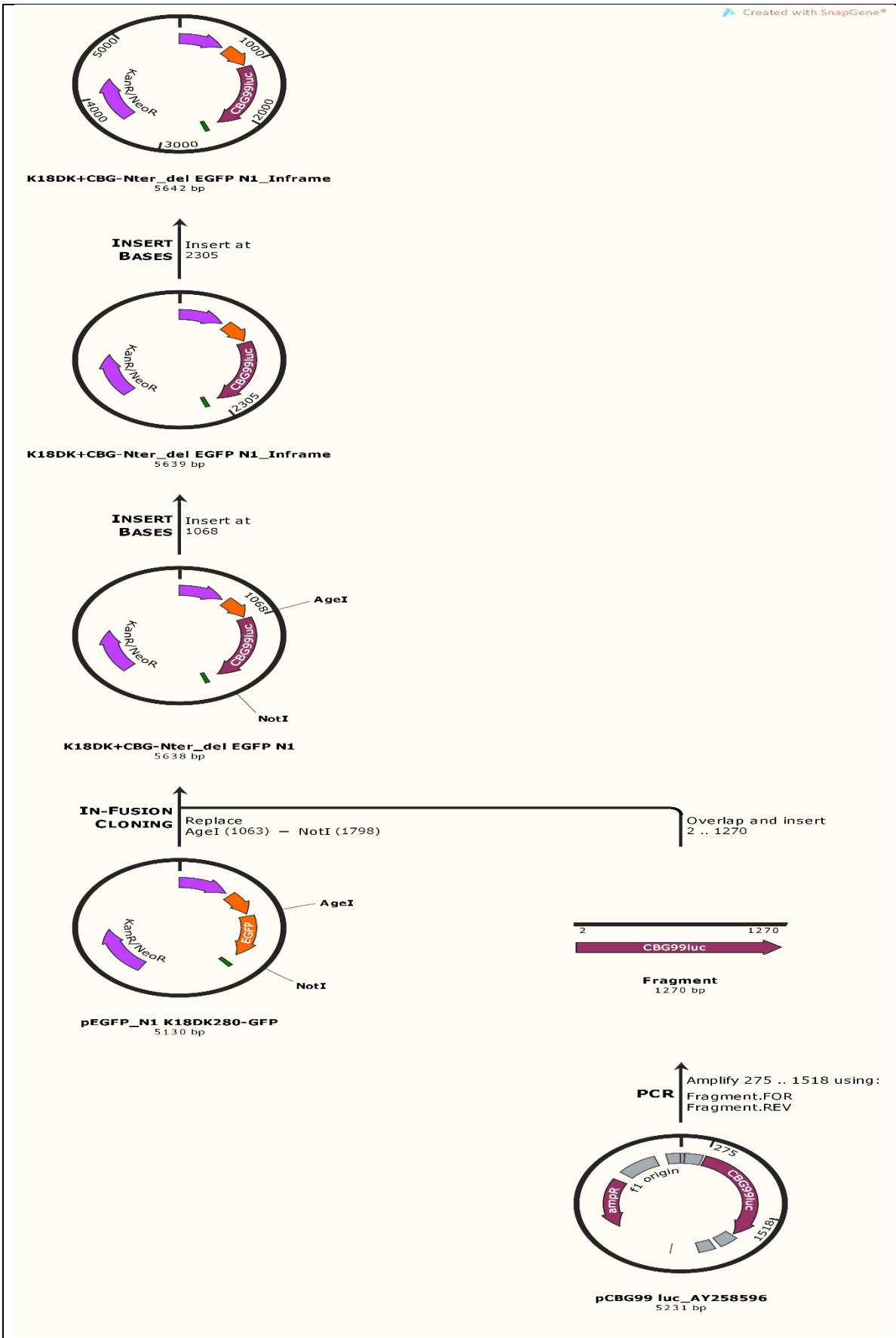


**I: Plasmid map of (K18DK280) Tau$^{RD\Delta K}$-Luc-N.**

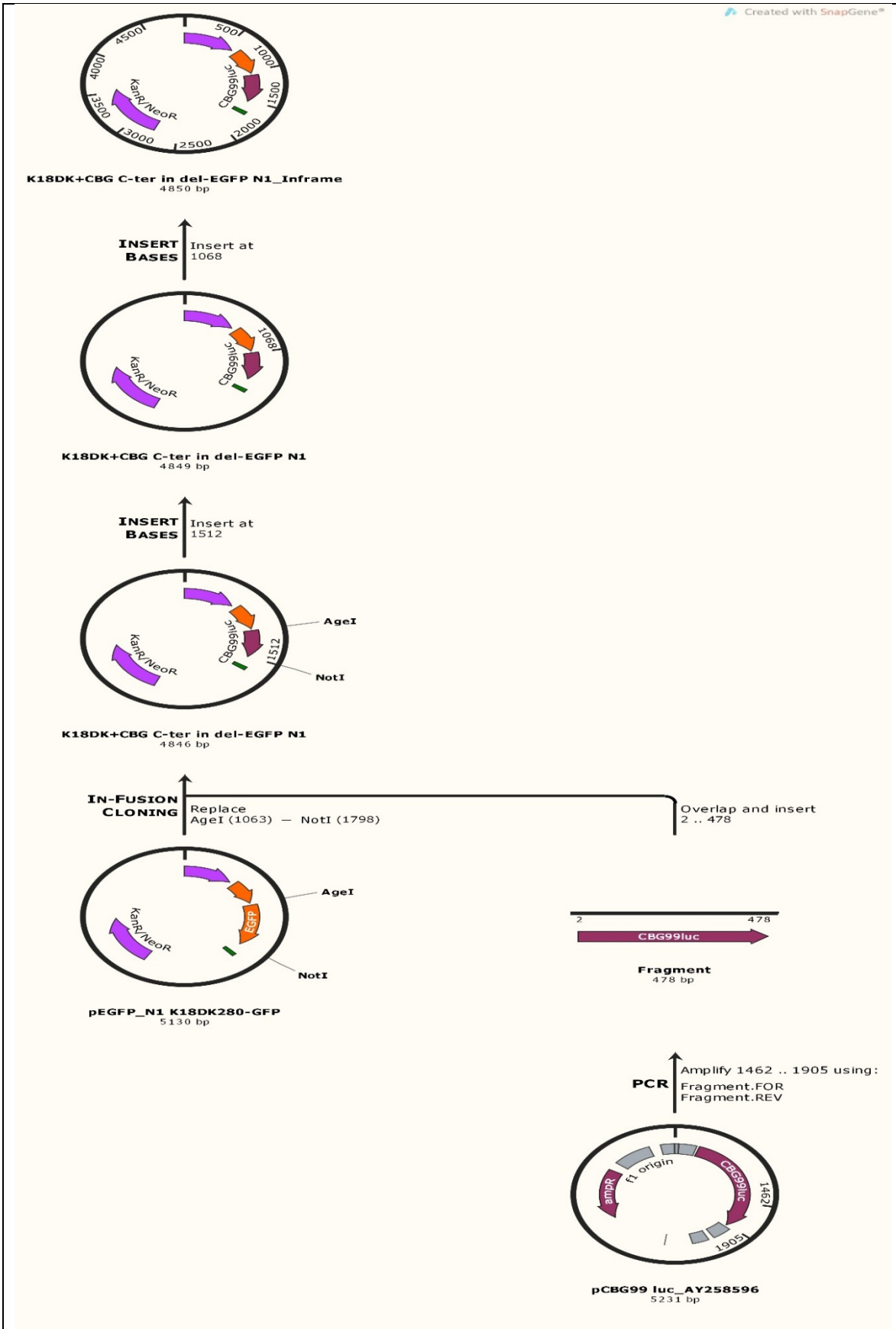


**II: Plasmid map of (K18DK280) Tau$^{RD\Delta K}$-Luc-C.**

**Acknowledgements**

Foremost, I would like to express my sincere gratitude to my advisors Dr. Eckhard Mandelkow and Dr. Eva-Maria Mandelkow for their continuous support of my PhD study and research. I would also like to thank Dr. Senthilvelrajan Kaniyappan, who helped me all the time with my research and writing of this thesis. I could not have imagined having a better friend and mentor for my PhD study.

I would like to thank Dr. Jacek Biernat for his valuable suggestions. I would like to thank my fellow lab mates for their constant support during my thesis work.

I would like to thank DZNE and CAESAR microscopy facility. I would also thank secretaries of MPI, DZNE and CAESAR for their support with the administrative tasks.

Last but not the least, I would like to thank my family, Tin Tin, Binu, Priya and Vignesh for their constant support and fun filled days which kept me through the years and years to come.